

Integrating Multidisciplinary Observations in Vent Environments (IMOVE): Decadal progress in deep-sea observatories at hydrothermal vents

1 **M. Matabos^{1*} & T. Barreyre^{2*}, S. K. Juniper³, M. Cannat⁴, D. Kelley⁵, J.M. Alfaro-Lucas⁶, V.
2 Chavagnac⁷, A. Colaco⁸, J. Escartin⁹, E. Escobar¹⁰, D. Fornari¹¹, J. Hasenlever¹², J.A. Huber¹³,
3 A. Laes¹, N. Lantéri¹, L.A. Levin¹⁴, S. Mihaly³, E. Mittelstaedt¹⁵, F. Pradillon¹, P.-M. Sarradin¹,
4 J. Sarrazin¹, B. Tomasi^{16,17}, R. Venkatesan¹⁸, C. Vic¹⁹, and the IMOVE InterRidge working
5 group.**

6 ¹ Ifremer, REM, IC MERS, F-29280 Plouzané, France

7 ² Department of Earth Science / Centre for Deep Sea Research, University of Bergen, Bergen, Norway
8 5020

9 ³ Ocean Networks Canada, University of Victoria, Victoria, British Columbia V8N 1V8, Canada

10 ⁴ Equipe de Géosciences Marines, Université de Paris, Institut de Physique du Globe de Paris, UMR
11 7154 CNRS, Paris, France

12 ⁵ School of Oceanography, University of Washington, Seattle, USA

13 ⁶ Department of Marine Zoology, Senckenberg Research Institute and Natural History Museum,
14 Frankfurt am Main, Germany

15 ⁷ Géosciences Environnement Toulouse CNRS UMR 5563 IRD/UPS/CNES, Université de Toulouse,
16 31400 Toulouse, France

17 ⁸ Instituto de Investigação em Ciências do Mar - Okeanos, Universidade dos Açores, Rua Professor
18 Doutor Frederico Machado 4, 9901-862 Horta, Portugal

19 ⁹ Laboratoire de Géologie, CNRS, UMR 8538, École Normale Supérieure, PSL University, Paris,
20 France

21 ¹⁰ Universidad Nacional Autónoma de México, Instituto de Ciencias del Mar y Limnología; CU 04510
22 Mexico City, Mexico

23 ¹¹ Geology and Geophysics Dept., Woods Hole Oceanographic Institution, Woods Hole, MA 02543
24 USA

25 ¹² Institute of Geophysics, CEN, Hamburg University, Germany

26 ¹³ Marine Chemistry and Geochemistry, Woods Hole Oceanographic Institution, Woods Hole, MA
27 02543

28 ¹⁴ Center for Marine Biodiversity and Conservation, Scripps Institution of Oceanography, UC San
29 Diego, La Jolla, CA USA

30 ¹⁵ Department of Earth and Spatial Sciences, University of Idaho, Moscow, ID, USA
31 ¹⁶ L@BISEN, ISEN Yncréa Ouest, Brest, France
32 ¹⁷ Norwegian Research Center, NORCE, Bergen, Norway
33 ¹⁸ National Institute of Ocean Technology, Chennai, India
34 ¹⁹ Univ. Brest, CNRS, IRD, Ifremer, Laboratoire d'Océanographie Physique et Spatiale, Plouzané,
35 France

36

37 * Correspondence:

38 *Equally first author: Marjolaine Matabos and Thibaut Barreyre

39 marjolaine.matabos@ifremer.fr; thibaut.barreyre@uib.no

40 **Keywords: Essential Ocean Variables (EOVs), Essential Biological Variables (EBVs), Mid-ocean**
41 **ridge (MOR), Sensors, seabed platforms, vent fluid dynamics, vent communities dynamics**

42

43 **Abstract**

44 The unique ecosystems and biodiversity associated with mid-ocean ridge (MOR) hydrothermal vent
45 systems contrast sharply with surrounding deep-sea habitats, however both may be increasingly
46 threatened by anthropogenic activity (e.g., mining activities at massive sulphide deposits). Climate
47 change can alter the deep-sea through increased bottom temperatures, loss of oxygen, and
48 modifications to deep water circulation. Despite the potential of these profound impacts, the
49 mechanisms enabling these systems and their ecosystems to persist, function and respond to oceanic,
50 crustal, and anthropogenic forces remain poorly understood. This is due primarily to technological
51 challenges and difficulties in accessing, observing and monitoring the deep-sea. In this context, the
52 development of deep-sea observatories in the 2000s focused on understanding the coupling between
53 sub-surface flow and oceanic and crustal conditions, and how they influence biological processes.
54 Deep-sea observatories provide long-term, multidisciplinary time-series data comprising repeated
55 observations and sampling at temporal resolutions from seconds to decades, through a combination of
56 cabled, wireless, remotely controlled, and autonomous measurement systems. The three existing vent
57 observatories are located on the Juan de Fuca and Mid-Atlantic Ridges (Ocean Observing Initiative,
58 Ocean Networks Canada and the European Multidisciplinary Seafloor and water column Observatory).
59 These observatories promote stewardship by defining effective environmental monitoring including
60 characterizing biological and environmental baseline states, discriminating changes from natural
61 variations versus those from anthropogenic activities, and assessing degradation, resilience and
62 recovery after disturbance. This highlights the potential of observatories as valuable tools for
63 environmental impact assessment (EIA) in the context of climate change and other anthropogenic
64 activities, primarily ocean mining. This paper provides a synthesis on scientific advancements enabled
65 by the three observatories this last decade, and recommendations to support future studies through
66 international collaboration and coordination. The proposed recommendations include: i) establishing
67 common global scientific questions and identification of Essential Ocean Variables (EOVs) specific to

68 MORs, ii) guidance towards the effective use of observatories to support and inform policies that can
69 impact society, iii) strategies for observatory infrastructure development that will help standardize
70 sensors, data formats and capabilities, and iv) future technology needs and common sampling
71 approaches to answer today's most urgent and timely questions.

72

73 **Introduction**

74 Over the past ~70 years, since the revolution in Earth and Ocean sciences precipitated by the
75 confirmation of seafloor spreading and plate tectonics, the technological challenges, limited access,
76 and high costs associated with deep-sea studies led to significant gaps in understanding spatial and
77 temporal changes associated with chemical, biological and physical phenomena in the deep ocean. This
78 has been especially true of seasonal processes that occur over a wide range of spatial and temporal
79 scales throughout the global oceans (e.g., Glover et al., 2010). To date, deep-sea time-series
80 investigations have documented notable environmental and biological variations from seconds to
81 decades in a wide range of ecosystems from bathyal and abyssal zones (e.g., Hartman et al., 2012;
82 Barreyre et al., 2014b; Cuvelier et al., 2014b; Doya et al., 2014; Matabos et al., 2014; Sarrazin et al.,
83 2014; Cuvelier et al., 2017; Lelièvre et al., 2017; Taylor et al., 2017; Chavagnac et al., 2018a; Taylor
84 et al., 2018; Durden et al., 2020). Increasing societal interest in deep-ocean resources has been
85 accompanied by a growing recognition of the urgent need for a comprehensive assessment of the status
86 and health of deep-sea ecosystems (Rogers et al., 2015; Franke et al., 2020). Robust environmental and
87 biological baselines as well as understanding of their natural dynamics are key to assessing and
88 predicting the impacts and responses of interconnected ecosystems to large-scale disturbances caused
89 by natural processes (e.g., earthquakes and volcanic eruptions), and anthropogenic activities (e.g.,
90 ocean acidification and warming and their climate and environmental impacts) (e.g., Ramirez-Llodra
91 et al., 2010; Danovaro et al., 2017, 2020). Multi-decadal and multidisciplinary time-series studies at

92 variable spatial scales are essential for discriminating between human-induced impacts, and long-term
93 natural periodic and episodic variability, and inform our assessment of the environmental drivers and
94 their biological consequences.

95 The need for long-term, time-series measurements of key ocean variables with a specific focus on the
96 deep-sea (Thiel et al., 1994), has been identified as a critical topic since the 1990s (National Research
97 Council, 2000), and has led to the development of seafloor-water column observatories. The
98 Committee on Seafloor Observatories, bringing together scientists from all fields of Ocean and Earth
99 sciences, gathered in 2000 to provide a vision for a global Seafloor Observatory Network including the
100 risks and benefits of ocean observation platforms (National Research Council, 2000). They defined
101 “seafloor observatories” as an autonomous “system of instruments, sensors, and command modules
102 connected either acoustically or via a seafloor junction box to a surface buoy or a fiber optic cable to
103 land”. This comprehensive report highlighted scientific questions that observatories could specifically
104 address. Observatories were foreseen as requiring a major investment of resources over many decades.
105 In the following two decades, a number of observatories have developed around the world, with
106 instruments distributed from seafloor to the water column (e.g., Kelley et al., 2014; Smith et al., 2018;
107 Dañobeitia et al., 2020). More recently an observatory was defined as an “integrated observing,
108 monitoring, and experimenting infrastructure which aims to collect high-resolution data in a restricted
109 geographical region” (Crise et al., 2018). One of the first areas of interest for observatories has been
110 highly-dynamic mid-ocean ridges and back-arc spreading centres, where seafloor volcanism and
111 tectonic activity predominate.

112 Mid-Ocean Ridge (MOR) and back-arc spreading systems host unique ecosystems and biodiversity
113 (Tunnicliffe, 1991; Ramirez-Llodra et al., 2010; Mullineaux et al., 2018; Chapman et al., 2019).
114 Hydrothermal circulation within these environments is responsible for significant transfer of heat and
115 chemical constituents between the oceanic lithosphere and the overlying hydrosphere, thus controlling

116 the thermo-mechanical state of the crust, its formation and deformation, rock alteration, and influencing
117 element balances in the ocean. (e.g., Boyd and Ellwood, 2010; Fitzsimmons et al., 2014). Hydrothermal
118 circulation also supports high-biomass chemosynthesis-based ecosystems that sharply contrast with
119 surrounding deep-sea habitats (e.g., Kelley et al., 2005; Lutz et al., 2008; Nees et al., 2008; Dick, 2019).
120 Hydrothermal vents sustain dense populations of endemic faunal species that rely on microbial dark
121 CO₂ fixation (Tunnicliffe, 1991; Tunnicliffe et al., 2003) that is coupled to the oxidation of reducing
122 elements (e.g., HS⁻, H₂, CH₄, etc.) in discharging hydrothermal fluids (Le Bris et al., 2019). Its footprint
123 impacts neighbouring water and seafloor and marine ecosystems (Levin et al., 2016). Vent fauna
124 communities are influenced by local population's demography and connected by dispersing planktonic
125 larvae, which impact the dynamics of the vent metacommunity at a regional scale (Mullineaux et al.,
126 2018). Challenging physico-chemical conditions at seafloor vents constrain faunal diversity
127 (Tunnicliffe, 1991), whereas highly diverse prokaryotes exploit a broad range of habitats (Dick, 2019).
128 These ecosystems broaden our understanding of the potential origins of life on Earth (Martin et al.,
129 2008; Barge et al., 2019) and of the possibilities for life on other worlds (e.g., Hand and German, 2018).
130 Furthermore, adaptations of vent fauna and microorganisms to extreme conditions have been a source
131 of inspiration for biotechnology, but also in Design and Art (reviewed in Van Dover, 2014). Growing
132 interests in the mining of polymetallic sulphide deposits raise concerns about the potential impacts of
133 mineral extraction on these unique ecosystems, stressing the need for research to inform environmental
134 policy and management strategies (Boschen et al., 2013; Van Dover, 2019; Orcutt et al., 2020; Smith
135 et al., 2020; Van Dover et al., 2020). Climate change is also expected to affect the deep sea through
136 increased bottom temperatures, loss of oxygen in certain areas of the ocean, and modifications to deep
137 water circulation (Levin and Le Bris, 2015; Sweetman et al., 2017; Galaasen et al., 2020; Levin et al.,
138 2020). Understanding how these changes will affect ecosystem integrity and function requires detailed
139 baseline knowledge of natural processes, with an understanding of the mechanisms involved.

140 Questions remain regarding the evolution of biological communities through time including non-
141 directional change (i.e., change in species compositions, symbiosis, and abundances due to
142 immigration, extinction, competition, predation), as well as on directional change (i.e., succession after
143 natural and/or anthropogenic disturbance). Those processes can only be addressed with robust baseline
144 knowledge provided by time series observations. Since the discovery of low-hydrothermal vents in
145 1977 (Ballard and Van Andel, 1977; Corliss et al., 1979), only a few areas have been repeatedly visited
146 (Glover et al., 2010; Fornari et al., 2012). Long-term time-series acquired at these sites, including 9°N
147 or 13°N along the East Pacific Rise, allowed significant advances in our understanding of community
148 dynamics and successional processes (e.g., Sarrazin et al., 1997; Shank et al., 1998; Marcus et al.,
149 2009; Cuvelier et al., 2011; Du Preez and Fisher, 2018; Mullineaux et al., 2020). However
150 understanding episodic and periodic hydrothermal and sub-seafloor processes that operate over time
151 scales of seconds to years (e.g., Tivey et al., 2002; Scheirer et al., 2006; Barreyre et al., 2014b, 2022),
152 and the associated faunal and microbial responses require continuous or at least annual *in situ*
153 monitoring and observations (e.g., Huber et al., 2003).

154 Cabled and autonomous deep-sea observatories can provide long-term time-series collection of multi-
155 disciplinary data (e.g., geological, physical, chemical, biological) at high temporal resolution and over
156 years to decades. Repeated submersible visits to study sites, combined with observatory maintenance,
157 have documented submarine volcanic eruptions and associated changes to hydrothermal vent fields
158 (e.g., Chadwick et al., 2012, 2013, 2022; Fornari et al., 2012; Nooner and Chadwick, 2016; Wilcock
159 et al., 2016; Barreyre et al., 2022), changes in community structure and activity (Shank et al., 1998;
160 Fortunato et al., 2018; Rommevaux et al., 2019) as well as interactions with other nearby
161 chemosynthetic and peripheral surrounding ecosystems (Levin et al., 2016). Together, these data
162 contribute to answering a number of questions across various disciplines from geophysics to
163 microbiology:

164 • How are hydrothermal heat, mass and chemical fluxes to the ocean impacted by seismicity,
165 volcanic activity and ground deformation at a diverging plate boundary?

166 • Does tectonic setting impact the long-term stability or temporal variability of these systems?

167 • How do steep axial valley topography and hydrothermal buoyancy flux affect the dynamics of
168 water masses, and how do local dynamics impact the dispersion of hydrothermal effluents?

169 • How do species compositions differ between habitats, geological settings, and ridges?

170 • How do pioneering species colonise new sites and which processes are involved?

171 • What are the impacts of telluric, climatic, and anthropogenic changes on deep seafloor
172 ecosystems and hydrothermal communities?

173 There are currently three observatory installations at hydrothermally active MOR systems. Plans for a
174 fourth at the Mohn Ridge (EMSO-Mohn), north of Jan Mayen, are ongoing
175 (<https://emso.eu/observatories-node/nordic-seas/>). In concert, these observatories provide Ocean and
176 Earth scientists, engineers, educators, policy makers, and the public opportunities to deepen
177 multidisciplinary understanding of myriad processes operating at MOR environments and utilization
178 and advancement of deep-sea technology. The InterRidge Working Group on Integrating
179 Multidisciplinary Observations in Vent Environments (IMOVE; <https://www.interridge.org/working->
180 group/wg_imove/) was created to advance and coordinate the integration of observatory research at
181 deep-sea vent fields. InterRidge (IR - www.interridge.org) is an international non-profit organization
182 created in 1992 that brings together ca. 1600 scientists from 20 nations involved in MOR research. IR
183 aims to (i) facilitate interdisciplinary, international collaboration; (ii) coordinate scientific exchange -
184 including information, technology and facilities; (iii) encourage the protection and environmental
185 management of ridge environments; and (iv) promote communication between scientists and members
186 of the society through coordinated outreach efforts. InterRidge Working Groups (WGs) are formed to

187 support the implementation of these objectives in priority areas. The IMOVE WG was formed to
188 advance multi-disciplinary research within and across the three MOR observatories.

189 A large volume of temporally- and spatially-variable multidisciplinary data has been collected at the
190 three presently active MOR vent observatories (Figure 1), requiring considerable support from funding
191 agencies. One of the goals of the IMOVE WG is to advance the integration of data from different
192 disciplines into quantitative, cross-disciplinary models relevant to hydrothermal processes on the
193 global MOR system. Coordinating the efforts of the scientific communities working at MOR
194 observatories has the potential to produce transformative research outcomes and major knowledge
195 advancements. The IMOVE WG held two international workshops (2019 and 2020) to set the stage for
196 such a global effort. The results of these workshops, including recommendations for future MOR
197 observatory science, are presented in this paper (IMOVE, 2019).

198 1 Current observatories at mid-ocean ridges

199 The three currently operating MOR ocean observatories are the Azores component of the European
200 Multidisciplinary Seafloor and water column Observatory (EMSO), the Endeavour node of Ocean
201 Networks Canada (ONC) and the Axial Seamount array of Ocean Observatory Initiative (OOI) (Figure
202 1, Box 1). EMSO-Azores, part of the EMSO European Research Infrastructure Consortium (ERIC), is
203 located on the slow-spreading Mid-Atlantic Ridge (MAR), at the summit of a magmatically robust
204 central volcano hosting the Lucky Strike hydrothermal field (Blandin et al., 2010; Colaço et al., 2011;
205 Cannat et al., 2016) (Figure 2). The two other observatories include submarine high power and
206 bandwidth cables spanning the intermediate-spreading Juan de Fuca Ridge (JdFR) in the NE Pacific.
207 ONC-Endeavour, located on the intensely hydrothermally-active Endeavour Segment, is significantly
208 influenced by seismicity, extensional tectonics and faulting and is operated by ONC (Kelley et al.,
209 2012, 2014) (Figure 3). OOI-Axial Seamount, located on the magmatically robust and volcanically
210 active Axial volcano is operated by the University of Washington for the US OOI (Kelley et al., 2014;

211 Delaney et al., 2016), as part of the OOI Regional Cable Array (RCA, Figure 4). All three observatories
212 support research aimed at understanding second, to daily, to multidecadal geophysical and geochemical
213 processes occurring at these submarine volcanoes and their vent systems, and, in turn, how these
214 processes affect the water column and drive biological responses in time and space, below, at, and
215 above the seafloor. The multidisciplinary observatories host sensors to characterise crustal dynamics,
216 hydrothermal circulation, fluid dynamics and composition both below and above ground, and
217 biological activity.

218 **1.1 The EMSO-Azores observatory, Lucky Strike vent field, Mid-Atlantic Ridge**

219 EMSO-Azores sits atop an active volcano close to the Azores Triple Junction on the northern part of
220 the Mid-Atlantic Ridge (MAR). The volcano hosts Lucky Strike, one of the largest active ridge-related
221 hydrothermal vent fields ($\sim 1 \text{ km}^2$, Langmuir et al., 1997; Barreyre et al., 2012; Beaulieu and Szafranski,
222 2020). This basalt-hosted field, situated at an average water depth of 1700 m, contains over twenty
223 active hydrothermal edifices distributed around a fossilised lava lake (Ondréas et al., 2009; Barreyre
224 et al., 2012), and overlying a magma chamber at ~ 3 km depth below seafloor (Singh et al., 2006). Part
225 of the venting area is included in a Marine Protected Area (MPA) in the Portuguese Exclusive
226 Economic Zone (EEZ) (Menini and Van Dover, 2019). Planning for this observatory began in October
227 1998 at an Interridge workshop dedicated to the long-term Monitoring of the Mid-Atlantic Ridge
228 (MoMAR). A series of follow-up MoMAR workshops (Santos et al., 2002; Barriga et al., 2005)
229 established scientific objectives, technical goals, and experimental designs. These plans served as a
230 basis for the implementation of the observatory, funded for the most part by the French ministry of
231 research with support over the years of several EC research grants. The autonomous observing system
232 EMSO-Azores, first deployed in 2010 (Cannat et al., 2011; Colaço et al., 2011; Legrand et al., 2019),
233 comprises two Sea Monitoring Nodes (SeaMoN) that provide local electrical power (28V), sensor
234 control, and data archiving, and limited satellite data transmission to shore via an acoustic connection

235 to a surface buoy (Figure 2). It supports research focused on understanding hydrothermal circulation
236 above the magmatic chamber to the seafloor, and its influence on deep-sea ecosystem functioning and
237 water column processes in the context of a magmatically robust slow-spreading ridge environment.
238 This multidisciplinary array has evolved over its, now, 11 years of continuous recording and the
239 following description concerns its present-day configuration.

240 The first node, SeaMoN west, is deployed at a former lava lake that formed within a series of rifted
241 volcanic cones at the summit of the central volcano (e.g., Ondréas et al., 2009; Escartín et al., 2014).
242 This node measures seafloor seismic activity, vertical seafloor motion, and is presently also equipped
243 withs the multisensor platform EGIM (EMSO Generic Instrumentation Module) that comprises a
244 turbidimeter, a CTD, an ADCP, one hydrophone, an Oxygen optode, and a pressure gauge (Lantéri et
245 al., 2022). The SeaMoN East node is deployed at the base of the Tour Eiffel active hydrothermal edifice
246 and is dedicated to physical, chemical and ecological studies. An High-Definition (HD) video camera
247 module (Sarrazin et al., 2007), chemical sensor (Laes et al., 2014), and thermistor string, support
248 studies of the dynamics of mussel assemblages and their environment. Biological and chemical
249 properties of high-temperature fluids are monitored with the microbial colonization module CISICS
250 (Connected In Situ Instrumented Colonizing System), and the *in situ* automated sampling of high-
251 temperature hydrothermal fluid device DEAFS (DEep sea Autonomous Fluid Sampler). The two nodes
252 are acoustically linked to a surface relay instrumented buoy, ensuring satellite communication to the
253 land base station in Brest, France. Data are archived, published with a DOI, and available on the
254 EMSO-Azores web page (Box 1).

255 In addition to these nodes, the observatory setup comprises several sets of autonomous instruments,
256 with data recovered during yearly maintenance cruises. The autonomous instruments deployed at
257 Lucky Strike include 4 short-period Ocean Bottom Seismometers (OBS), 2 pressure gauges, a physical
258 oceanography mooring, a seabed array of four cabled hydrophones that supports microseismicity and

259 marine sound studies at the Tour Eiffel site, a vast array of temperature probes distributed in hot and
260 diffuse vents through the hydrothermal field, several bottom current meters and over 20 autonomous
261 faunal colonization devices. A complementary ship-based field program is implemented during the
262 cruises and contributes to increasing the set of accessible parameters and their temporal and spatial
263 coverage (e.g., fluid and rock sampling, ecological studies, surveys of active and inactive areas, *in situ*
264 experimentations and repeated high-resolution mapping and 3D imaging of the venting areas). The
265 EMSO-Azores observatory is maintained annually during the MoMARSat cruises (Cannat and
266 Sarradin, 2010). All seafloor system components are recovered, serviced onboard and redeployed by
267 either the Remote Operated Vehicle (ROV) Victor 6000 or the Human Occupied Vehicle (HOV)
268 Nautile. Each dataset is linked to the relevant cruises, which are listed in the data DOI, and each cruise
269 DOI includes a list of the available data with their DOIs (Box 1).

270 1.2 **ONC-Endeavour**

271 The hydrothermally active Endeavour Segment, located on the northern part of the intermediate-
272 spreading Juan de Fuca Ridge, is 10 km long, with a 1 km wide axial valley that has rift walls reaching
273 200 m. Endeavour Segment hosts five major hydrothermal vent fields (Kelley et al., 2012, 2014) that
274 are underlain by magma lenses at depths of ~2-3 km (e.g., Van Ark et al., 2007) with microseismic
275 activity linked to hydrothermal circulation between the magma lens and the seafloor (e.g., Toomey et
276 al., 2009; Hooft et al., 2010). The Endeavour Hydrothermal Vents (EHV) became Canada's first MPA,
277 following an act of parliament in 2003. Ocean Networks Canada has been operating real-time
278 observing systems there since September 2010.

279 The scientific goals of the Endeavour observatory were established during a series of workshops,
280 following which researchers developed a multi-disciplinary community experiment proposal that
281 competed for instrumentation funds with other community experiment proposals during the design and
282 instrumentation phase of the ONC NEPTUNE (NorthEast Pacific Time-series Undersea Networked

283 Experiments) network. The observatory design had to be compliant with the MPA Management Plan,
284 which allowed for two of the vent fields, Mothra and Main Endeavour Field (MEF), to be cabled with
285 scientific instrumentation and experiments. A third vent field, High Rise, was to be left in its natural
286 state, and monitored through ROV visits and occasional deployments of autonomous instruments. The
287 Endeavour Node is sited 5 km east of the axial valley on a relatively flat seafloor. Three fibre optic
288 extension cables provide power and two-way data communications to seafloor junction boxes located
289 in the Mothra and Main Endeavour vent fields, and at a site north of the High Rise field (Figure 3).
290 The junction boxes provide power and communication to sensors and instruments on seafloor platforms
291 and water column moorings. The Main Endeavour Field instrumentation was initially concentrated on
292 a nearly 50 m-across, actively venting sulphide edifice named Grotto (Kelley et al., 2014; Juniper et
293 al., 2019). A seismometer array, designed to precisely locate shallow micro-seismic events in the
294 hydrothermal up-flow zone below the seafloor, supports study of their links to vent fluid discharge. On
295 Grotto, several different temperature sensor technologies monitor hydrothermal discharge at vents that
296 vary from a >335°C black smoker vent to diffuse warm flows. Two camera modules look out onto a
297 tubeworm assemblage and new sulphide worm habitat, and three monitoring systems provide data on
298 chemical properties of the vent environment. Outside of the vent fields, two pairs of water column
299 moorings (RCM), one pair between High Rise and Salty Dawg, the other between Mothra and MEF,
300 monitor water column properties and currents to constrain buoyancy-driven flow in the axial valley
301 (Figure 3). A Junction Box (JB) placed near the northern RCM pair supports a broadband seismometer
302 and bottom pressure recorder on the western flank of the Endeavour segment, about two kilometers
303 west of the MEF, on the Pacific Plate.

304 A near-tripling of ONC's observing system at the Endeavour hydrothermal vents is nearing completion.
305 This expansion will enhance the simultaneous, real-time monitoring in the Mothra and Main Endeavor
306 vent fields (Figure 3), with new sensors (including additional cameras and instruments for *in situ*

307 hydrothermal fluid chemistry), and the completion of the larger scale seismometer network around the
308 segment with deployments at the Endeavour node on the JdF plate. The extension of the observing
309 system to the Mothra vent field provides biologists with new settings to test hypotheses about the
310 coupling of vent communities to habitat dynamics. Expansion of the observing system began in 2016
311 with the installation of extension optical cables to connect the Endeavour node to the Mothra vent field
312 and a site north of the High Rise field. Installation of new sensors and camera systems began in 2019
313 and are scheduled for completion in 2022. All data are available for download and visualisation through
314 an online query interface linked to the data archive and GIS database (Box 1).

315 During the deployment of the 840 km backbone NEPTUNE cable, a spur cable (with a cable
316 termination assembly) was extended to the Middle Valley hydrothermal area, to the north of the
317 Endeavour Segment (Figure 3). This installation could support future development of a node and
318 instruments to contrast the hydrothermal activity at the sedimented Middle Valley, with the sediment-
319 starved spreading centre at Endeavour. This would also support extension of the network onto the
320 Pacific Plate to the west, and the Sovanco Fracture Zone to the northeast.

321 1.3 Ocean Observatories Initiative (OOI): Regional Cabled Array on Axial Seamount

322 Axial Seamount is the largest and most magmatically active volcano along the JdFR (Kelley et al.,
323 2014, 2016; Smith et al., 2018). It is also the best imaged submarine volcano worldwide, with multiple
324 3D seismic surveys delineating two magma chambers and a series of stacked feeder sills (West et al.,
325 2001; Arnulf et al., 2014, 2018; Carbotte et al., 2020). Repeated high resolution (1 m) bathymetric
326 surveys acquired with deep-sea autonomous vehicles of the caldera and surrounding walls have
327 allowed documentation of the volcanic and hydrothermal geomorphology, and the extent and volume
328 of different volcanic eruptions and of vertical seafloor displacements (e.g., Caress et al., 2012; Clague
329 et al., 2017).

330 The OOI marine infrastructure was designed and built to meet science requirements developed through
331 community workshops, which identified broad-ranging critical ocean science questions requiring
332 comprehensive and sustained (up to ~25 years) ocean observing infrastructure, enabling examination
333 of processes at multiple spatial (ocean basin to tidal basin) and temporal (short-term, stochastic events
334 and large-scale decadal cycles) scales. The Axial observatory is part of the RCA (Box 1; Figure 4). A
335 525 km-long, high power (10 kV) and bandwidth (10 gb/s) submarine fiber optic cable provides power
336 and two-way communication from Pacific City, Oregon, to the volcano. In 2014, the RCA observatory
337 was installed at the base and within the caldera of Axial Seamount. Axial Caldera currently hosts a
338 diverse array of 23 core seafloor instruments (Figure 4). In 2016, following commissioning of the RCA,
339 NSF opened the door to Principal Investigators (PI) to add infrastructure onto the RCA through funding
340 outside of OOI. Within Axial Caldera, nine PI instruments are now on the cable and there are three
341 uncabled instruments. Twenty additional cabled and uncabled instruments are funded for installation
342 in the caldera and on its walls. Infrastructure located in Axial Caldera is focused at four sites: The
343 ASHES and International District Hydrothermal Fields, and the Central Caldera and Eastern Caldera
344 sites focused on geophysical investigations (Figure 4).

345 The geophysical instruments positioned within the caldera that monitor seismic and volcanic activity
346 – including explosive events (Wilcock et al., 2016; Caplan-Auerbach et al., 2017; Chadwick et al.,
347 2022) – include five short-period seismometers, in addition to two pairs of broadband seismometers
348 and low-frequency hydrophones. Four bottom pressure-tilt instruments situated in the Central and
349 Eastern Caldera regions, and the ASHES and International District vent fields, monitor, in real time,
350 changes in seafloor elevation/tilt associated with the inflation/deflation of the magma chamber and are
351 being used for forecast future volcanic eruptions (Box 1). Also distributed within the caldera are three
352 CTDs (Central Caldera, Eastern Caldera, and ASHES) to monitor hydrothermal fluid interactions with
353 crustal and seafloor processes (e.g., diking-eruptive events).

354 At the ASHES vent field (Figure 4), a 3D-thermistor array and a collocated osmotic-based fluid
355 sampler provide temperature distribution in a diffuse flow site along with physical samples for shore-
356 based chemical analysis of emanating fluids. A HD video camera focused on the 4 m tall actively
357 venting ‘Mushroom’ edifice provides real-time streaming imagery every 3 hrs covering the entire
358 edifice to monitor changes in chimney development and biological communities colonizing the edifice
359 and surrounding seafloor (Box 1). The site also hosts a COVIS multibeam sonar system focused on the
360 4 m tall edifice Inferno and surrounding diffuse flow sites, and thermistor arrays within diffuse flow.

361 At the International District vent field (Figure 4), an instrument suite is used for real-time monitoring
362 of temperatures and fluid chemistry of hydrothermal vents and collecting fluids and DNA for later
363 shore-based chemical analyses (Kelley et al., 2014). A high-temperature, resistivity, and redox
364 potential probe (TRHPH/BARS) is installed in the Escargot hydrothermal chimney to examine boiling
365 processes. A high-temperature probe (THSPH) that measures H₂, H₂S, and pH is installed in the Diva
366 hydrothermal chimney. Instruments positioned at the Tiny Towers site include a mass spectrometer to
367 measure dissolved gases in the venting fluids, coupled microbial DNA (PPS) and hydrothermal fluid
368 (RAS) samplers with temperature co-registered vent fluid temperature. These instruments’ intakes are
369 collocated in a ‘vent cap’ positioned atop emanating diffuse flow thereby providing real-time
370 monitoring of dissolved gas concentrations in hydrothermal fluids while simultaneously allowing for
371 collection of microbial DNA and fluids for post-recovery metagenomic and chemical analyses. A
372 digital still camera at this site allows monitoring of the hydrothermal activity, changes in biological
373 communities, and condition of the previous instrument installations. A 3D single point current meter
374 provides real-time monitoring of currents near the seafloor. A second nearby bare-rock site, includes a
375 short-period seismometer, current meter, and bottom pressure tilt instrument. This site is the focus of
376 an International Ocean Discovery Program proposal to include an array of holes with cabled CORKED

377 observatories to examine the deep biosphere, crustal hydrogeology, and magma injection and crustal
378 deformation (Huber et al., 2021).

379 The Central Caldera site has become a key site for testing of geodetic instruments to examine seafloor
380 deformation with follow-on applications to monitoring the Cascadia Subduction Zone. Here, the co-
381 registration of two different kinds of self-calibrating pressure sensors and a “flipping” tilt meter along-
382 side Core OOI instrumentation allows cross referencing of these new technologies. Also hosted at this
383 site is a newly developed ADCP to image the entire ~ 1500 m of water column. Finally, two state-of-
384 the-art instrumented cabled profiling moorings at the base of the seamount provide environmental
385 measurements from ~ 2600 m to 125 m to 5 m beneath the ocean’s surface. In concert, the two moorings
386 host a diverse suite of 24 instruments, provide insight into internal waves and may capture the
387 formation-evolution of the next megaplume (Kelley et al., 2016; Devine et al., 2020).

388 2 **Ten years of observatory research at vents**

389 Understanding the functioning and dynamics of vent ecosystems requires resolving the range of scales
390 at which processes operate. The three seafloor observatories have supported a decade of
391 multidisciplinary research at hydrothermal environments hosted in a basaltic upper crust, and overlying
392 magma chambers at varying depths. The data and follow-on research have enabled significant
393 advancements in our understanding of processes occurring at multiple scales from the sub-seafloor to
394 the water column. These magmatic sites are visited every year as part of the maintenance cruises
395 allowing for systematic surveys and sampling and integration of the different scales of biological and
396 environmental data. The following section summarises results obtained using seafloor observatories
397 during the last 10 years, based on both time-series analyses and modelling.

398 2.1 **Crustal processes**

399 While MOR's represent the world's largest hydrothermal-volcanic system, we still lack an in-depth
400 understanding of the complex interplay of magmatic, tectonic, and hydrothermal processes that take
401 place along the ~65,000 km of ridge axis. Comprehensive databases acquired in recent decades show
402 that hydrothermal fluids expelled at vents along magmatically robust sections of a MOR have a large
403 spatial and temporal variability in exit fluid velocity, temperature, and chlorinity (e.g., Scheirer et al.,
404 2006; Larson et al., 2007; Sohn, 2007; Sarrazin et al., 2009; Barreyre et al., 2014b; Germanovich et
405 al., 2015; Xu et al., 2017). Monitoring seafloor deformation and seismic activity at active volcanoes
406 provided insights into magma movement at depth (Chadwick et al., 2016; Nooner and Chadwick, 2016;
407 Wilcock et al., 2016) and into the location and time-evolution of the domain of hydrothermal heat
408 extraction (Tolstoy et al., 2006; Crawford et al., 2013; Wilcock et al., 2016). The RCA infrastructure,
409 online for the Axial 2015 eruption, captured the first real-time cabled observatory data of the timing,
410 location, dynamics and volume of eruption-related magma movements, eruptive explosions and
411 fissuring, and egress of fluids out of the subseafloor (Chadwick et al., 2016; Wilcock et al., 2016;
412 Caplan-Auerbach et al., 2017; Spietz et al., 2018). Additionally, an eruption response has been
413 observed in high-temperature vents at Axial instrumented with data logging temperature probes. After
414 the 2011 eruption, temperatures in some high-temperature vents adjacent to the eruptive area dropped
415 to just over 100°C, perhaps as a consequence of rapid recharge of cold seawater that replenished warm
416 fluids injected into the caldera and formation of spectacular snow blowers from which issued microbes
417 and microbial material flowing from the subseafloor (Kelley et al., 2014).

418 Being on a slow spreading ridge, the Lucky Strike volcano has a significantly lower melt flux than the
419 JdF ridge vent areas, resulting in less frequent eruptions (Rubin et al., 2012). Monitoring full cycles of
420 volcanic activity at a slow spreading ridge is beyond human time scales. Indications for recent
421 magmatic activity at the Lucky Strike volcano include an earthquake swarm interpreted as due to a

422 dike injection in 2001 (Dziak et al., 2004), and increased CO₂ content in the vent fluids in 2008 (Pester
423 et al., 2012) and 2010 (Chavagnac et al., 2015; Rommevaux et al., 2019).

424 One of the most critical crustal accretion variables, and one that is commonly poorly constrained, is
425 indeed permeability, as it is a major control on fluid flow below the seafloor. The use of the natural
426 forcing from ocean tides to constrain crustal dynamics and permeability structure of MOR
427 hydrothermal fields brought new insights in the study of hydrothermal circulation processes and fluxes
428 in the oceanic crust (e.g., Crone and Wilcock, 2005; Barreyre et al., 2018). Using a time series of fluid
429 temperature data, differences in phase lags between tides and the thermal response of exit fluids were
430 shown to correspond to variations in the shallow crustal permeability structure and therefore in mass
431 and heat fluxes (Barreyre et al., 2018). Similar approaches also showed a strong control of shallow
432 spatial variations in permeability on diffuse exit fluids at the ASHES vent field and Lucky Strike (e.g.,
433 Mittelstaedt et al., 2016). Recent studies have investigated the feasibility of using models of the
434 poroelastic response to tidal loading manifested in exit-fluid velocity and temperature records to obtain
435 shallow crustal permeability constraints below MOR vent fields (e.g., Jupp and Schultz, 2004; Crone
436 and Wilcock, 2005; Barreyre et al., 2014a, 2018; Barreyre and Sohn, 2016). High-resolution seismic
437 studies provide additional constraints into possible subseafloor heterogeneities and related fluid paths
438 between the axial magma chamber and the seafloor (e.g., Marjanović et al., 2019).

439 While these data sets pertaining to seismic and fluid flow studies provide valuable constraints for
440 coupled geodynamic-hydrothermal models (e.g., Theissen-Krah et al., 2016), these snapshots of the
441 “current state” at a specific location are difficult to interpret in the context of a dynamically evolving
442 hydrothermal and magmatic system. At the same time, numerical models have evolved in recent years
443 and can now handle more realistic thermodynamic fluid properties and two-phase flow phenomena
444 (Coumou et al., 2009; Lewis and Lowell, 2009; Afanasyev et al., 2018; Vehling et al., 2021). An
445 outstanding strength of numerical forward models is their ability to establish process-based causal links

446 between different observations and data sets, including spatial and temporal dependencies. Time series
447 data sets from recurring expeditions to the same geographical location or, ideally, permanent
448 installations, are extremely valuable and enable the stringent design and calibration of models and
449 facilitate non-ambiguous interpretation of transient model results. The combination of state-of-the-art
450 numerical modelling techniques and data from (nearly) continuous monitoring will enhance our
451 understanding of processes and mechanisms taking place at inaccessible locations inside the Earth.

452 **2.2 Interface and biological response**

453 Integrated studies at the interface of the subseafloor and the water column have contributed to a better
454 understanding of links between geological, geochemical and biological processes. At the Lucky Strike
455 seafloor, the hydrothermal fluid fluxes of 14 monitored vents (Leleu, 2017) have immediate impact on
456 trace element dispersion within the hydrosphere and microbial development. For example, high fluid
457 CO₂ contents, induced by replenishment of the magmatic chamber at depth stimulate the thriving of
458 thermophilic and anaerobic Archaea and Bacteria (Archaeoplobales, Nautiliales and
459 Nitratiruptoraceae) (Rommevaux et al., 2019). In addition, the progressive mixing of end-member
460 hydrothermal fluid and surrounding seawater leads to the formation of hydrothermally-derived
461 minerals, in particular sulfate-bearing minerals (anhydrite and barite) which control dissolved rare
462 earth element fluxes and the Nd isotope signature of the hydrothermal plume (Chavagnac et al., 2018b).
463 At Axial Seamount, the past three eruptions provide some insights into subseafloor hydrothermal
464 processes because these eruptions have significantly affected crustal hydrology, fluid geochemistry,
465 and microbial communities. This is exemplified by the development of low-temperature, diffuse
466 snowblower vents formed within ~50 m of eruptive fissures by subsurface circulation of warm,
467 volatile-rich fluids, which results in microbial growth and discharge, indicating a near-instantaneous
468 increase in heat and mass fluxes, followed by exponential decay (Cann et al., 1997; Butterfield et al.,
469 2004; Chadwick et al., 2013; Meyer et al., 2013; Nooner and Chadwick, 2016). Diffuse vent fluids at

470 Axial are hotspots of primary production in the deep ocean, while also providing access points to infer
471 microbial and geochemical processes in the subseafloor (e.g., Butterfield et al., 2004; Huber et al.,
472 2007; Fortunato and Huber, 2016; Olins et al., 2017; Fortunato et al., 2018). Time-series microbial and
473 geochemical studies of these fluids at Axial began in 1998, shortly after the volcano erupted. These
474 multi-year studies at Axial showed that individual vent sites maintained microbial communities and
475 specific populations, with spatially distinct communities and activities mediated by both endemic and
476 unique groups at each site (Opatkiewicz et al., 2009; Fortunato et al., 2018). Such results, combined
477 with cultivation experiments and modelling efforts, suggest that the type and quantity of subseafloor
478 microbes beneath particular vents is controlled by a combination of geochemistry and local geology at
479 individual sites, leading to spatially and temporally stable fluid paths that allow for the persistence of
480 distinct subseafloor microbial communities (Opatkiewicz et al., 2009; Fortunato et al., 2018; Stewart
481 et al., 2019).

482 In the mixing zone, recurrent *in situ* sampling with filtration and analysis during maintenance cruises
483 allowed the investigation of the dissolved and particulate partitioning of metals in the early buoyant
484 plume (4–150°C) of smokers at Lucky Strike (Cotte et al., 2020). Noted spatial variability of the
485 chemical composition (Fe and Cu) of the buoyant plume throughout the vent field was limited in the
486 warmest part of the plume. Even though metal partitioning was strongly affected by different
487 precipitation and oxidation processes, hydrothermal iron was almost completely preserved (> 90%) in
488 the dissolved fraction along the mixing gradient (Laës-Huon et al., 2016; Waeles et al., 2017; Cotte et
489 al., 2018). A long-term *in situ* study of reactive iron (CHEMINI) in a diffuse vent at the base of the
490 Tour Eiffel active edifice showed that reactive iron stabilization over time prevented precipitation and
491 could enhance iron availability to the local biological community structure (Laës-Huon et al., 2016).
492 These studies highlight that metal stabilization processes allow the export of hydrothermally sourced
493 iron and copper into the deep ocean.

494 Observatory studies of biological responses to habitat variability combine sensor data on habitat
495 conditions with imagery that documents species presence/absence and behaviour. The few long-term
496 studies at the assemblage-scale have shown faunal communities to be relatively stable in relation to
497 baseline environmental variability (Sarrazin et al., 2014). At the organism-scale, analyses of imagery
498 have highlighted species behavioural responses that correlate with tides and surface storms, both on
499 the MAR and the JdFR (Cuvelier et al., 2014b, 2017; Lee et al., 2015; Lelièvre et al., 2017; Mat et al.,
500 2020). Deep current inversions in response to tides affect the mixing of hydrothermal fluid inputs with
501 surrounding seawater, thus modifying local environmental conditions in vent habitats. Symbiotic vent
502 mussels at Lucky Strike open and close, and tubeworms from MEF extract and retract, following the
503 tidal cycle, probably in response to their physiological/endosymbiont needs (Cuvelier et al., 2014b;
504 Mat et al., 2020). On the JdFR, non-symbiotic species also appear to respond to environmental
505 variability by adjusting their position and behaviour, possibly as a trade-off between resource
506 availability/predation and physiological tolerance (Lelièvre et al., 2017). Daily recording of video
507 imagery has also proved to be a good tool for characterising the behaviour and interactions of species
508 that could not otherwise be reared in aquaria under controlled conditions (Matabos et al., 2015). It
509 remains a challenge to relate micro environmental changes to life history strategies and physiological
510 tolerances. Combining imagery with multi-variable sensor data should improve our ability to relate
511 recruitment to local environmental cues and broader oceanographic drivers, and consequently better
512 understand regional reproductive patterns.

513 Maintenance cruises offer opportunities to sample and describe natural communities (e.g., Sarrazin et
514 al., 2015, 2020; Husson et al., 2017; Lelièvre et al., 2018) and perform manipulative and colonizing
515 experiments over time. Extensive experiments conducted during maintenance cruises (e.g., Cannat and
516 Sarradin, 2010) have produced key insights into the biodiversity, functional diversity, and ecology of
517 MAR hydrothermal communities. These include (re-)colonization processes and relationships between

518 vent and cognate communities along a vent gradient and on different types of substrata (Cuvelier et al.,
519 2014a; Zeppilli et al., 2015; Plum et al., 2016; Baldrighi et al., 2018; Alfaro-Lucas et al., 2020; Cowart
520 et al., 2020; Marticorena et al., 2021). Biological samples have contributed to increasing basic
521 knowledge of species biology (Husson et al., 2017; Marticorena et al., 2020), trophic interactions
522 (Lelièvre et al., 2018; Portail et al., 2018; Zeppilli et al., 2019), biological rhythms (Mat et al., 2020)
523 and physiology (Husson et al., 2018), leading to a growing understand of vent faunal functional traits
524 (Chapman et al., 2019; Alfaro-Lucas et al., 2020; Murdock et al., 2021). Post-eruption succession
525 patterns have been studied at Axial, particularly following the 1998 eruption, from repeated visits both
526 pre-eruption as well as 7-, 18-, 30-, and 42-months post-eruption (Marcus et al., 2009).

527 2.3 Water column: deep circulation, fluid dispersal and connectivity

528 The ocean dynamics above MOR systems and specifically around vents are complex. Broadly, they
529 feature three families of processes with their own phenomenology and impacts. First, the interaction
530 of oscillating tidal currents with the rough seafloor topography generates internal waves at tidal
531 frequencies called internal tides. These waves are unstable and eventually break close to their
532 generation sites, provoking irreversible vertical mixing (St. Laurent and Garrett, 2002; Vic et al.,
533 2018a). Although the astronomical (tidal) forcing is now easily predicted and appears to be remarkably
534 in-phase with the local tidal energy density over ridges (Vic et al., 2021), the spatio-temporal variability
535 of mixing remains poorly quantified, due to sparse data. Studies conducted these last decades
536 highlighted key processes associated with internal tides, including their interactions with seafloor
537 topography and background currents, leading to dynamical modifications of the mean state of the deep
538 ocean (Thomson et al., 1990, 2003; Lahaye et al., 2019, 2020).

539 Second, low-frequency currents drag on the valley walls and destabilise, generating small-scale
540 swirling structures called submesoscale coherent vortices (SCVs, Vic et al., 2018b). SCVs can feature
541 lifespans of many months and travel thousands of kilometres (recent survey in McCoy et al., 2020).

542 Thus, they are effective at trapping and spreading deep-ocean material to the ocean interior (e.g., Bower
543 et al., 2013; Vic et al., 2018b). Observations of SCVs are very sparse in general and even more
544 specifically at depths of MOR.

545 Third, hydrothermal venting introduces a heat flux that generates mixing of vent fluids with ambient
546 waters near the seabed. In addition, hydrothermal plumes that form over the vent field contain chemical
547 constituents, larvae and microbes. These plumes have buoyant and neutrally-buoyant components.
548 Buoyant plumes rise into the water column, entraining surrounding seawater, until they achieve neutral
549 buoyancy through dilution and cooling. Near the bottom, this upward buoyancy flux drives an inflow
550 towards the vent field and is effective in the retention of plankton (Thomson et al., 2003).
551 Hydrothermal plumes can also carry plankton up into the ambient oceanic currents to be dispersed in
552 along the axis, or off-axis to possibly a less hospitable deep-sea environment. In contrast, organisms
553 with the ability to swim vertically or alter their density can utilise these dynamics and larvae have been
554 shown to actively alter their positions to stay near their preferred environment (Mullineaux et al., 2013).
555 The influence of hydrothermal venting on the chemistry of the deep-sea near the Endeavour segment
556 has been investigated by Coogan et al. (2017). Using tow-yo hydrocasts, sediment traps and push cores
557 they revealed that the plume heat and particulate anomalies indicate a half contribution from the
558 particle-poor diffuse flow and half from (particle rich) high-temperature venting. Coogan et al. (2017)
559 also found that less than 2% of all measured elements accumulate on the seafloor within 1.5
560 km of the individual vent fields. This implies that most of the chemical flux is transported significant
561 distances away. The variability of plume position at higher frequencies is regulated by the local
562 oscillatory currents in the inertial, tidal and weather bands (Xu and Di Iorio, 2012) and the periodicity
563 of the immediate fallout from the plume, in addition to the direct effects of the local currents, appears
564 to have an effect on the benthic ecology (Lelièvre et al., 2017). Above the neutrally buoyant plume,
565 towed nets along with acoustical methods identified a deep scattering layer associated with the

566 aggregation of zooplankton (e.g., Burd and Thomson, 2012). This deep scattering layer has been shown
567 to have a complex seasonal and higher frequency (20-40d) variability likely due to a combination of
568 both ontogenetic migration and dynamic advective processes (Burd and Thomson, 2019). In the rift
569 valley of the northern MAR, the compilation of different *in situ* data acquired by CTD-LADCP casts
570 and mooring deployments during repeated visits (Lahaye et al., 2019), combined with modelling
571 studies (Vic et al., 2018b) has revealed consistent north-eastward along-valley currents below 2000 m
572 at sub-inertial time scales. Current variability, dominated by slow time scales (weeks), favours the
573 northward dispersion of tracers. Over the Endeavour segment of the JdFR, data from current meters
574 and tracking of the neutrally buoyant plume, indicate that the long-term mean current tends to the
575 southwest (Thomson et al., 2003; Coogan et al., 2017), with observations suggesting it has been steady
576 for decades.

577 Integrating ecological/biogeochemical/physical data with modelling approaches can help address
578 dispersion and connectivity questions (e.g., Owen and Sponaugle, 2009; Artigue et al., 2021). In coastal
579 studies, sub-kilometre-grid, primitive-equation models have been used to perform Lagrangian
580 dispersion since the 2000's ('reef-scale' models; Werner et al., 2007). No such method has been used
581 in deep-ocean studies until recently. Mesoscale-resolving models (Young et al., 2012; Breusing et al.,
582 2016) and submesoscale-permitting models (Bracco et al., 2016; Cardona et al., 2016; Mitarai et al.,
583 2016; Vic et al., 2018b) have been employed to study connectivity between benthic communities at
584 depths below 1000 m, resulting in improved realism of flow-topography interactions in many ways
585 (Bracco et al., 2016; Vic et al., 2018b). Notably, tidal currents, hitherto absent from high-resolution
586 regional models, are found to increase the vertical spreading of particles and help them cross
587 topographic barriers (Vic et al., 2018b).

588 **3 Towards a coordinated understanding of MOR hydrothermal vents and their ecosystems**

589 The IMOVE working group seeks to refine common process-oriented research questions that can be
590 addressed with data in hand, and identifying what is needed to address questions raised by today's
591 societal challenges, in order to help and foster interoperability across vent observatory platforms. The
592 locations of the three observatories permits the study of hydrothermal processes in contrasting
593 environments and settings. Each is representative of different dynamics of seafloor spreading and
594 volcanism, from slow (MAR) to intermediate (JdFR) spreading rates, and the relative importance of
595 tectonic (Endeavour) and volcanic (Lucky Strike, Axial Volcano) processes. They also provide
596 contrasting examples of hydrothermal plume behaviour: with episodic megaplume generation during
597 eruptions at Axial volcano, (e.g., Palmer and Ernst, 1998; Baker et al., 2019) a continuously present
598 intense plume generated by multiple hydrothermal vents along the axis of the Endeavour segment
599 (Thomson et al., 2003; Kelley et al., 2012), whereas megaplume events were yet never detected at
600 Lucky Strike. Early international workshops in the 90s and 2000s (National Research Council, 2000)
601 set the scene for a globally-coordinated design of seafloor observatories. Following this collaborative
602 effort, programmatic and funding realities have resulted in each observatory having its own
603 infrastructure design, research goals, and specific scientific questions (Barnes and Tunnicliffe, 2008;
604 Favali and Beranzoli, 2009; Cannat et al., 2011). Since their deployment, large volumes of data have
605 been acquired from all three current observatories, creating opportunities for studies that extend across
606 locations. The first workshop (IMOVE, 2019) defined priority themes and vent processes, establishing
607 a basis for setting common scientific questions. This framework was then used to structure the science-
608 based workshop at which participants developed a set of scientific questions and related societal
609 challenges. This provided a basis for further exploiting existing data, and for identifying EOVs and
610 Essential Biodiversity Variables (EBVs) that need to be measured to improve our understanding of
611 hydrothermal processes (see Section 4).

612 Processes of particular interest include fluid flow geometry, fluxes (heat, mass, chemical), their
613 variability (i.e. periodic and episodic) and how they partition, local oceanographic currents and
614 associated biological responses (Figure 5). These processes can be divided in three domains: the
615 subseafloor, the interface at the ocean floor, and the water column. In the subseafloor, ground
616 deformation, heat transfer, fluid-rock interactions affect fluid flow geometry, fluid composition and
617 crustal stress and permeability, fluid residence times and recharge, and microbial community
618 composition. At the seafloor interface, where the fluid meets the cold background seawater, thermo-
619 chemical exchanges and mixing impact fluid flow characteristics, microbial and vent species
620 distributions and biomass, and energy flow (e.g., carbon flux) (Le Bris et al., 2019). Finally, in the
621 water column, oceanographic forcing, including currents, tides and their interactions with the local
622 topography, drives plume dispersal, hydrothermal fluxes and exports to the ocean, faunal distribution,
623 behaviour and larval dispersal, and influences species connectivity (Table 1, Figure 5). The
624 multidisciplinary approach enabled by observatories through the concomitant acquisition of
625 environmental and biological variables provides a unique opportunity to integrate this wide range of
626 processes and assess mechanisms driving vent ecosystem function and temporal trajectories. Four key,
627 integrative questions emerged from the two IMOVE workshops:

- 628 • How does hydrothermal circulation and associated heat and matter fluxes respond to crustal
629 and oceanographic forces at varying temporal scales?
- 630 • How does the interaction between hydrothermal circulation and shallow mixing with seawater
631 control fluid chemistry, flux and temperature in the mixing zone where microbial communities
632 and vent fauna develop?
- 633 • How do the hydrothermal biological communities respond to changes in environmental
634 conditions?

635 • How do vent fluxes, productivity, and communities influence the surrounding deep-sea
636 ecosystems and vice versa?

637 This fundamental knowledge is prerequisite to evaluating faunal responses to anthropogenic
638 disturbances, elaborating conservation strategies, and addressing the societal challenges that mid-ocean
639 ridge systems are increasingly facing.

640 *Anthropogenic challenges and the scientific questions to address them*

641 The three main current or foreseeable anthropogenic challenges to deep-sea vent environments are
642 climate change, pollution (e.g., microplastics, persistent organic pollutants) and deep-sea mining.
643 Fisheries are not discussed since most MOR vents are at (currently) non-fishable depths and do not
644 host significant standing stocks of fish. Observatories contribute to enhancing our fundamental
645 knowledge of ecosystem function, and yearly visits on site offer opportunities for seafloor experiments
646 (Alfaro-Lucas et al., 2020; Marticorena et al., 2021) and collection of biological samples to increase
647 our knowledge of species biology and ecology (e.g., Husson et al., 2017; Lelièvre et al., 2018; Murdock
648 et al., 2021). Directly assessing the potential impacts of deep-sea mining will require similar
649 experimental and sampling approaches. Regular sampling is also needed to characterise the abundance
650 and composition of microplastics in these environments and understand how local and regional
651 hydrography impacts their distribution. Standardised protocols should be defined and shared in order
652 to ensure cross-comparison between observatories and the detection of long-term trends. Future
653 research will also contribute to a new, more environmentally responsible relationship between
654 terrestrial society and the deep sea, in the form of regulations, best practices, environmental ethic, and
655 societal awareness. Section 6 discusses these new research avenues and how they can benefit from
656 observatory infrastructure and associated maintenance cruises.

657 4 Essential variables and common best practices for MOR vent observatories

658 The first workshop (IMOVE, 2019) identified all variables currently measured or acquired by the
659 different existing sensors at each established observatory. Each variable was then translated into an
660 observable belonging to a biological, geophysical or geochemical domain (Table 2). As an example, a
661 video camera (the sensor) allows counting the visible species (variable) to measure species distribution
662 and abundance (observable) in the biology (domain) (Table 2). The final table revealed a number of
663 commonalities among the three observatories highlighting the potential for defining common
664 measurable characteristics. Based on this table and the list of common scientific questions, discussions
665 during the second workshop resulted in a list of EOVs to be monitored across the different
666 observatories. Some of the variables measured are mature EOVs, especially the ones related to physics
667 and geochemistry. The biological related EOVs are not yet mature, most of the seabed ones are still at
668 the merging phase, and the specificity of the different environments, require standardisation and
669 calibration (e.g., EOVs body size, or biomass or % cover, which are based on imagery, need a
670 standardisation towards automation, and calibration of surface observable, calibration size, weight,
671 etc). This list was built in light of work previously conducted by international networks including The
672 Group on Earth Observations Biodiversity Observation Network (GEO BON; Pereira et al., 2013) and
673 the Deep Ocean Observing Strategy (DOOS; Levin et al., 2019). A number of EOVs recommended by
674 GOOS and DOOS were considered as observables to measure at vents in the context of seafloor
675 observatories and associated maintenance cruises. Table 3 reports these variables that can be measured
676 and provides new ones to be considered when conducting observations at vents. Box 2 summarises
677 recommendations issued during the second workshop.

678 The DOOS demonstration projects in the Azores and NE Pacific offer opportunities to feature
679 hydrothermal vents within the concept of integrated observing (Levin et al., 2019). The linkage of
680 multiple platforms and sensors operation both inside (observatories, repeat visits) and outside but
681 proximate to the vents in these regions (e.g., Argo floats, Ocean Sites moorings, GoSHIP tracks, Ocean

682 exploration activities, gliders), can contribute to a powerful multidimensional understanding in space
683 and time of the external forces affecting vent communities and the influence of these ecosystems on
684 surrounding environments.

685 **4.1 Monitoring long-term changes in the context of climate change**

686 By enabling sub-daily to multidecadal monitoring, seafloor observatories harbour a great potential to
687 assess long-term changes in the context of climate change. The deep-sea is expected to lose oxygen,
688 increase in temperature and change in pH (Levin and Le Bris, 2015; Sweetman et al., 2017; Levin et
689 al., 2020). One big common question that the scientific community can tackle using an integrated
690 approach is the impact of water column and subseafloor processes on global climate, not only through
691 the emission of gases like CH₄ and CO₂, which in general are negligible, but also as organic carbon
692 producers, CO₂ consumers, and O₂ consumption (Le Bris et al., 2019).

693 Processes identified during the first workshop that should be considered when addressing climate
694 change are the carbon cycle and geochemical and thermal fluxes impacts on the ocean (Table 1). The
695 next paragraphs summarise the recommendations issued during the second workshop.

696 In an environment characterised by high environmental heterogeneity over limited spatial scales, it
697 appears essential to monitor background seawater characteristics. Although basic, this type of data is
698 not routinely acquired today at all sites. EMSO developed, in the framework of the European
699 Commission H2020 EMSODev project (Grant Agreement 676555), the EGIM, designed to
700 continuously measure long-term series of key variables (Lantéri et al., 2022). EGIM is originally
701 equipped with a CTD, ADCP, oxygen sensor, pressure temperature, turbidity meter and hydrophone
702 to measure conductivity, precise pressure, dissolved O₂, turbidity, passive acoustics, and ocean currents
703 but can host additional sensors. The module has been successfully deployed on a number of EMSO-
704 ERIC observatories and can actively contribute to the international effort undertaken by the Global

705 Ocean Observing System on Essential Ocean Variables (Levin et al., 2019; Sloyan et al., 2019). A first
706 recommendation is thus to deploy an EGIM-like module at each observatory site, away from vent
707 influence. This will require the definition of standardised instruments and calibration protocols and the
708 development of new sensors, in particular for long-term pH measurements.

709 By measuring water mass circulation, dissolved oxygen concentrations, temperature, POC fluxes and
710 chemical and heat exchanges, the vent observatory community can contribute to address some of the
711 key questions raised by DOOS (Levin et al., 2019). However, because yearly maintenance involves
712 recovery and redeployment of platforms, change in sensors and their potential location, some common
713 good practices must be adopted to help make sense of data acquired, and are supported by existing Best
714 Practices guides (Coppola et al., 2016). Groundtruthing measurements and sampling should be
715 performed whenever possible and at every maintenance cruise. This includes oxygen calibration with
716 Winkler measurements, characterising seawater particulate load by sampling bottom water, *in situ*
717 temperature measurements using high resolution, reliable and properly calibrated temperature sensors.

718 The nature of the coupling of water column processes to benthic processes is critical to understanding
719 the ocean's carbon cycle and its link to climate change and biodiversity (Cathalot et al., 2021 and
720 reference therein). Long term observations of benthic-pelagic coupling can address vent stimulation of
721 photosynthetic productivity or dark carbon fixation, influences on microbes, pelagic larvae and adults
722 of vent and non-vent species, and alteration of food supply for mixotrophic vent species (Levin et al.,
723 2016). These have relevance for the biological pump and opportunities for carbon sequestration. Newly
724 developed seafloor rovers such as RB-II or other benthic crawlers that have potential to track carbon
725 inputs, remineralisation rates and oxygen levels can associate with cabled observatories to obtain power
726 and transmit data in association with other observatory monitoring (Smith et al., 2021).

727 **4.2 Crustal and surface processes**

728 During the first IMOVE workshop, several processes were identified as important when addressing
729 subsurface processes: seafloor dynamics including compliance and ground deformation, plumbing
730 system and fluid flow geometry, subsurface characterization, crustal geothermal signature, subseafloor
731 microbial communities, and forcing of sub-seafloor processes on seafloor systems (Figure 5, Table 1).

732 Similarly, the first workshop identified several processes as important when addressing fluid fluxes
733 and heat exchanges at the interface: forcing of sub-seafloor processes on seafloor systems, chemical
734 signature, dynamic coupling of diffuse/focused venting, crustal plumbing system and fluid flow
735 geometry, phase separation, and sub-surface and post-exit fluid mixing (Figure 5, Table 1).

736 During the workshop, several approaches were proposed to better constrain models of fluid circulation
737 and characterise fluid flux dynamics on a local scale. Repeat mapping of smoker vents at certain sites
738 (e.g., Barreyre et al., 2012; Girard et al., 2020) can help better characterise the long-term changes and
739 stability of vent circulation in different ridge settings. Such repeat mapping could occur during
740 maintenance cruises by a submersible or by future drones linked to connected or autonomous benthic
741 docking stations allowing power recharge and data transfer (see section 5). Taking this standardised
742 approach to fluid flow characterization will foster comparison among different ridge systems and help
743 better understand how temporal and spatial changes in the distribution of hydrothermal venting impacts
744 ecosystem stability and species' adaptation to their environment (e.g., reproductive biology, growth,
745 mobility). A benefit of the above approach is the ease with which it could be extended to other systems
746 where repeated visits allow for temporal monitoring (e.g., East Pacific Rise, Lau Basin, Guaymas
747 Basin).

748 As part of repeated monitoring efforts, the use of non-invasive video sequence analyses could be key
749 for volume, heat, and chemical flux estimations at smoker vents. Using pixel-based correlation methods
750 (Particle Image Velocimetry or Diffuse Fluid Velocimetry; Crone et al., 2010; Mittelstaedt et al., 2010,
751 2012; Escartín et al., 2015; Puzenat et al., 2021), the flow of high-temperature and low-temperature

752 fluids can be estimated with reasonable accuracy and in relatively short image capture sequences. To
753 allow uniform, inter-comparable results using these techniques requires a common protocol with
754 guidelines for image acquisition (camera distance; use of chessboard for image calibration; Escartin et
755 al., 2013; minimum image resolution and frame rate guidelines), the implementation of a user-friendly
756 computer program to process images as part of routine maintenance visits to vent sites, and sufficiently
757 stable imaging platforms to avoid image motion related to currents and/or vehicle motions. To
758 constrain heat and chemical fluxes, the above techniques for estimating flow rates should be coupled
759 with simultaneous exit-temperature and near-simultaneous fluid sampling data.

760 4.3 Biological responses to hydrothermal forcing

761 Processes identified during the first workshop that should be considered when addressing biological
762 responses at the interface are: chemical signature, dynamic coupling of diffuse/focused venting,
763 mixing, recruitment dynamics, energy flow and fluxes (Figure 5, Table 2).

764 A number of common variables were identified as potential ridge EBVs and were discussed in relation
765 to the work already done by Significant Ecological Components (SECs, DFO, 2006), DOOS (Levin et
766 al., 2019) and GEO BON (Pereira et al., 2013). Variables that can contribute to the ones already defined
767 or proposed by GOOS and DOOS respectively, are presented in Table 3, and new ones are proposed
768 in the context of ridge monitoring. Repeated visits and cameras deployed on the seafloor provide
769 information on species presence/absence, faunal abundance in relation to oceanographic variables.
770 However, because it is not possible to generalise fixed-point observations to regional scale, routine
771 transects should be conducted during cruises when possible to extend the spatial extent of observations.
772 Protocols should be standardised and shared to enable large-scale comparisons and should include the
773 use of a common real-time dive logging strategies and terminology (i.e. annotation of fauna, geological
774 or chemical features, litter) (Schoening et al., 2020). Alternatively, this acquisition could be achieved
775 by resident drones or AUVs in parallel with chemical and geological features mapping (see section 5).

776 Time-series observations should focus on species and habitats that are indicators of change (e.g.,
777 Sarrazin et al., 2015). Deep pelagic ecosystems represent more than 90% of the biosphere but remain
778 the most unexplored and least understood environment (Webb et al., 2010). Maintenance cruises can
779 contribute to enhancing our knowledge of this ecosystem by routinely recording vertical video transect
780 during the ascent and descent of submersibles, coupled with CTD measurements and discrete water
781 samples.

782 Video imagery collected during observatory maintenance activities is a potentially important and
783 currently undervalued source of information on the spatial distribution and biomass of visible vent and
784 non-vent organisms and on seasonal and inter-annual variability in species abundances and diversity.
785 A structured approach to real-time and post-cruise annotations of video records can greatly increase
786 their usefulness for extraction of biodiversity information. The value of these annotations can be further
787 enhanced by the standardisation of vocabularies and their alignment with recognized terms used by
788 international organisations such as the World Registry of Marine Species (WoRMS). Ocean Networks
789 Canada has recently collaborated with WoRMS and the US National Oceanic and Atmospheric
790 Administration (NOAA) Office of Ocean Exploration & Research (OER) to develop a standardised
791 video annotation system. The SeaTube interface allows users at sea or via telepresence to annotate live
792 video streams, and permits post cruise annotation of ROV video recordings. Annotations may be
793 entered as free-format text or structured annotations adhering to custom or standard taxonomies (such
794 as WoRMS, CMECS, etc.). Ancillary data from both ROV and ship mounted sensors are also displayed
795 in conjunction with the video, all synchronised with the video timestamp (Figure 6). Live links to the
796 WoRMS database while annotating allows for near-real-time validation of species identifications
797 against known geographic distributions, and the flagging of potential new occurrences or identification
798 errors.

799 Finally, maintenance cruises represent unique opportunities for repeated sampling and have enabled a
800 better characterisation of the geological, geochemical and biological settings of vent ecosystems (see
801 section 2). These cruises should be further used to collect opportunistic samples following standardised
802 protocols to monitor microplastics distribution, environmental DNA (eDNA), or other EOVs and
803 pollutants but also to characterise ecosystem function and services (Danovaro et al., 2020). One
804 solution to optimise the acquisition and processing of samples is to involve and offer access to cruises
805 for external researchers which will contribute to fostering a mutualisation of the infrastructures. Such
806 an effort is currently under development within the EMSO-Eric through the establishment of access
807 services including the Transnational Access (TNA) to EMSO ERIC observatories
808 (<https://emso.eu/transnational-access/>).

809 4.4 Water column: deep circulation, fluid dispersal and connectivity

810 Processes identified during the first workshop that should be considered when addressing fluid
811 dispersal and connectivity are: plume characterization and dispersal, turbulent mixing and energy
812 dissipation, forcing of ocean dynamics on seafloor systems, connectivity between vents, seafloor
813 topography, mounds, ridges, and role of ocean circulation on larval and free-living microorganisms
814 dispersal (Table 2).

815 One of the next challenges needed to be addressed in deep-ocean modelling with likely implications
816 for Lagrangian spreading is the representation of the thermal plume dynamics. Due to the lack of
817 sustained measurements in the deep ocean, spatial scale coverage, assessing the realism of numerical
818 models remains arduous. Another challenge is to understand if the mesoscale processes are periodic,
819 or asynchronous, having implications on the connectivity of species, and consequently succession
820 patterns and community resilience. Numerical models of the deep-ocean circulation are now routinely
821 reaching submesoscale-resolving and internal wave-resolving resolutions ($dx < 1$ km). Although the
822 phenomenology of resolved processes is widening, uncovering smaller eddies and turbulent processes,

823 we lack a trustworthy 3-D *in situ* picture to assess the models' performances. A rather low-cost solution
824 to address this limitation would be to deploy an array of moorings equipped with deep T-S sensors and
825 current-meters and distant by ca. 1 km to mimic the scales resolved by numerical models. This would
826 allow the measurement of the gradients of the essential properties of oceanic flows, i.e., velocity and
827 density, and a direct comparison with modelled data.

828 The routine acquisition of EOVs currently not measured on autonomous observing systems requires
829 the development of new technologies and sensors, more particularly for biological and biogeochemical
830 variables that currently require *in situ* sampling. The collection of samples calls for dedicated time
831 during the yearly maintenance cruises which are already demanding in terms of human and operational
832 resources. The group agreed on the need to reduce and optimise maintenance cruises and several
833 solutions made possible by the current technological developments emerged (see section 5).

834

835 5 Ocean Sensing Technology and Future Directions

836 R&D activities on ocean observing sensors is expected to reach USD 128.56 billion by 2025,
837 registering a CAGR of 8.86%, during the period of 2020-2025 (van den Burg et al., 2021). The global
838 underwater drone market integrating these sensors is projected to reach USD 7391 million by 2027,
839 registering a CAGR (i.e. Compouned Annual Growth Rate) of 11.7% (van den Burg et al., 2021). The
840 reason for this growth is the need for precise, reliable, and pervasive sensing technology to measure
841 and follow multiscale spatio-temporal dynamics of ocean physical, geochemical, and biological
842 processes. This technology aims to explore and quantify the role of the ocean and seafloor processes
843 in climate change, in provisioning of rare minerals and unexplored biological resources, and
844 availability of biomass. The future directions on ocean sensors development are within the design of i)
845 novel sensing technology, such as underwater mass spectrometer, eDNA collectors and *in situ*

846 sequencing, ii) energy efficient and/or resilient solutions to minimise battery consumption and/or
847 harvest ocean energy, iii) use of Artificial Intelligence (AI) to reduce energy/data storage by “pre-
848 filtering” data or allow adaptive sampling, and iv) new networking architectures that integrate the
849 sensor networks at the surface, e.g., as described in Aguzzi et al., 2019 and Mariani et al., 2021 with
850 the underwater sensor networks.

851 *Sensing and monitoring platforms*

852 Platforms that integrate ocean sensors and operate over a long time at sea can be fixed, e.g., surface
853 buoys, moorings and landers, or mobile such as Argo floats, crawlers, surface vehicles, gliders and
854 Autonomous Underwater Vehicles (AUV) (Aguzzi et al., 2019; Rountree et al., 2020). These platforms
855 can be cabled with power and data transmission ensured from the shore - but unchangeable location
856 strongly constrains the cable route and price -, or wireless with battery and data storage capabilities
857 dimensioned according to the duration of the foreseen deployment on board the seabed station
858 (Matabos et al., 2016). The future directions on platforms’ development need to address a number of
859 limitations highlighted through the experience acquired over a decade of operation (also see Rountree
860 et al., 2020): i) The operational cost is high, partly because underwater vehicles are required for
861 maintenance operation to place the sensor with precision and perform underwater connection; ii) the
862 time between the maintenance operations is limited due to requirement for sensor calibration and, in
863 case of wireless system, for energy pack and data storage replacement ; iii) the spatial coverage is
864 limited to the close surrounding of the seabed station ; iv) new regulation will urge for new deployment
865 processes with low environmental footprint; v) a larger number and variety of sensors are fundamental
866 for multidisciplinary approaches and the amount of energy and volume of data storage needed keeps
867 increasing.

868 These limitations call for technological and operational breakthrough, and the future trends in fixed-
869 point long-term observation are central to developments going on in the field (Figure 7). First,
870 decreasing operational cost requires combining various efforts to reduce the time and means required
871 for maintenance operation at sea. In terms of means, this can be achieved by improving the global
872 robustness of the system to insure the endurance to meteorological and other heavy environmental
873 conditions. Surface buoys relaying the information to the shore, sensitive to storms, can be replaced by
874 autonomous surface vehicle patrolling to recover the data weather permitting. The development of
875 submarine tools specialised and optimised for deployment and recovery of systems could carry out the
876 maintenance from a small ship instead of large multipurpose ROVs. Wireless contacts to recharge
877 batteries and recover data would avoid plugging connectors underwater and can reduce the number of
878 packages to be recovered onboard for refurbishing and contribute to reducing time at sea (Aguzzi et
879 al., 2019). Increasing the intervals between maintenance requires technological developments at the
880 platform and sensor level. For a wireless autonomous system, the amount of energy and data storage
881 volume available are fundamental parameters to determine maintenance frequency considering the
882 growing ambition of observatories (more sensors, better images definitions, etc.). Spare energy and
883 data storage require establishing strategies to collect the data (e.g., optimise multidisciplinary
884 integration and reinforce collaborative strategies), reduce the duration of measurements, and/or trigger
885 measurements on predictable (foreseeable) events detected using sensors with low power needs or
886 using *in situ* decisions based on IA algorithms for pattern recognition (Aguzzi et al., 2022). An
887 alternative is to harvest energy in small yet decisive quantities from heat exchange occurring at mid-
888 ocean ridges. Technologies are progressing quickly and high capacity energy and data storage are
889 expected in the coming years. As an example, optical fibre cable, supporting fast data transmission,
890 can also power over a few kilometres from the central station low consumption sensors (Matsuura,
891 2021). This technology by reducing the cable cost also contributes to extending the observations spatial
892 coverage.

893 Extended spatial coverage is a challenge for ocean observation. Fixed observatories, in particular, give
894 a very partial view of the seafloor generally limited to a few metres around the central place (Rountree
895 et al., 2020). There are already a few examples of static or moving devices expanding the scope around
896 the central station, for instance the 100 m thermistance chain deployed on EMSO Azores or the Internet
897 Operated Deep-Sea Crawler Wally (Chatzivangelou et al., 2020) at ONC. Developments are on the
898 way to deep-sea autonomous mobile vehicles operating from a seabed station with large excursion
899 capacities and wireless docking stations to refill batteries and download data (e.g., Costanzi et al.,
900 2020). However with the technologies presently available to store the energy, the feasibility of a vehicle
901 operating around a non-cabled observatory is not conceivable and will be first limited to cables
902 observatories. Things are however changing very quickly in this field. Fuel cells tomorrow, or quantum
903 batteries in the future, could drastically increase the amount of energy available.

904 Finally, environmental footprint concerns appeared some 10 years ago and the number of marine
905 protected areas has increased since then. Research activities and observations are a source of
906 disturbance to marine ecosystems (Juniper et al., 2019) and constitute an additional constraint when
907 designing observation systems and operation scenarios.

908

909 *Internet of Things (IoT)*

910 These platforms can communicate at the surface through IoT protocols, as described in Mariani et al
911 2021 or underwater through underwater acoustic, optical, and/or magnetic inductive modems. Acoustic
912 waves propagate over long ranges (orders of km) but can transfer limited data rate (some kbps) optical
913 modem can reach a few tens of meters with data rates of up to 500 kbps and finally magnetic inductive
914 modems can support contactless data transfer (very short range few cm). Even though the internet of
915 underwater things (Jahanbakht et al., 2021) is a concept introduced a decade ago, and underwater

916 sensor networks have been studied for two decades (Heidemann et al., 2012), it is only recently that *in*
917 *situ* underwater networks have been deployed for scientific and industrial use cases (Qiu et al., 2019).
918 Examples of services enabled by this technology are:

919 (1) Real-time data transfer to a node connected to the end user through IT infrastructure.
920 (2) Machine-to-machine communication to remotely operate instrumentation, e.g., in hazardous
921 conditions.
922 (3) Extended spatial coverage data acquisition through resident autonomous drones.
923 (4) On-demand data offloading of standalone sensors.

924 The challenges of underwater acoustic communication relate to the impact of environmental factors on
925 acoustic waves propagation in shallow and deep water (Tomasi et al., 2010, 2011). In deep waters,
926 variations in sound speed alter the direction of propagation of acoustic waves (i.e., sound refraction).
927 This causes shadow zones and reflected echoes from seabed also affects communication.

928 The future directions on underwater networks development are within the design of novel networking
929 solutions where both stationary and mobile nodes can connect and coordinate towards a common
930 mission defined by the end user and provide an underwater positioning system. One shift of paradigm
931 that could be enabled by this development is going from ocean observatories to *in situ* ocean
932 laboratories and virtual laboratories.

933

934 *Geochemical sensors*

935 Along with the evolution of the platforms, a larger number and variety of sensors are expected to
936 complement data acquisition. The sensor required for ocean measurements has undergone various
937 phases of technological advancements to meet requirements of robustness, reliability and low

938 maintenance in harsh environments. Some examples of the last technology available to measure
939 chemical properties are based on optical measurement. Optical sensors provide conventional
940 measurements by providing highly stable values for long term applications. As an example, the ECO
941 (Environment Characterisation Optics-SBE) technology is used for measuring various parameters such
942 as turbidity, fluorescence, Coloured Dissolved Organic Matter (CDOM), Photosynthetically Active
943 Radiation or chlorophyll. For pH, usage of glass electrode-based measurement often poses challenges
944 at remote locations in the ocean and are prone to drift with errors. The recent advancement in pH
945 measurement is by using the state-of- the- art ion-sensitive electronic devices such as ion-sensitive
946 field effect transistors (IISFET-Ion Sensitive Field Effect Transistor - Seabird Electronics (SBE)) that
947 uses advanced transistor-based technology. The MBARI Submersible Ultraviolet Nitrate Analyser
948 provides a highly stable measurement of nutrients over a wide range of environmental conditions
949 although their sensitivity and accuracy are poorer than those of wet chemical analyzers in conditions
950 of high turbidity and high CDOM (Daniel et al., 2020). These sensors use MBARI-ISUS (*In Situ*
951 Ultraviolet Spectrophotometer) nitrate measurement technology based on the absorption characteristics
952 of nitrate in the UV light spectrum. *In situ* pCO₂ values of seawater are measured using 4 broad
953 approaches such as gas based, electrochemical, wet-chemical or fluorescent. The partial pressure of
954 carbon dioxide in surface ocean waters is a key parameter used to study ocean CO₂ absorption,
955 acidification, primary productivity, carbon cycle, source, and sinks of CO₂, and biogeochemistry.
956 Finally, better understanding metals transfer from the hydrothermal sources to the open ocean column
957 needs the development of sensors capable of measuring trace metal micronutrients at levels found in
958 the open ocean. There is a clear gap in the development of more sensitive techniques for trace metal
959 analysis and the sensor support infrastructure needs to be redesigned to fully access their dynamic
960 distribution and impact on ocean productivity (Grand et al., 2019).

961

962 *Biological sensors*

963 One example of technological development in the last decade that includes these three technological
964 developments is represented by high-throughput sequencing solutions that are increasingly used in
965 ecology and environmental management studies. eDNA studies are also applied in the deep ocean
966 (Laroche et al., 2020). The available technology requires *a priori* knowledge of deep-sea taxonomy,
967 meaning that a large effort of species barcoding is needed (Cowart et al., 2020). However, in well-
968 known areas observatory site time series where fluid/DNA samplers exist and are coupled to fluid-
969 temperature samplers, we can track changes in microbial communities over time and in response to
970 perturbation events (e.g., Huber et al., 2003; Fortunato et al., 2018). Because lifeforms in the ocean
971 contain or leave behind a biomolecular trace that can be analysed directly from a seawater sample, 4D
972 seascapes could be a possibility with the development of multi-omic biodiversity sensing capabilities
973 by integrating probes or sensors to existing observing systems (Stefanni et al., 2022). These latter offer
974 the opportunity to integrate additional concomitant biological, biogeochemical and physical parameters
975 to take in consideration the influence of habitat heterogeneity, fluid and larvae dispersion, as well as
976 regional and local oceanography.

977

978 If eDNA and other high-throughput sequencing technologies hold great promise to uncover the
979 multiple facets of deep-sea biodiversity, understanding fundamental processes involved in population's
980 persistence and resilience still requires observations of the organisms themselves, throughout their life
981 cycle, particularly at early life-stages. The development of biophysical modelling to predict
982 connectivity patterns simulating larval trajectories requires *in situ* observations for model validation
983 and biological parametrization. Taking advantage of the infrastructure of established observatories,
984 where combinations of existing plankton collection tools could be integrated, would most effectively

985 foster rapid advancement in deep-sea larval biology. For example, large volume plankton samplers
986 such as the SyPRID currently deployed on the Woods Hole Oceanographic Institution Sentry AUV
987 (Billings et al., 2017) could be further developed and miniaturised for integration with other platforms,
988 such as small mobile long-range vehicle docking on a seabed station, which could greatly expand the
989 spatial coverage of deep-sea plankton observations. Development of imaging, automated taxonomic
990 identification through machine learning algorithms, and adaptive sampling can also accelerate deep-
991 sea larval research. Recent technological advancements in *in situ* plankton imaging such as the
992 Underwater Vision Profiler (UVP, Picheral et al., 2010) or holographic cameras (e.g., LISST-Holo2,
993 Sequoia, Lombard et al., 2019) are currently being further developed for deployment on diverse deep-
994 sea observing platforms (e.g., Picheral et al., 2021). New imaging techniques are currently under
995 development to document spawning or larval settlement events in conjunction with multi-parameter
996 sensors to identify environmental cues or oceanographic patterns driving life cycles in the deep sea.
997 Machine-learning can allow for rapid identification of high-volume image samples, as well as enable
998 the collection of higher-resolution samples following detection of an anomaly (adaptive sampling).
999 While such technological innovation could greatly accelerate our knowledge on deep-sea benthic and
1000 planktonic communities, most deep-sea species are still undescribed in their adult form, and this is only
1001 amplified for their larval forms. Therefore, their identification from images still requires the collection
1002 of physical specimens for morphological or genetic analyses, which will feed biodiversity baseline
1003 databases and provide training sets for machine learning (e.g., Stefanni et al., 2022).

1004

1005 6 Observatories and new societal approaches to deep-sea environments

1006 Seafloor observatories are a natural platform for collaboration within the ocean science and technology
1007 sectors and offer unique opportunity for demonstrations to the public and policy makers about oceanic
1008 and ocean floor processes that can stimulate society's interest in the marine realm and impacts that

1009 society is having on oceanic processes. Looking to the future, seafloor observatories have an important
1010 role to play in understanding and mitigating the effects of climate change and resource exploitation on
1011 deep-sea ecosystems.

1012 **6.1 A tool to inform environmental managers and policy makers**

1013 Because observatories constitute technological development platforms, they can support the design,
1014 testing and implementation of environmental monitoring strategies and evolve with new emergent
1015 technologies and the innovation of instrumentation for sustained, systematic data acquisition (e.g.,
1016 Danovaro et al., 2017). The Endeavour nodes of ONC and EMSO-Azores are both located within an
1017 MPA. Together, these seafloor infrastructures constitute an essential tool to inform MPA management
1018 and efficiency for the benefits of the local governments but also of international instances such as the
1019 International Seafloor Authority (ISA) which is currently developing the standards and guidelines of
1020 the international mining code. As an example, ONC has developed SeaTube (Box 1), a software system
1021 for assembling ROV dive navigation logs and video records, including real-time annotations, into an
1022 online archive and a GIS database. The database can be queried to generate maps for researchers and
1023 MPA managers that illustrate the spatial distribution of seafloor features of interest. Juniper et al.
1024 (2019) provide examples of how this geodatabase can be used to analyse the distribution of species of
1025 interest, debris, and human pressures resulting from research activity. All observatory sensor data and
1026 ROV expedition video and navigation records from the Endeavour Hydrothermal Vent MPA are
1027 archived and made publicly available by ONC (Box 1). The combined data archive therefore has the
1028 potential to support adaptation of the EHV MPA management plan and conservation objectives to a
1029 growing understanding of natural rates and scales of environmental and ecosystem change, and the
1030 spatial distribution of research activity.

1031 To standardise and implement these conservation objectives at a larger scale, regular workshops should
1032 be organised with various stakeholders, including the ISA, State environmental ministries, Non-

1033 Governmental Organisations (NGOs), Business/Industry, Science Networks and the civil society to
1034 identify their respective needs and work towards the co-design, co-development and co-delivery of
1035 commonly defined monitoring approaches and tools. Sustained funding together with governance are
1036 required to guarantee future long-term systematic observations.

1037 **6.2 Outreach and education**

1038 Real-time data available on-line and the associated data archives are an under-tapped resource for
1039 educational purposes and for general public communication. Hydrothermal systems are dynamic, and
1040 the different links between physical and biological processes could be included in education curricula,
1041 at all levels. The associated annual cruises also provide unprecedented opportunities to develop
1042 outreach and educational projects. The colossal imagery archive of hydrothermal systems can be
1043 exploited and showcased to attract the general public's interest towards these systems in particular, and
1044 oceanography and deep-sea research in general, while increasing the awareness regarding the unknown
1045 and endangered ecosystem that the deep ocean still has to reveal fully both to science and society. In
1046 the context of increased anthropogenic activities, it is of utmost importance to engage with the next
1047 generation and inform the society about our research, especially since they occur in inaccessible areas.

1048 For the last 10 years, various original actions have been proposed in all three observatories to make the
1049 science, the people and life onboard accessible to the public. Primary outreach activities are related to
1050 maintenance expeditions at sea at all three MOBs (Box 3). At Ocean Networks Canada, live-streaming
1051 video with commentary by shipboard personnel allows members of the public to follow ROV dives
1052 and on-deck action on the research vessel. The audience for these live streams has been greatly
1053 augmented in recent years through a partnership with the Ocean Exploration Trust (OET). ONC has
1054 frequently chartered the Exploration Vessel Nautilus with Hercules ROV to perform maintenance
1055 activity at the Endeavour observatory. OET has a large global audience for their Nautilus Live program
1056 and Education and Outreach staff on the vessel are experienced in interpreting science for the public,

1057 providing live commentary during dives and fielding questions from the online audience. OET's
1058 Science Communication Fellowship and Science and Engineering Internship Program allows educators
1059 and students to join the outreach staff at sea.

1060 A well-established University of Washington experiential at-sea learning program 'VISIONS' supports
1061 outreach at the Axial Seamount component of OOI's RCA. Since 2010, over 160 undergraduate and
1062 graduate students have participated in this uniquely interdisciplinary, hands-on at-sea program that
1063 provides training in research and engagement related to many important oceanographic processes
1064 operating within the Northeast Pacific ocean and on the seafloor. The oceanographic expeditions are
1065 an important component of the National Science Foundations' OOI RCA operations and maintenance
1066 cruises using the global class research ships the R/V Thompson (University of Washington, UW), the
1067 R/V Revelle (Scripps Institution of Oceanography, SIO), and the R/V Atlantis (Woods Hole
1068 Oceanographic Institution, WHOI). All cruises utilize state-of-the-art underwater robotic vehicles
1069 (ROV) that allow students to directly witness some of the most extreme environments on Earth. On all
1070 annual expeditions, similar to ONC, live video is continuously streamed from the ship and from the
1071 ROV's to viewers around the globe. In addition, the UW RCA team has developed the
1072 interactiveoceans website (Box 3) that provides rich and diverse content about the RCA sites,
1073 technologies, expeditions and educational components of the RCA.

1074 In addition to live interactions during cruises, other original actions have been developed including,
1075 among others, participative science and art & science projects. AbyssBox, the first permanent public
1076 exhibition of live deep-sea hydrothermal fauna maintained at *in situ* pressure (170 bars, Shillito et al.,
1077 2015), is a first step towards maintaining a variety of deep-sea fauna year-round, serving both scientific
1078 and public purposes. The Deep Sea Spy (DSS) project (Box 3), developed by Ifremer allows society
1079 to be involved in the research process by contributing to the annotation of deep-sea hydrothermal vent
1080 imagery acquired by seafloor observatories. To date, over 1300 citizens annotated almost 50,000

1081 images through the DSS platform building a reference database for machine algorithms developments.
1082 This alternative approach to the study of ecosystems, by increasing public engagement, also provides
1083 scientific transparency which can improve the credibility and relevance of the research process. The
1084 SPLUJ and DONVOR (Box 3), two radiophonic theatre plays, co-created in 2018 by Ifremer scientists
1085 and the professional theatre company Teatr PIBA, invite the public to explore the unknown and the
1086 imaginary by "doing" and "living" in a complete sensitive immersion. This artistic approach helped
1087 take up the challenge to reach "different" public: those who are not naturally attracted to science or
1088 those living far from the ocean. To date, over 22 000 spectators have assisted to one of the plays and
1089 over 50 representations are expected in 2022. Finally, the visit of the Tour Eiffel edifice in an
1090 immersive environment using virtual goggles provides a unique way to experience and comprehend an
1091 otherwise inaccessible environment (Box 3). This innovative way of accessing the deep ocean
1092 significantly increases the outreach potential to raise ocean awareness in the general public. It is
1093 essential to develop a wide range of outreach material exploring all five senses to reach the widest
1094 range of people. Collaboration with artists, writers and musicians, whose multifaceted visions allow us
1095 to explore the unknown in original and diverse fashions, can help meet this objective.

1096 The DSS project supported the development of educational resources for kids from 3 to 11 years old
1097 (Box 3), promoting the use of the annotation online platform as a tool in school programs. Similar
1098 resources, based on the use of data, can support programs for students in middle school and high-school
1099 in several languages. Immersive environments offered by virtual goggles, such as the one developed
1100 with the active edifice Tour Eiffel, can allow « field work » in remote environments, including
1101 exploration, observation and annotation and harbour valuable application in training by bringing
1102 students on a «field trip». More should be achieved with kids and young people in Least Developed
1103 Countries (LDCs) and Small Island Developing States (SIDs), more particularly those in the Pacific
1104 and the Caribbean Sea that are increasingly concerned with future deep-seabed mining.

1105 While some of these projects result from individual/few scientist initiatives, an important step could
1106 be achieved by hiring communication specialists dedicated to each observatory, especially to cope with
1107 the numerous media available (e.g., Youtube, Instagram, Twitter). For example, in the EMSO-ERIC
1108 European infrastructure, a communication service group exists but is composed of overloaded
1109 scientists/engineers and has no targeted budget. At ONC, a communications team supports outreach
1110 activities during expeditions that use the Nautilus, and ensures at-sea outreach activities during
1111 maintenance expeditions that use other vessels and ROVs.

1112

1113 **Conclusions**

1114 The InterRidge IMOVE workgroup aimed to internationally coordinate and optimise ridge seafloor
1115 infrastructures in terms of technology, scientific questions through a multinational and multi-
1116 collaborative endeavour. However, given the variability of hydrothermal systems, particularly at slow-
1117 spreading ridges, it is also clear that this limited number of sites, focused in magmatic ridge systems,
1118 do not cover key hydrothermal systems such as that are hosted in peridotite, or displaying only low-
1119 temperature hydrothermal outflow and temporal studies at these distinct systems are required.

1120 This review offers an overarching umbrella that can help community-based experiments to react to
1121 specific events, and help in designing, as well as coordinating observatory maintenance and
1122 complementary samples during cruises. The paper presents the state of the art in terms of results and
1123 advances enabled by these observation systems, as well as data, tools and the infrastructure available
1124 to address scientific, technological, educational and societal issues. Data acquired the last 10 years
1125 enabled great advancement in our understanding of ridges, and more particularly vent ecosystems
1126 dynamics. The next step will be to integrate across disciplines to better constrain the overall ecosystem
1127 functioning, from geological processes to biological communities' distribution and responses. This can

1128 be achieved by a joint effort in defining common variables, sensors and protocols for complementary
1129 systematic samples and data acquisition. Science service groups, such as the ones proposed through
1130 the EMSO network can help propagate ocean good practices guidelines of surveying ecosystems from
1131 the seafloor to the water column and create a global capacity development initiative that includes data
1132 management and accessibility. A wealth of data is being acquired through a number of observing
1133 programs and observatories in coastal and global oceans. An effort should be made to link the data to
1134 surrounding observations (e.g., Argo, deep Argo, GoSHIP, OceanSITES, OTN) in order to reach an
1135 integrated and multidisciplinary understanding of ecosystems functioning at the regional scale. More
1136 particularly, the DOOS proposed region-specific interdisciplinary projects to demonstrate the
1137 feasibility of sustained deep-ocean observing. Two of the three proposed locations include the Azores
1138 Archipelago and the Northeast Pacific from the Cascadian Margin to the Juan de Fuca Ridge. The
1139 implementation of such projects provides the opportunity to develop a community-based approach for
1140 large-scale interdisciplinary studies, placing the ridge environment and its influence on the global
1141 ocean.

1142 Our ten years' experience also proved that observatories constitute great means to involve and inform
1143 the society about the importance of the deep sea and the challenges we are facing to maintain a healthy
1144 ocean and the ecosystem services it provides. However, more should be done to expand our capacity
1145 building endeavour and widen the public to be reached. The scientific community needs to imagine
1146 new ways to exchange outreach, arts & science experiences across observatories by building dedicated
1147 communication plans. The complexity of marine ecosystems in relation to climate change and other
1148 anthropogenic impacts confronts us with the need to interact with many scientific disciplines.
1149 Researchers from fields in Social and Human Sciences need to be involved to conduct science in the
1150 context of sustainability and socio-ecosystems and help develop regulations. They can help in new
1151 ways to engage public and policy makers/public administration and advise environmental scientists in

1152 the development and management of multi and transdisciplinary studies in order to optimise the
1153 societal scope, including the traditional knowledge holders where feasible, and impact of deep-sea
1154 research projects in accordance with today's society mandates.

1155 **Conflict of Interest**

1156 *The authors declare that the research was conducted in the absence of any commercial or financial
1157 relationships that could be construed as a potential conflict of interest.*

1158 **Author Contributions**

1159 MM and TB lead the working group, conceived the review and wrote a first draft of the manuscript.
1160 All authors contributed the manuscript ideas and text.

1161 **Funding**

1162 The first workshop in Bergen was additionally funded by the K.G. Jebsen Centre for Deep Sea
1163 Research and the University of Bergen. The second workshop was supported by ISblue project,
1164 Interdisciplinary graduate school for the blue planet (ANR-17-EURE-0015) and co-funded by a grant
1165 from the French government under the program "Investissements d'Avenir". Additional funding was
1166 provided by Ifremer, and the département du Finistère. The operation and maintenance of the EMSO-
1167 Azores observatory is funded by the by the EMSO-FR Research Infrastructure (MESR), which is
1168 managed by an Ifremer-CNRS collaboration. The operation and maintenance of the Endeavour
1169 observatory is funded by the Canada Foundation for Innovation's Major Science Infrastructure
1170 program and the Department of Fisheries and Oceans (Canada). The operation and maintenance of the
1171 Axial Seamount observatory is funded by the National Science Foundation as part of the Ocean
1172 Observatories Initiative Regional Cabled Array. AC• was supported by the Figures

1173 **Acknowledgments**

1174 The authors acknowledge the support of the InterRidge office in Paris, Nadine Lebris, Jérôme Dyment
1175 and Kamil Szafrański. Thanks to Jina Mousseau (ONC) for creating Figure 3. We thank the captains
1176 and crews of the research vessels that enabled infrastructure maintenance: RV Pourquoi Pas?, RV
1177 L'Atalante, RV Thalassa, CCGS John P. Tully, RV Thomas G Thompson, EV Nautilus. We are also
1178 grateful to the pilots of the submersible Nautile, Victor6000, ROPOS, Hercules, Argus, Odysseus. The

1179 work reviewed in this paper would have not been possible without the help of all mechanical, electric
 1180 and computer engineers and technicians from Ifremer (RDT and RIC), ONC and OOI. The working
 1181 group was supported by InterRidge (2017-2020). Other participants in IMOVE Working Group: Lise
 1182 Artigue, Loïc Van Audenhaege, Valérie Ballu, Catherine Borremans, Greace Crystle, Cécile Cathalot,
 1183 Jerome Dyment, Aida Farough, Anne Godfroy, Sabine Gollner, Zhikui Guo, Orest Kawka, Noé
 1184 Lahaye, Marie Eide Lien, Anna Lim, Jean-Arthur Olive, Giuliana Panieri, Rolf Birger Pedersen,
 1185 Eoghan Reeves, Celine Rommevaux, Guillaume Roullet, Lars Rüpke, Ben Snook, Adam Soule, Kamil
 1186 Szafranski, Julie Tourolle, Benjamin Wheeler. Finally the group would like to thank to anonymous
 1187 reviewers and Jacopo Aguzzi for their comments.

1188 **References**

1189 Afanasyev, A., Blundy, J., Melnik, O., and Sparks, S. (2018). Formation of magmatic brine lenses via
 1190 focussed fluid-flow beneath volcanoes. *Earth Planet. Sci. Lett.* 486, 119–128.
 1191 doi:10.1016/j.epsl.2018.01.013.

1192 Aguzzi J., Chatzivangelou D., Marini S., Fanelli E., Danovaro R., Flögel S., Lebris N., Juanes F., De
 1193 Leo F., Del Rio J., Thomsen L., S., Costa C., Riccobene G., Tamburini C., Lefevre D., Gojak C.,
 1194 Poulain P.M., Favali P., Griffa A., Purser A., Cline D., Edington D., Navarro J., Stefanni S.,
 1195 Company J.B. 2019. New high-tech interactive and flexible networks for the future monitoring of deep-
 1196 sea ecosystems. *Environmental Science and Technology*, 53: 6616-6631.

1197 Aguzzi J., Flögel S., Marini S., Thomsen L., Iblez J., Weiss P., Picardi G., Calisti M., Stefanni S.,
 1198 Mirimin L., Vecchi F., Laschi C., Branch A., Clark E.B., Foing B., Wedler A., Chatzivangelou D.,
 1199 Tangherlini M., Purser A., Danovaro R. 2022. Developing technological synergies between deep-sea
 1200 and space research. *Elementa-Science of the Anthropocene*, 10: 1-9.

1201 Alfaro-Lucas, J. M., Pradillon, F., Zeppilli, D., Michel, L. N., Martinez-Arbizu, P., Tanaka, H., et al.
 1202 (2020). High environmental stress and productivity increase functional diversity along a deep-sea
 1203 hydrothermal vent gradient. *Ecology* 101, 1–13. doi:10.1002/ecy.3144.

1204 Arnulf, A. F., Harding, A. J., Kent, G. M., Carbotte, S. M., Canales, J. P., and Nedimović, M. R. (2014).
 1205 Anatomy of an active submarine volcano. *Geology* 42, 655–658. doi:10.1130/G35629.1.

1206 Arnulf, A. F., Harding, A. J., Kent, G. M., and Wilcock, W. S. D. (2018). Structure, Seismicity, and
1207 Accretionary Processes at the Hot Spot-Influenced Axial Seamount on the Juan de Fuca Ridge. *J.*
1208 *Geophys. Res. Solid Earth* 123, 4618–4646. doi:<https://doi.org/10.1029/2017JB015131>.

1209 Artigue, L., Wyatt, N. J., Lacan, F., Mahaffey, C., and Lohan, M. C. (2021). The Importance of Water
1210 Mass Transport and Dissolved-Particle Interactions on the Aluminum Cycle in the Subtropical North
1211 Atlantic. *Global Biogeochem. Cycles* 35, e2020GB006569.
1212 doi:<https://doi.org/10.1029/2020GB006569>.

1213 Baker, E. T., Walker, S. L., Chadwick, W. W., Butterfield, D. A., Buck, N. J., and Resing, J. A. (2019).
1214 Posteruption Enhancement of Hydrothermal Activity: A 33-Year, Multieruption Time Series at Axial
1215 Seamount (Juan de Fuca Ridge). *Geochemistry, Geophys. Geosystems* 20, 814–828.
1216 doi:<https://doi.org/10.1029/2018GC007802>.

1217 Baldighi, E., Zeppilli, D., Crespin, R., Chauvaud, P., Pradillon, F., and Sarrazin, J. (2018).
1218 Colonization of synthetic sponges at the deep-sea Lucky Strike hydrothermal vent field (Mid-Atlantic
1219 Ridge): a first insight. *Mar. Biodivers.* 48, 89–103. doi:10.1007/s12526-017-0811-3.

1220 Ballard, R. D., and Van Andel, T. H. (1977). Project FAMOUS: Operational techniques and American
1221 submersible operations. *GSA Bull.* 88, 495–506. doi:10.1130/0016-
1222 7606(1977)88<495:PFOTAA>2.0.CO;2.

1223 Barge, L. M., Flores, E., Baum, M. M., Velde, D. G. V., and Russell, M. J. (2019). Redox and pH
1224 gradients drive amino acid synthesis in iron oxyhydroxide mineral systems. *Proc. Natl. Acad. Sci. U.*
1225 *S. A.* 116, 4828–4833. doi:10.1073/pnas.1812098116.

1226 Barnes, C. R., and Tunnicliffe, V. (2008). Building the World's First Multi-node Cabled Ocean
1227 Observatories (NEPTUNE Canada and VENUS, Canada): Science, Realities, Challenges and
1228 Opportunities. in *OCEANS 2008 - MTS/IEEE Kobe Techno-Ocean* (IEEE), 1–8.
1229 doi:10.1109/OCEANSKOBE.2008.4531076.

1230 Barreyre, T., Escartín, J., García, R., Cannat, M., Mittelstaedt, E., and Prados, R. (2012). Structure,
1231 temporal evolution, and heat flux estimates from the Lucky Strike deep-sea hydrothermal field derived
1232 from seafloor image mosaics. *Geochemistry, Geophys. Geosystems* 13. doi:10.1029/2011GC003990.

1233 Barreyre, T., Escartin, J., Sohn, R., and Cannat, M. (2014a). Permeability of the Lucky Strike deep-sea
1234 hydrothermal system: Constraints from the poroelastic response to ocean tidal loading. *Earth Planet.*
1235 *Sci. Lett.* 408, 146–154. doi:10.1016/j.epsl.2014.09.049.

1236 Barreyre, T., Escartín, J., Sohn, R. A., Cannat, M., Ballu, V., and Crawford, W. C. (2014b). Temporal
1237 variability and tidal modulation of hydrothermal exit-fluid temperatures at the Lucky Strike deep-sea
1238 vent field, Mid-Atlantic Ridge. *J. Geophys. Res. Solid Earth.* doi:10.1002/2013JB010478.

1239 Barreyre, T., and Sohn, R. A. (2016). Poroelastic response of mid-ocean ridge hydrothermal systems
1240 to ocean tidal loading: Implications for shallow permeability structure. *Geophys. Res. Lett.* 43, 1660–
1241 1668. doi:10.1002/2015GL066479.

1242 Barreyre, T., Olive, J. A., Crone, T. J., and Sohn, R. A. (2018). Depth-dependent permeability and heat
1243 output at basalt-hosted hydrothermal systems across mid-ocean ridge spreading rates. *Geochemistry,*
1244 *Geophys. Geosystems* 19, 1259–1281. doi:10.1002/2017GC007152.

1245 Barreyre, T., Parnell-Turner, R., Wu, J.N. and Fornari, D.J., 2022. Tracking crustal permeability and
1246 hydrothermal response during seafloor eruptions at the East Pacific Rise, 9° 50'N. *Geophysical*
1247 *Research Letters*, 49(3), p.e2021GL095459.

1248 Barriga, F. J. A. S., Colaço, A., Escartín, J., Hooft, E., Humphris, S. E., Le Bris, N., et al. (2005). Long-
1249 term monitoring of the Mid-Atlantic Ridge: Proceedings of the III MOMAR Workshop. Long-Term
1250 Monit. Mid-Atlantic Ridge P, 63.

1251 Beaulieu, S. E., and Szafranski, K. M. (2020). InterRidge Global Database of Active Submarine
1252 Hydrothermal Vent Fields Version 3.4. doi:10.1594/PANGAEA.917894.

1253 Billings, A., Kaiser, C., Young, C. M., Hiebert, L. S., Cole, E., Wagner, J. K. S., et al. (2017). SyPRID
1254 sampler: A large-volume, high-resolution, autonomous, deep-ocean precision plankton sampling
1255 system. *Deep Sea Res. Part II Top. Stud. Oceanogr.* 137, 297–306.
1256 doi:<https://doi.org/10.1016/j.dsr2.2016.05.007>.

1257 Blandin, J., Colaço, A., Legrand, J., Cannat, M., Sarradin, P., and Sarrazin, J. (2010). The MoMAR-D
1258 project : a challenge to monitor in real time the Lucky Strike hydrothermal vent field. *ICES J. Mar.*
1259 *Sci.* 68, 416–424.

1260 Boschen, R. E., Rowden, A. A., Clark, M. R., and Gardner, J. P. A. (2013). Mining of deep-sea seafloor
1261 massive sulfides: A review of the deposits, their benthic communities, impacts from mining, regulatory
1262 frameworks and management strategies. *Ocean Coast. Manag.* 84, 54–67.
1263 doi:10.1016/j.ocecoaman.2013.07.005.

1264 Bower, D. J., Gurnis, M., and Seton, M. (2013). Lower mantle structure from paleogeographically
1265 constrained dynamic Earth models. *Geochemistry, Geophys. Geosystems* 14, 44–63.
1266 doi:<https://doi.org/10.1029/2012GC004267>.

1267 Boyd, P. W., and Ellwood, M. J. (2010). The biogeochemical cycle of iron in the ocean. *Nat. Geosci.*
1268 3, 675–682. doi:10.1038/ngeo964.

1269 Bracco, A., Choi, J., Joshi, K., Luo, H., and McWilliams, J. C. (2016). Submesoscale currents in the
1270 northern Gulf of Mexico: Deep phenomena and dispersion over the continental slope. *Ocean Model.*
1271 101, 43–58. doi:<https://doi.org/10.1016/j.ocemod.2016.03.002>.

1272 Breusing, C., Biastoch, A., Drews, A., Metaxas, A., Jollivet, D., Vrijenhoek, R. C., et al. (2016).
1273 Biophysical and Population Genetic Models Predict the Presence of “Phantom” Stepping Stones
1274 Connecting Mid-Atlantic Ridge Vent Ecosystems. *Curr. Biol.* 26, 2257–2267.
1275 doi:10.1016/j.cub.2016.06.062.

1276 Burd, B. J., and Thomson, R. E. (2012). Estimating zooplankton biomass distribution in the water
1277 column near the Endeavour segment of Juan de Fuca ridge using acoustic backscatter and concurrently
1278 towed nets. *Oceanography* 25, 269–276. doi:doi:10.5670/oceanog.2012.25.

1279 Burd, B. J., and Thomson, R. E. (2019). Seasonal patterns in deep acoustic backscatter layers near vent
1280 plumes in the northeastern Pacific Ocean. *FACETS* 4, 183–209. doi:doi:10.1139/facets-2018-0027.

1281 Butterfield, D. A., Roe, K. K., Lilley, M. D., Huber, J. A., Baross, J. A., Embley, R. W., et al. (2004).
1282 Mixing, Reaction and Microbial Activity in the Sub-Seafloor Revealed by Temporal and Spatial
1283 Variation in Diffuse Flow Vents at Axial Volcano. *Subseafloor Biosph. Mid-Ocean Ridges*, 269–289.
1284 doi:<https://doi.org/10.1029/144GM17>.

1285 Cann, J. R., Elderfield, H., Laughton, A., Butterfield, D. A., Jonasson, I. R., Massoth, G. J., et al.
1286 (1997). Seafloor eruptions and evolution of hydrothermal fluid chemistry. *Philos. Trans. R. Soc.
1287 London. Ser. A Math. Phys. Eng. Sci.* 355, 369–386. doi:10.1098/rsta.1997.0013.

1288 Cannat, M., and Sarradin, P. (2010). MOMARSAT : MONITORING THE MID ATLANTIC RIDGE.
1289 doi:<https://doi.org/10.18142/130>.

1290 Cannat, M., Sarradin, P., Blandin, J., Ballu, V., Barreyre, T., Chavagnac, V., et al. (2016). EMSO-
1291 Azores : Monitoring seafloor and water column processes at the Mid-Atlantic Ridge. Fix03 - Proj.
1292 Newsletter. Serv. Act. Spec. 3.

1293 Cannat, M., Sarradin, P., Blandin, J., Escartín, J., and Colaço, A. (2011). MoMar-Demo at Lucky
1294 Strike. A near-real time multidisciplinary observatory of hydrothermal processes and ecosystems at the
1295 Mid-Atlantic Ridge. in AGU Fall meeting, Abstract OS22A-05 (San Francisco).

1296 Caplan-Auerbach, J., Dziak, R. P., Haxel, J., Bohnenstiehl, D. R., and Garcia, C. (2017). Explosive
1297 processes during the 2015 eruption of Axial Seamount, as recorded by seafloor hydrophones.
1298 *Geochemistry, Geophys. Geosystems* 18, 1761–1774. doi:<https://doi.org/10.1002/2016GC006734>.

1299 Carbotte, S. M., Arnulf, A., Spiegelman, M., Lee, M., Harding, A., Kent, G., et al. (2020). Stacked sills
1300 forming a deep melt-mush feeder conduit beneath axial seamount. *Geology* 48, 693–697.
1301 doi:[10.1130/G47223.1](https://doi.org/10.1130/G47223.1).

1302 Cardona, Y., Ruiz-Ramos, D. V., Baums, I. B., and Bracco, A. (2016). Potential connectivity of
1303 coldwater black coral communities in the northern Gulf of Mexico. *PLoS One* 11.
1304 doi:[10.1371/journal.pone.0156257](https://doi.org/10.1371/journal.pone.0156257).

1305 Caress, D. W., Clague, D. A., Paduan, J. B., Martin, J. F., Dreyer, B. M., Chadwick, W. W., et al.
1306 (2012). Repeat bathymetric surveys at 1-metre resolution of lava flows erupted at Axial Seamount in
1307 April 2011. *Nat. Geosci.* 5, 483–488. doi:[10.1038/ngeo1496](https://doi.org/10.1038/ngeo1496).

1308 Cathalot, C., Roussel, E. G., Perhirin, A., Creff, V., Donval, J. P., Guyader, V., et al. (2021).
1309 Hydrothermal plumes as hotspots for deep-ocean heterotrophic microbial biomass production. *Nat.*
1310 *Commun.* 12, 4–13. doi:[10.1038/s41467-021-26877-6](https://doi.org/10.1038/s41467-021-26877-6).

1311 Chadwick, W. W., Clague, D. A., Embley, R. W., Perfit, M. R., Butterfield, D. A., Caress, D. W., et
1312 al. (2013). The 1998 eruption of Axial Seamount: New insights on submarine lava flow emplacement
1313 from high-resolution mapping. *Geochemistry, Geophys. Geosystems* 14, 3939–3968.
1314 doi:<https://doi.org/10.1002/ggge.20202>.

1315 Chadwick, W. W., Nooner, S. L., Butterfield, D. A., and Lilley, M. D. (2012). Seafloor deformation
1316 and forecasts of the April 2011 eruption at Axial Seamount. *Nat. Geosci.* 5, 474–477. doi:doi:
1317 10.1038/ngeo1464.

1318 Chadwick, W. W., Paduan, J. B., Clague, D. A., Dreyer, B. M., Merle, S. G., Bobbitt, A. M., et al.
1319 (2016). Voluminous eruption from a zoned magma body after an increase in supply rate at Axial
1320 Seamount. *Geophys. Res. Lett.* 43, 12,12-63,70. doi:https://doi.org/10.1002/2016GL071327.

1321 Chadwick, W. W., Wilcock, W. S. D., Nooner, S. L., Beeson, J. W., Sawyer, A. M., and Lau, T.-K.
1322 (2022). Geodetic Monitoring at Axial Seamount Since Its 2015 Eruption Reveals a Waning Magma
1323 Supply and Tightly Linked Rates of Deformation and Seismicity. *Geochemistry, Geophys. Geosystems*
1324 23, e2021GC010153. doi:https://doi.org/10.1029/2021GC010153.

1325 Chapman, A. S. A., Beaulieu, S. E., Colaço, A., Gebruk, A. V., Hilario, A., Kihara, T. C., et al. (2019).
1326 sFDvent: A global trait database for deep-sea hydrothermal-vent fauna. *Glob. Ecol. Biogeogr.* 28,
1327 1538–1551. doi:10.1111/geb.12975.

1328 Chatzievangelou, D., Aguzzi, J., Ogston, A., Suárez, A., and Thomsen, L. (2020). Visual monitoring
1329 of key deep-sea megafauna with an Internet Operated crawler as a tool for ecological status assessment.
1330 *Prog. Oceanogr.* 184, 102321. doi:https://doi.org/10.1016/j.pocean.2020.102321.

1331 Chavagnac, V., Leleu, T., Boulart, C., Barreyre, T., Castillo, A., Menjot, L., et al. (2015). Deep-Sea
1332 Observatory EMSO-Azores (Lucky Strike, 37°17'N MAR): Impact of Fluid Circulation Pathway on
1333 Chemical Hydrothermal Fluxes. in *AGU Fall Meeting Abstracts*, OS42A-07.

1334 Chavagnac, V., Leleu, T., Fontaine, F. J., Cannat, M., Ceuleneer, G., and Castillo, A. (2018a). Spatial
1335 Variations in Vent Chemistry at the Lucky Strike Hydrothermal Field, Mid-Atlantic Ridge (37°N):
1336 Updates for Subseafloor Flow Geometry From the Newly Discovered Capelinhos Vent. *Geochemistry,*
1337 *Geophys. Geosystems* 19, 4444–4458. doi:10.1029/2018GC007765.

1338 Chavagnac, V., Saleban Ali, H., Jeandel, C., Leleu, T., Destrigneville, C., Castillo, A., et al. (2018b).
1339 Sulfate minerals control dissolved rare earth element flux and Nd isotope signature of buoyant
1340 hydrothermal plume (EMSO-Azores, 37°N Mid-Atlantic Ridge). *Chem. Geol.* 499, 111–125.
1341 doi:10.1016/j.chemgeo.2018.09.021.

1342 Clague, D., Paduan, J., Caress, D., Chadwick, W. W., Le Saout, M., Dreyer, B., et al. (2017). High-
1343 Resolution AUV Mapping and Targeted ROV Observations of Three Historical Lava Flows at Axial
1344 Seamount. *Oceanography* 30. doi:10.5670/oceanog.2017.426.

1345 Colaço, A., Blandin, J., Cannat, M., Carval, T., Chavagnac, V., Connelly, D. P., et al. (2011). MoMAR-
1346 D: a technological challenge to monitor the dynamics of the Lucky Strike vent ecosystem. *ICES J.*
1347 *Mar. Sci. J. du Cons.* 68, 416–424.

1348 Coogan, L. A., Attar, A., Mihaly, S. F., Jeffries, M., and Pope, M. (2017). Near-vent chemical
1349 processes in a hydrothermal plume: Insights from an integrated study of the Endeavour segment.
1350 *Geochemistry Geophys. Geosystems* 18, 1641–1660. doi:doi:10.1002/2016GC006747.

1351 Coppola, L., Ntoumas, M., Bozzano, R., Bensi, M., Hartman, S. E., Charcos Llorens, M., et al. (2016).
1352 Handbook of best practices for open ocean fixed observatories. European Commission, FixO3 Project
1353 Available at: doi: <https://doi.org/10.25607/OPB-1488>.

1354 Corliss, J. B., Dymond, J., Gordon, L. I., Edmond, J. M., Von Herzen, R. P., Ballard, R. D., et al.
1355 (1979). Submarine thermal springs on the Galapagos Rift. *Science* (80-). 203, 1073–1083.

1356 Costanzi, R., Fenucci, D., Manzari, V., Micheli, M., Morlando, L., Terracciano, D., et al. (2020).
1357 Interoperability Among Unmanned Maritime Vehicles: Review and First In-field Experimentation.
1358 *Front. Robot. AI* 7, 1–15. doi:10.3389/frobt.2020.00091.

1359 Cotte, L., Chavagnac, V., Pelleter, E., Laes-Huon, A., Cathalot, C., Dulaquais, G., et al. (2020). Metal
1360 partitioning after in situ filtration at deep-sea vents of the Lucky Strike hydrothermal field (EMSO-
1361 Azores, Mid-Atlantic Ridge, 37 degrees N). *Deep Sea Res. Part I Oceanogr. Res. Pap.* 157, 103204.
1362 doi:10.1016/j.dsr.2019.103204.

1363 Cotte, L., Omanović, D., Waeles, M., Laës, A., Cathalot, C., Sarradin, P., et al. (2018). On the nature
1364 of dissolved copper ligands in the early buoyant plume of hydrothermal vents. *Environ. Chem.* 15, 58–
1365 73. doi:10.1071/EN17150.

1366 Coumou, D., Driesner, T., Weis, P., and Heinrich, C. (2009). Phase separation, brine formation, and
1367 salinity variation at Black Smoker hydrothermal systems. *J. Geophys. Res.* 114.
1368 doi:10.1029/2008JB005764.

1369 Cowart, D. A., Matabos, M., Brandt, M. I., Marticorena, J., and Sarrazin, J. (2020). Exploring
1370 environmental DNA (eDNA) to assess biodiversity of hard substratum faunal communities on the
1371 Lucky Strike vent field (Mid-Atlantic Ridge) and investigate recolonization dynamics after an induced
1372 disturbance. *Front. Mar. Sci.* 6, 1–21. doi:10.3389/fmars.2019.00783.

1373 Cowen, R. K., and Sponaugle, S. (2009). Larval dispersal and marine population connectivity. *Ann.*
1374 *Rev. Mar. Sci.* 1, 443–466. doi:10.1146/annurev.marine.010908.163757.

1375 Crawford, W. C., Rai, A., Singh, S. C., Cannat, M., Escartín, J., Wang, H., et al. (2013). Hydrothermal
1376 seismicity beneath the summit of Lucky Strike volcano, Mid-Atlantic Ridge. *Earth Planet. Sci. Lett.*
1377 373, 118–128.

1378 Crise, A., d'Alcalà, M. R., Mariani, P., Petihakis, G., Robidart, J., Iudicone, D., et al. (2018). A
1379 conceptual framework for developing the next generation of Marine OBservatories (MOBs) for science
1380 and society. *Front. Mar. Sci.* 5, 1–8. doi:10.3389/fmars.2018.00318.

1381 Crone, T. J., and Wilcock, W. S. D. (2005). Modeling the effects of tidal loading on mid-ocean ridge
1382 hydrothermal systems. *Geochemistry, Geophys. Geosystems* 6. doi:10.1029/2004GC000905.

1383 Crone, T. J., Wilcock, W. S. D., and McDuff, R. E. (2010). Flow rate perturbations in a black smoker
1384 hydrothermal vent in response to a mid-ocean ridge earthquake swarm. *Geochemistry, Geophys.*
1385 *Geosystems* 11, 1–13. doi:10.1029/2009GC002926.

1386 Cuvelier, D., Beesau, J., Ivanenko, V. N., Zeppilli, D., Sarradin, P., and Sarrazin, J. (2014a). First
1387 insights into macro-and meiofaunal colonisation patterns on paired wood/slate substrata at Atlantic
1388 deep-sea hydrothermal vents. *Deep Sea Res. Part I Oceanogr. Res. Pap.* 87, 70–81.

1389 Cuvelier, D., Legendre, P., Laës-Huon, A., Sarradin, P., and Sarrazin, J. (2017). Biological and
1390 environmental rhythms in (dark) deep-sea hydrothermal ecosystems. *Biogeosciences* 14, 2955–2977.
1391 doi:10.5194/bg-14-2955-2017.

1392 Cuvelier, D., Legendre, P., Laes, A., Sarradin, P., and Sarrazin, J. (2014b). Rhythms and Community
1393 Dynamics of a Hydrothermal Tubeworm Assemblage at Main Endeavour Field—A Multidisciplinary
1394 Deep-Sea Observatory Approach. *PLoS One* 9, e96924.

1395 Cuvelier, D., Sarrazin, J., Colaço, A., Copley, J. T. P., Glover, A. G., Tyler, P. A., et al. (2011).
1396 Community dynamics over 14 years at the Eiffel Tower hydrothermal edifice on the Mid-Atlantic
1397 Ridge. *Limnol. Oceanogr.* 56, 1624–1640.

1398 Daniel, A., Laës-Huon, A., Barus, C., Beaton, A. D., Blandfort, D., Guigues, N., et al. (2020). Toward
1399 a Harmonization for Using in situ Nutrient Sensors in the Marine Environment . *Front. Mar. Sci.* 6.

1400 Dañobeitia, J. J., Pouliquen, S., Johannessen, T., Basset, A., Cannat, M., Gerrit Pfeil, B., et al. (2020).
1401 Toward a Comprehensive and Integrated Strategy of the European Marine Research Infrastructures for
1402 Ocean Observations. *Front. Mar. Sci.* 7, 180. doi:10.3389/fmars.2020.00180.

1403 Danovaro R., Aguzzi J., Fanelli E., Billet D. Gjerde K., Jamieson A., Ramirez-Llodra E, Smith C.R.,
1404 Snelgrove P.V.R., Thomsen L., Van Dover C. 2017. A new international ecosystem-based strategy for
1405 the global deep ocean. *Science*, 355: 452-454.

1406 Danovaro, R., Corinaldesi, C., Dell'Anno, A., and Snelgrove, P. V. R. (2017). The deep-sea under
1407 global change. *Curr. Biol.* doi:10.1016/j.cub.2017.02.046.

1408 Danovaro, R., Fanelli, E., Aguzzi, J., Billett, D., Carugati, L., Corinaldesi, C., et al. (2020). Ecological
1409 variables for developing a global deep-ocean monitoring and conservation strategy. *Nat. Ecol. Evol.* 4,
1410 181–192. doi:10.1038/s41559-019-1091-z.

1411 Delaney, J. R., Kelley, D. S., Marburg, A., Stoermer, M., Hadaway, H., Juniper, S. K., et al. (2016).
1412 Axial Seamount - wired and restless: A cabled submarine network enables real-time, tracking of a Mid-
1413 Ocean Ridge eruption and live video of an active hydrothermal system Juan de Fuca Ridge, NE Pacific.
1414 OCEANS 2016 MTS/IEEE Monterey, 1–8. doi:10.1109/OCEANS.2016.7761484.

1415 Devine, B. M., Baker, K. D., Edinger, E. N., and Fisher, J. A. D. (2020). Habitat associations and
1416 assemblage structure of demersal deep-sea fishes on the eastern Flemish Cap and Orphan Seamount.
1417 Deep. Res. Part I *Oceanogr. Res. Pap.* 157, 103210. doi:10.1016/j.dsr.2019.103210.

1418 DFO (2006). Identification of Ecologically Significant Species and Community Properties. DFO Can.
1419 Sci. Advis. Sec. Sci. Advis. Rep. 2006/04.

1420 Dick, G. J. (2019). The microbiomes of deep-sea hydrothermal vents: distributed globally, shaped
1421 locally. *Nat. Rev. Microbiol.* 17, 271–283. doi:10.1038/s41579-019-0160-2.

1422 Doya, C., Aguzzi, J., Pardo, M., Matabos, M., Company, J. B., Costa, C., et al. (2014). Diel behavioral
1423 rhythms in sablefish (*Anoplopoma fimbria*) and other benthic species, as recorded by the Deep-sea
1424 cabled observatories in Barkley canyon (NEPTUNE-Canada). *J. Mar. Syst.* 130, 69–78. Available at:
1425 <http://dx.doi.org/10.1016/j.jmarsys.2013.04.003>.

1426 Du Preez, C., and Fisher, C. R. (2018). Long-term stability of back-arc basin hydrothermal vents. *Front.*
1427 *Mar. Sci.* 5, 1–10. doi:10.3389/fmars.2018.00054.

1428 Durden, J. M., Bett, B. J., Huffard, C. L., Pebody, C., Ruhl, H. A., and Smith, K. L. (2020). Response
1429 of deep-sea deposit-feeders to detrital inputs: A comparison of two abyssal time-series sites. *Deep.*
1430 *Res. Part II Top. Stud. Oceanogr.* 173, 104677. doi:10.1016/j.dsr2.2019.104677.

1431 Dziak, R. P., Smith, D. K., Bohnenstiehl, D. W. R., Fox, C. G., Desbruyeres, D., Matsumoto, H., et al.
1432 (2004). Evidence of a recent magma dike intrusion at the slow spreading Lucky Strike segment, Mid-
1433 Atlantic Ridge. *J. Geophys. Res. Solid Earth* 109, 1–15. doi:10.1029/2004JB003141.

1434 Escartin, J., Garcia, R., Barreyre, T., Cannat, M., Gracias, N., Shihavuddin, A., et al. (2013). Optical
1435 methods to monitor temporal changes at the seafloor: The Lucky Strike deep-sea hydrothermal vent
1436 field (Mid-Atlantic Ridge). in 2013 IEEE International Underwater Technology Symposium (UT
1437 2013) (Tokyo, France: IEEE), 1–6. doi:10.1109/UT.2013.6519838.

1438 Escartín, J., Barreyre, T., Cannat, M., Garcia, R., Gracias, N., Deschamps, A., et al. (2015).
1439 Hydrothermal activity along the slow-spreading Lucky Strike ridge segment (Mid-Atlantic Ridge):
1440 Distribution, heatflux, and geological controls. *Earth Planet. Sci. Lett.* 431, 173–185.
1441 doi:10.1016/j.epsl.2015.09.025.

1442 Escartín, J., Soule, S. A., Cannat, M., Fornari, D. J., Düsünür, D., and Garcia, R. (2014). Lucky Strike
1443 seamount: Implications for the emplacement and rifting of segment-centered volcanoes at slow
1444 spreading mid-ocean ridges. *Geochemistry Geophys. Geosystems* 15, 4157–4179. doi:doi:
1445 10.1002/2014GC005477.

1446 Favali, P., and Beranzoli, L. (2009). EMSO: European multidisciplinary seafloor observatory. *Nucl.*
1447 *Instruments Methods Phys. Res. Sect. A Accel. Spectrometers, Detect. Assoc. Equip.* 602, 21–27.
1448 doi:10.1016/j.nima.2008.12.214.

1449 Fitzsimmons, J. ., Boyle, E. A., and Jenkins, W. J. (2014). Distal transport of dissolved hydrothermal
1450 iron in the deep South Pacific Ocean. *Proc. Natl. Acad. Sci.* 111, 16654–16661.
1451 doi:10.1073/pnas.1418778111.

1452 Fornari, D. J., Von Damm, K. L., Bryce, J. G., Cowen, J. P., Ferrini, V., Fundis, A., et al. (2012). The
1453 East Pacific Rise between 9°N and 10°N: Twenty-five years of integrated, multidisciplinary oceanic
1454 spreading center studies. *Oceanography* 25, 18–43. doi:10.5670/oceanog.2012.02.

1455 Fortunato, C. S., and Huber, J. A. (2016). Coupled RNA-SIP and metatranscriptomics of active
1456 chemolithoautotrophic communities at a deep-sea hydrothermal vent. *ISME J.* 10, 1925–1938.
1457 doi:10.1038/ismej.2015.258.

1458 Fortunato, C. S., Larson, B., Butterfield, D. A., and Huber, J. A. (2018). Spatially distinct, temporally
1459 stable microbial populations mediate biogeochemical cycling at and below the seafloor in hydrothermal
1460 vent fluids. *Environ. Microbiol.* 20, 769–784. doi:10.1111/1462-2920.14011.

1461 Franke, A., Blenckner, T., Duarte, C. M., Ott, K., Fleming, L. E., Antia, A., et al. (2020).
1462 Operationalizing Ocean Health: Toward Integrated Research on Ocean Health and Recovery to
1463 Achieve Ocean Sustainability. *One Earth* 2, 557–565. doi:10.1016/j.oneear.2020.05.013.

1464 Galaasen, E. V., Ninnemann, U. S., Kessler, A., Irvalı, N., Rosenthal, Y., Tjiputra, J., et al. (2020).
1465 Interglacial instability of North Atlantic Deep Water ventilation. *Science* 367, 1485–1489.
1466 doi:10.1126/science.aay6381.

1467 Germanovich, L. N., Hurt, R. S., Smith, J. E., Genc, G., and Lowell, R. P. (2015). Journal of
1468 Geophysical Research: Solid Earth hydrothermal environments. *J. Geophys. Res. Solid Earth* 120,
1469 8031–8055. doi:10.1002/2015JB012245. Received.

1470 Girard, F., Sarrazin, J., Arnaubec, A., Cannat, M., Sarradin, P., Wheeler, B., et al. (2020). Currents and
1471 topography drive assemblage distribution on an active hydrothermal edifice. *Prog. Oceanogr.* 187.
1472 doi:10.1016/j.pocean.2020.102397.

1473 Glover, A. G., Gooday, A. J., Bailey, D., Billet, D. S. M., Chevaldonné, P., Colaço, A., et al. (2010).
1474 Temporal change in deep-sea benthic ecosystems: a review of the evidence from recent time-series
1475 studies. *Adv. Mar. Biol.* 58, 1–95. doi:10.1016/B978-0-12-381015-1.00001-0.

1476 Grand, M. M., Laes-Huon, A., Fietz, S., Resing, J. A., Obata, H., Luther III, G. W., et al. (2019).
1477 Developing autonomous observing systems for micronutrient trace metals. *Front. Mar. Sci.* 6, 35.

1478 Hand, K. P., and German, C. R. (2018). Exploring ocean worlds on Earth and beyond. *Nat. Geosci.* 11,
1479 2–4. doi:10.1038/s41561-017-0045-9.

1480 Hartman, S. E., Lampitt, R. S., Larkin, K. E., Pagnani, M., Campbell, J., Gkritzalis, T., et al. (2012).
1481 The Porcupine Abyssal Plain fixed-point sustained observatory (PAP-SO): variations and trends from
1482 the Northeast Atlantic fixed-point time-series. *ICES J. Mar. Sci.* 69, 776–783.

1483 Heidemann, J., Stojanovic, M., and Zorzi, M. (2012). Underwater sensor networks: applications,
1484 advances and challenges. *Philos. Trans. R. Soc. A* 370, 158–175. Available at:
1485 <https://doi.org/10.1098/rsta.2011.0214>.

1486 Hooft, E. E. E., Patel, H., Wilcock, W., Becker, K., Butterfield, D., Davis, E., et al. (2010). A seismic
1487 swarm and regional hydrothermal and hydrologic perturbations: The northern Endeavour segment,
1488 February 2005. *Geochemistry, Geophys. Geosystems* 11. doi:<https://doi.org/10.1029/2010GC003264>.

1489 Huber, J. A., Butterfield, D. A., and Baross, J. A. (2003). Bacterial diversity in a subseafloor habitat
1490 following a deep-sea volcanic eruption. *FEMS Microbiol. Ecol.* 43, 393–409. doi:10.1016/S0168-
1491 6496(02)00451-8.

1492 Huber, J. A., Crone, T. J., and Soule, D. (2021). Integrating the Regional Cabled Array with ocean
1493 drilling to facilitate observatory-based subseafloor science at Axial Seamount. *Ocean Observatories
1494 Initiative Facility Board, Ocean Observatories Initiative (OOI) science plan: Exciting science
1495 opportunities using OOI data.*

1496 Huber, J. A., David, B. M. W., Morrison, H. G., Huse, S. M., Neal, P. R., Butterfield, D. A., et al.
1497 (2007). Microbial Population Structures in the Deep Marine Biosphere. *Science* (80-.). 318, 97–100.
1498 doi:10.1126/science.1146689.

1499 Husson, B., Sarradin, P., Zeppilli, D., and Sarrazin, J. (2017). Picturing thermal niches and biomass of
1500 hydrothermal vent species. *Deep. Res. Part II Top. Stud. Oceanogr.* 137, 6–25.
1501 doi:10.1016/j.dsr2.2016.05.028.

1502 Husson, B., Sarrazin, J., van Oevelen, D., Sarradin, P., Soetaert, K., and Menesguen, A. (2018).
1503 Modelling the interactions of the hydrothermal mussel *Bathymodiolus azoricus* with vent fluid. *Ecol.*
1504 *Modell.* 377, 35–50. doi:10.1016/j.ecolmodel.2018.03.007.

1505 IMOVE, working group (2019). IMOVE - Integrating Multidisciplinary Observations in Vent
1506 Environments. An InterRidge Working Group. Workshop, Feb. 6-8, Bergen, Norway. Available at:
1507 <https://archimer.ifremer.fr/doc/00623/73522/>.

1508 Jahanbakht, M., Xiang, W., Hanzo, L., and Azghadi, M. R. (2021). Internet of Underwater Things and
1509 Big Marine Data Analytics—A Comprehensive Survey. *IEEE Commun. Surv. Tutorials* 23, 904–956.
1510 doi:10.1109/COMST.2021.3053118.

1511 Juniper, S. K., Thornborough, K., Douglas, K., and Hillier, J. (2019). Remote monitoring of a deep-
1512 sea marine protected area: The Endeavour Hydrothermal Vents. *Aquat. Conserv. Mar. Freshw.*
1513 *Ecosyst.* 29, 1–19. doi:10.1002/aqc.3020.

1514 Jupp, T. E., and Schultz, A. (2004). Physical balances in subseafloor hydrothermal convection cells. *J.*
1515 *Geophys. Res. Solid Earth* 109, 1–12. doi:10.1029/2003JB002697.

1516 Kelley, D. S., Carbotte, S. M., Caress, D. W., Clague, D. A., Delaney, J. R., Gill, J. B., et al. (2012).
1517 Endeavour segment of the Juan de Fuca Ridge: one of the most remarkable places on Earth.
1518 *Oceanography* 25, 44–61.

1519 Kelley, D. S., Delaney, J. R., and Juniper, S. K. (2014). Establishing a new era of submarine volcanic
1520 observatories: Cabling Axial Seamount and the Endeavour Segment of the Juan de Fuca Ridge. *Mar.*
1521 *Geol.* 352, 426–450. doi:10.1016/j.margeo.2014.03.010.

1522 Kelley, D. S., Delaney, J. R., and Team, C. A. (2016). NSF’s Cabled Array: A wired tectonic plate and
1523 overlying ocean. *Ocean. 2016 MTS/IEEE Monterey, OCE 2016.*
1524 doi:10.1109/OCEANS.2016.7761398.

1525 Kelley, D. S., Karson, J. A., Früh-Green Gretchen, L., Yoerger, D. R., Shank, T. M., Butterfield, D.
1526 A., et al. (2005). A Serpentinite-Hosted Ecosystem: The Lost City Hydrothermal Field. *Science* (80-
1527). 307, 1428–1434. doi:10.1126/science.1102556.

1528 Laës-Huon, A., Cathalot, C., Legrand, J., Tanguy, V., and Sarradin, P. (2016). Long-Term In Situ
 1529 Survey of Reactive Iron Concentrations at the EMSO-Azores Observatory. *IEEE J. Ocean. Eng.* 41,
 1530 744–752. doi:10.1109/JOE.2016.2552779.

1531 Laes, A., Bucas, K., Le Piver, D., Matabos, M., Sarradin, P., Legrand, J., et al. (2014). Chemini : Long
 1532 term in situ survey of total dissolved iron concentrations in deep ocean. Colloque des 10 ans de la
 1533 station instrumentée MAREL Carnot. 12-13 juin 2014, Boulogne-sur-mer. Available at:
 1534 <https://w3.ifremer.fr/archimer/doc/00197/30860/>.

1535 Lahaye, N., Gula, J., and Roullet, G. (2020). Internal tide cycle and topographic scattering over the
 1536 North Mid-Atlantic Ridge. *J. Geophys. Res. Ocean.*, 1–21. doi:10.1029/2020jc016376.

1537 Lahaye, N., Gula, J., Thurnherr, A. M., Reverdin, G., Bouruet-Aubertot, P., and Roullet, G. (2019).
 1538 Deep currents in the rift valley of the north mid-atlantic ridge. *Front. Mar. Sci.* 6.
 1539 doi:10.3389/fmars.2019.00597.

1540 Langmuir, C. H., Humphris, S. E., Fornari, D. J., Van Dover, C. L., Von Damm, K., Tivey, M. K., et
 1541 al. (1997). Hydrothermal vents near a mantle hot spot: the Lucky Strike vent field at 37°N on the Mid-
 1542 Atlantic Ridge. *Earth Planet. Sci. Lett.* 148, 69–91. doi:10.1016/S0012-821X(97)00027-7.

1543 Lantéri, N., Ruhl, H.A., Gates, A., Martínez, E., del Rio Fernandez, J., Aguzzi, J., Cannat, M., Delory,
 1544 E., Embriaco, D., Huber, R. and Matabos, M., 2022. The EMSO Generic Instrument Module (EGIM):
 1545 Standardized and interoperable instrumentation for ocean observation. *Frontiers in Marine Science*,
 1546 p.205.

1547 Laroche, O., Kersten, O., Smith, C. R., and Goetze, E. (2020). From Sea Surface to Seafloor: A Benthic
 1548 Allochthonous eDNA Survey for the Abyssal Ocean. *Front. Mar. Sci.* 7, 1–16.
 1549 doi:10.3389/fmars.2020.00682.

1550 Larson, B. I., Olson, E. J., and Lilley, M. D. (2007). In situ measurement of dissolved chloride in high
 1551 temperature hydrothermal fluids. *Geochim. Cosmochim. Acta* 71, 2510–2523.
 1552 doi:10.1016/j.gca.2007.02.013.

1553 Le Bris, N., Yücel, M., Das, A., Sievert, S. M., LokaBharathi, P. P., and Girguis, P. R. (2019).
 1554 Hydrothermal energy transfer and organic carbon production at the deep seafloor. *Front. Mar. Sci.* 5,
 1555 1–24. doi:10.3389/fmars.2018.00531.

1556 Lee, R. W., Robert, K., Matabos, M., Bates, A. E., and Juniper, S. K. (2015). Temporal and spatial
1557 variation in temperature experienced by macrofauna at Main Endeavour hydrothermal vent field. Deep.
1558 Res. Part I Oceanogr. Res. Pap. 106, 154–166. doi:10.1016/j.dsr.2015.10.004.

1559 Legrand, J., Sarradin, P., and Cannat, M. (2019). EMSO Azores Deep-sea Observatory : 9 years of
1560 operations. doi:0.

1561 Leleu, T. (2017). Variabilité spatio-temporelle de la composition des fluides hydrothermaux
1562 (observatoire fond de mer EMSO-Açores, Lucky Strike) : traçage de la circulation hydrothermale et
1563 quantification des flux chimiques associées / Spatial and temporal variability of the composition of
1564 hydrothermal fluids (Deep sea observatory EMSO-Azores, Lucky Strike) : tracing the hydrothermal
1565 pathway and quantification of the associated chemical fluxes. PhD Thesis, Université de Toulouse..
1566 Available at: <https://archimer.ifremer.fr/doc/00692/80380/>.

1567 Lelièvre, Y., Legendre, P., Matabos, M., Mihaly, S., Lee, R. W., Sarradin, P., et al. (2017).
1568 Astronomical and atmospheric impacts on deep-sea hydrothermal vent invertebrates. Proc. R. Soc.
1569 London B Biol. Sci. 284.

1570 Lelièvre, Y., Sarrazin, J., Marticorena, J., Schaal, G., Day, T., Legendre, P., et al. (2018). Biodiversity
1571 and trophic ecology of hydrothermal vent fauna associated with tubeworm assemblages on the Juan de
1572 Fuca Ridge. Biogeosciences 15. doi:10.5194/bg-15-2629-2018.

1573 Levin, L. A., Baco, A. R., Bowden, D. A., Colaço, A., Cordes, E. E., Cunha, M. R., et al. (2016).
1574 Hydrothermal Vents and Methane Seeps: Rethinking the Sphere of Influence. Front. Mar. Sci. 3, 72.
1575 doi:10.3389/fmars.2016.00072.

1576 Levin, L. A., Bett, B. J., Gates, A. R., Heimbach, P., Howe, B. M., Janssen, F., et al. (2019). Global
1577 Observing Needs in the Deep Ocean. Front. Mar. Sci. 6, 1–32. doi:10.3389/fmars.2019.00241.

1578 Levin, L. A., and Le Bris, N. (2015). The deep ocean under climate change. Science (80-.). 350.
1579 doi:10.1126/science.aad0126.

1580 Levin, L. A., Wei, C. L., Dunn, D. C., Amon, D. J., Ashford, O. S., Cheung, W. W. L., et al. (2020).
1581 Climate change considerations are fundamental to management of deep-sea resource extraction. Glob.
1582 Chang. Biol. 26, 4664–4678. doi:10.1111/gcb.15223.

1583 Lewis, K., and Lowell, R. P. (2009). Numerical modeling of two-phase flow in the NaCl-H₂O system:
1584 Introduction of a numerical method and benchmarking. *J. Geophys. Res.* 114, B05202.
1585 doi:doi:10.1029/2008JB006029.

1586 Lutz, R. A., Shank, T. M., Luther, G. W., Vetriani, C., Tolstoy, M., Nuzzio, D. B., et al. (2008).
1587 Interrelationships Between Vent Fluid Chemistry, Temperature, Seismic Activity, and Biological
1588 Community Structure at a Mussel-Dominated, Deep-Sea Hydrothermal Vent Along the East Pacific
1589 Rise. *J. Shellfish Res.* 27, 177–190. doi:10.2983/0730-8000(2008)27[177:IBVFCT]2.0.CO;2.

1590 Marcus, J., Tunnicliffe, V., and Butterfield, D. A. (2009). Post-eruption succession of macrofaunal
1591 communities at diffuse flow hydrothermal vents on Axial Volcano, Juan de Fuca Ridge, Northeast
1592 Pacific. *Deep Sea Res. Part II Top. Stud. Oceanogr.* 56, 1586–1598. doi:10.1016/j.dsr2.2009.05.004.

1593 Mariani, P., Bachmayer, R., Kosta, S., Pietrosemoli, E., Ardelan, M. V., Connelly, D. P., et al. (2021).
1594 Collaborative Automation and IoT Technologies for Coastal Ocean Observing Systems. *Front. Mar.
1595 Sci.* 8. doi:10.3389/fmars.2021.647368.

1596 Marjanović, M., Barreyre, T., Fontaine, F. J., and Escartín, J. (2019). Investigating Fine-Scale
1597 Permeability Structure and Its Control on Hydrothermal Activity Along a Fast-Spreading Ridge (the
1598 East Pacific Rise, 9°43'–53°N) Using Seismic Velocity, Poroelastic Response, and Numerical
1599 Modeling. *Geophys. Res. Lett.* 46, 11799–11810. doi:<https://doi.org/10.1029/2019GL084040>.

1600 Marticorena, J., Matabos, M., Ramirez-Llodra, E., Cathalot, C., Laes-Huon, A., Leroux, R., et al.
1601 (2021). Recovery of hydrothermal vent communities in response to an induced disturbance at the
1602 Lucky Strike vent field (Mid-Atlantic Ridge). *Mar. Environ. Res.*, 105316.
1603 doi:10.1016/j.marenvres.2021.105316.

1604 Marticorena, J., Matabos, M., Ramirez-Llodra, E., and Sarrazin, J. (2020). Contrasting reproductive
1605 biology of two hydrothermal gastropods from the Mid - Atlantic Ridge : implications for resilience of
1606 vent communities. *Mar. Biol.*, 1–19. doi:10.1007/s00227-020-03721-x.

1607 Martin, W., Baross, J., Kelley, D. S., and Russell, M. (2008). Hydrothermal vents and the origin of life.
1608 *Nat Rev Micro* 6(11): 805-814. *Nat. Rev. Microbiol.* 6, 805–814. doi:10.1038/nrmicro1991.

1609 Mat, A. M., Sarrazin, J., Markov, G. V., Apremont, V., Dubreuil, C., Eché, C., et al. (2020). Biological
1610 rhythms in the deep-sea hydrothermal mussel *Bathymodiolus azoricus*. *Nat. Commun.* 11, 1–12.
1611 doi:10.1038/s41467-020-17284-4.

1612 Matabos, M., Best, M., Blandin, J., Hoeberichts, M., Juniper, S. K., Pirenne, B., et al. (2016). “Seafloor
1613 Observatories,” in *Biological Sampling in the Deep Sea*, eds. M. R. Clark, M. Consalvey, and A. A.
1614 Rowden (Wiley), 306–337. doi:10.1002/9781118332535.ch14.

1615 Matabos, M., Bui, A. O. V., Mihaly, S., Aguzzi, J., Juniper, S. K., and Ajayamohan, R. S. (2014). High-
1616 frequency study of epibenthic megafaunal community dynamics in Barkley Canyon: A multi-
1617 disciplinary approach using the NEPTUNE Canada network. *J. Mar. Syst.* 130, 56–68.
1618 doi:10.1016/j.jmarsys.2013.05.002.

1619 Matabos, M., Cuvelier, D., Brouard, J., Shillito, B., Ravaux, J., Zbinden, M., et al. (2015). Behavioural
1620 study of two Hydrothermal crustacean decapods: *Mirocaris fortunata* and *Segonzacia mesatlantica*,
1621 from the lucky strike vent field (mid-Atlantic ridge). *Deep Sea Res. Part II Top. Stud. Oceanogr.* 121,
1622 146–158. doi:<http://dx.doi.org/10.1016/j.dsr2.2015.04.008>.

1623 Matsuura, M. (2021). Recent Advancement in Power-over-Fiber Technologies. *Photonics* 8, 335.

1624 McCoy, D., Bianchi, D., and Stewart, A. L. (2020). Global observations of submesoscale coherent
1625 vortices in the ocean. *Prog. Oceanogr.* 189, 102452. doi:<https://doi.org/10.1016/j.pocean.2020.102452>.

1626 Menini, E., and Van Dover, C. L. (2019). An atlas of protected hydrothermal vents. *Mar. Policy* 108,
1627 103654. doi:10.1016/j.marpol.2019.103654.

1628 Meyer, J., Akerman, N., Proskurowski, G., and Huber, J. (2013). Microbiological characterization of
1629 post-eruption “snowblower” vents at Axial Seamount, Juan de Fuca Ridge. *Front. Microbiol* 4.
1630 Available at: <https://www.frontiersin.org/article/10.3389/fmicb.2013.00153>.

1631 Mitarai, S., Watanabe, H., Nakajima, Y., Shchepetkin, A. F., and McWilliams, J. C. (2016).
1632 Quantifying dispersal from hydrothermal vent fields in the western Pacific Ocean. *Proc. Natl. Acad.*
1633 *Sci. U. S. A.* 113, 2976–2981. doi:10.1073/pnas.1518395113.

1634 Mittelstaedt, E., Davaille, A., Van Keken, P. E., Gracias, N., and Escartin, J. (2010). A noninvasive
 1635 method for measuring the velocity of diffuse hydrothermal flow by tracking moving refractive index
 1636 anomalies. *Geochemistry, Geophys. Geosystems* 11. doi:10.1029/2010GC003227.

1637 Mittelstaedt, E., Escartín, J., Gracias, N., Olive, J. A., Barreyre, T., Davaille, A., et al. (2012).
 1638 Quantifying diffuse and discrete venting at the Tour Eiffel vent site, Lucky Strike hydrothermal field.
 1639 *Geochemistry, Geophys. Geosystems* 13. doi:10.1029/2011GC003991.

1640 Mittelstaedt, E., Fornari, D. J., Crone, T. J., Kinsey, J., Kelley, D. S., and Elend, M. (2016). Diffuse
 1641 venting at the ASHES hydrothermal field: Heat flux and tidally modulated flow variability derived
 1642 from in situ time-series measurements. *Geochemistry, Geophys. Geosystems* 17, 1435–1453.
 1643 doi:<https://doi.org/10.1002/2015GC006144>.

1644 Mullineaux, L. S., McGillicuddy, D. J., Mills, S. W., Kosnyrev, V. K., Thurnherr, A. M., Ledwell, J.
 1645 R., et al. (2013). Active positioning of vent larvae at a mid-ocean ridge. *Deep Sea Res. Part II Top.*
 1646 *Stud. Oceanogr.* 92, 46–57. doi:10.1016/j.dsr2.2013.03.032.

1647 Mullineaux, L. S., Metaxas, A., Beaulieu, S. E., Bright, M., Gollner, S., Grupe, B. M., et al. (2018).
 1648 Exploring the Ecology of Deep-Sea Hydrothermal Vents in a Metacommunity Framework. *Front. Mar.*
 1649 *Sci.* 5. doi:10.3389/fmars.2018.00049.

1650 Mullineaux, L. S., Mills, S. W., Bris, N. Le, Beaulieu, S. E., Sievert, S. M., and Dykman, L. N. (2020).
 1651 Prolonged recovery time after eruptive disturbance of a deep-sea hydrothermal vent community. *Proc.*
 1652 *R. Soc. B.* 287: 20202070. <https://doi.org/10.1098/rspb.2020.2070>.

1653 Murdock, S., Tunnicliffe, V., Boschen-Rose, R. E., and Juniper, S. K. (2021). Emergent “core
 1654 communities” of microbes, meiofauna and macrofauna at hydrothermal vents. *ISME Commun.* 1.
 1655 doi:10.1038/s43705-021-00031-1.

1656 National Research Council (2000). *Illuminating the Hidden Planet: The Future of Seafloor Observatory*
 1657 *Science*. Washington, DC, USA doi:<https://doi.org/10.17226/9920>.

1658 Nees, H. A., Moore, T. S., Mullaugh, K. M., Holyoke, R. R., Janzen, C. P., Ma, S., et al. (2008).
 1659 Hydrothermal Vent Mussel Habitat Chemistry, Pre- and Post-Eruption at 9°50'N on the East
 1660 Pacific Rise. *J. Shellfish Res.* 27, 169–175. doi:10.2983/0730-
 1661 8000(2008)27[169:HVMHCP]2.0.CO;2.

1662 Noon, S. L., and Chadwick, W. W. (2016). Inflation-predictable behavior and co-eruption
1663 deformation at Axial Seamount. *Science* (80-). 354, 1399–1403. doi:10.1126/science.aah4666.

1664 Olins, H. C., Rogers, D. R., Preston, C., Ussler, W., Pargett, D., Jensen, S., et al. (2017). Co-registered
1665 Geochemistry and Metatranscriptomics Reveal Unexpected Distributions of Microbial Activity within
1666 a Hydrothermal Vent Field. *Front. Microbiol.* 8.

1667 Ondréas, H., Cannat, M., Fouquet, Y., Normand, A., Sarradin, P., and Sarrazin, J. (2009). Recent
1668 volcanic events and the distribution of hydrothermal venting at the Lucky Strike hydrothermal field,
1669 Mid-Atlantic Ridge. *Geochemistry, Geophys. Geosystems* 10. doi:10.1029/2008GC002171.

1670 Opatkiewicz, A. D., Butterfield, D. A., and Baross, J. A. (2009). Individual hydrothermal vents at Axial
1671 Seamount harbor distinct subseafloor microbial communities. *FEMS Microbiol. Ecol.* 70, 413–424.
1672 doi:<https://doi.org/10.1111/j.1574-6941.2009.00747.x>.

1673 Orcutt, B. N., Bradley, J. A., Brazelton, W. J., Estes, E. R., Goordial, J. M., Huber, J. A., et al. (2020).
1674 Impacts of deep-sea mining on microbial ecosystem services. *Limnol. Oceanogr.*, 1–22.
1675 doi:10.1002/lno.11403.

1676 Palmer, M. R., and Ernst, G. G. J. (1998). Generation of hydrothermal megaplumes by cooling of
1677 pillow basalts at mid-ocean ridges. *Nature* 393, 643–647. Available at:
1678 <https://doi.org/10.1038/31397%0A>.

1679 Pereira, H. M., Ferrier, S., Walters, M., Geller, G. N., Jongman, R. H. G., Scholes, R. J., et al. (2013).
1680 Essential biodiversity variables. *Science* (80-). 339, 277–278. doi:10.1126/science.1229931.

1681 Pester, N. J., Reeves, E. P., Rough, M. E., Ding, K., Seewald, J. S., and Seyfried, W. E. (2012).
1682 Subseafloor phase equilibria in high-temperature hydrothermal fluids of the Lucky Strike Seamount
1683 (Mid-Atlantic Ridge, 37°17'N). *Geochimica Cosmochim. Acta* 90, 303–322.
1684 doi:10.1016/j.gca.2012.05.018.

1685 Picheral, M., Catalano, C., Brousseau, D., Claustre, H., Coppola, L., Leymarie, E., et al. (2021). The
1686 Underwater Vision Profiler 6: an imaging sensor of particle size spectra and plankton, for autonomous
1687 and cabled platforms. *Limnol. Oceanogr. Methods, Association for the Sciences of Limnology and*
1688 *Oceanography*, 2021, doi:<https://doi.org/10.1002/lom3.10475>.

1689 Picheral, M., Guidi, L., Stemmann, L., Karl, D. M., Iddaoud, G., and Gorsky, G. (2010). The
1690 Underwater Vision Profiler 5: An advanced instrument for high spatial resolution studies of particle
1691 size spectra and zooplankton. *Limnol. Oceanogr. Methods* 8, 462–473. doi:10.4319/lom.2010.8.462.

1692 Plum, C., Pradillon, F., Fujiwara, Y., and Sarrazin, J. (2016). Copepod colonization of organic and
1693 inorganic substrata at a deep-sea hydrothermal vent site on the Mid-Atlantic Ridge. *Deep Sea Res. Part*
1694 *II Top. Stud. Oceanogr.* 137. doi:10.1016/j.dsr2.2016.06.008.

1695 Portail, M., Brandily, C., Cathalot, C., Colaço, A., Gélinas, Y., Husson, B., et al. (2018). Food-web
1696 complexity across hydrothermal vents on the Azores triple junction. *Deep. Res. Part I Oceanogr. Res.*
1697 *Pap.* 131, 101–120. doi:10.1016/j.dsr.2017.11.010.

1698 Puzenat, V., Escartín, J., Martelat, J. E., Barreyre, T., Le Moine Bauer, S., Nomikou, P., et al. (2021).
1699 Shallow-water hydrothermalism at Milos (Greece): Nature, distribution, heat fluxes and impact on
1700 ecosystems. *Mar. Geol.* 438. doi:10.1016/j.margeo.2021.106521.

1701 Qiu, T., Zhao, Z., Zhang, T., Chen, C., and Chen, C. L. P. (2019). Underwater Internet of Things in
1702 Smart Ocean: System Architecture and Open Issues. *IEEE Trans. Ind. Informatics* 16, 4297–4307.
1703 doi:10.1109/TII.2019.2946618.

1704 Ramirez-Llodra, E., Brandt, a., Danovaro, R., De Mol, B., Escobar, E. G., German, C. R., et al. (2010).
1705 Deep, diverse and definitely different: unique attributes of the world's largest ecosystem.
1706 *Biogeosciences* 7, 2851–2899. doi:10.5194/bg-7-2851-2010.

1707 Rogers, A., Brierley, A., Croot, P., Cunha, M., Danovaro, R., Devey, C., et al. (2015). Delving Deeper:
1708 Critical challenges for 21st century deep-sea research. Larkin KE, Donaldson K and McDonough N
1709 (Eds.) *Position Paper 22 of the European Marine Board*, Ostend, Belgium. 224 pp. ISBN 978-94-
1710 920431-1-5. , eds. K. E. Larkin, K. Donaldson, and N. McDonough Osten, Belgium: Position Paper 22
1711 of the European Marine Board doi:10.13140/RG.2.1.4077.0009.

1712 Rommevaux, C., Henri, P., Degboe, J., Chavagnac, V., Lesongeur, F., Godfroy, A., et al. (2019).
1713 Prokaryote Communities at Active Chimney and In Situ Colonization Devices After a Magmatic
1714 Degassing Event (37°N MAR, EMSO-Azores Deep-Sea Observatory). *Geochemistry, Geophys.*
1715 *Geosystems* 20, 3065–3089. doi:10.1029/2018GC008107.

1716 Rountree, R. A., Aguzzi, J., Marini, S., Fanelli, E., DE LEO, F. C., Rio, J. Del, et al. (2020). "Towards
1717 an optimal design for ecosystem-level ocean observatories," in *Oceanography and Marine Biology*,
1718 79–105. doi:10.1201/9780429351495-2.

1719 Rubin, K. H., Soule, S. A., Chadwick, W. W., Fornari, D. J., Clague, D. A., Embley, R. W., et al.
1720 (2012). Volcanic eruptions in the deep sea. *Oceanography* 25, 143–157. doi:10.5670/oceanog.2012.12.

1721 Santos, R. S., Escartín, J., Colaço, A., and Adamczewska (2002). Towards planning of seafloor
1722 observatory programs for the MAR region : Proceedings of the II MoMAR Workshop.

1723 Sarrazin, J., Blandin, J., Delauney, L., Dentrecolas, S., Dorval, P., Dupont, J., et al. (2007). TEMPO:
1724 a new ecological module for studying deep-sea community dynamics at hydrothermal vents. in
1725 OCEANS 2007-Europe (Ieee), 1–4.

1726 Sarrazin, J., Cuvelier, D., Peton, L., Legendre, P., and Sarradin, P. (2014). High-resolution dynamics
1727 of a deep-sea hydrothermal mussel assemblage monitored by the EMSO-Açores MoMAR observatory.
1728 *Deep Sea Res. Part I Oceanogr. Res. Pap.* 90, 62–75. doi:10.1016/j.dsr.2014.04.004.

1729 Sarrazin, J., Legendre, P., de Busserolles, F., Fabri, M.-C., Guilini, K., Ivanenko, V. N., et al. (2015).
1730 Biodiversity patterns, environmental drivers and indicator species on a high-temperature hydrothermal
1731 edifice, Mid-Atlantic Ridge. *Deep Sea Res. Part II Top. Stud. Oceanogr.* 121, 177–192.
1732 doi:10.1016/j.dsr2.2015.04.013.

1733 Sarrazin, J., Portail, M., Legrand, E., Cathalot, C., Laes, A., Lahaye, N., et al. (2020). Endogenous
1734 versus exogenous factors: What matters for vent mussel communities? *Deep. Res. Part I Oceanogr.*
1735 *Res. Pap.* 160, 103260. doi:10.1016/j.dsr.2020.103260.

1736 Sarrazin, J., Robigou, V., Juniper, S. K., and Delaney, J. R. (1997). Biological and geological dynamics
1737 over four years on a high-temperature sulfide structure at the Juan de Fuca Ridge hydrothermal
1738 observatory. *Mar. Ecol. Prog. Ser.* 153, 5–24. doi:10.3354/meps153005.

1739 Sarrazin, J., Rodier, P., Tivey, M. K., Singh, H., Schultz, A., and Sarradin, P. (2009). A dual sensor
1740 device to estimate fluid flow velocity at diffuse hydrothermal vents. *Deep. Res. Part I Oceanogr. Res.*
1741 *Pap.* 56, 2065–2074. doi:10.1016/j.dsr.2009.06.008.

1742 Scheirer, D. S., Shank, T. M., and Fornari, D. J. (2006). Temperature variations at diffuse and focused
1743 flow hydrothermal vent sites along the northern East Pacific Rise. *Geochemistry Geophys. Geosystems*
1744 7, Q03002. doi:10.1029/2005GC001094.

1745 Schoening, T., Purser, A., Langenkämper, D., Suck, I., Taylor, J., Cuvelier, D., et al. (2020).
1746 Megafauna community assessment of polymetallic-nodule fields with cameras: platform and
1747 methodology comparison. *Biogeosciences* 17, 3115–3133. doi:10.5194/bg-17-3115-2020.

1748 Shank, T. M., Fornari, D. J., Von Damm, K. L., Lilley, M. D., Haymon, R. M., and Lutz, R. A. (1998).
1749 Temporal and spatial patterns of biological community development at nascent deep-sea hydrothermal
1750 vents (9°50'N, East Pacific Rise). *Deep. Res. Part II Top. Stud. Oceanogr.* 45, 465–515.

1751 Shillito, B., Ravaux, J., Sarrazin, J., Zbinden, M., Sarradin, P., and Barthelemy, D. (2015). Long-term
1752 maintenance and public exhibition of deep-sea Hydrothermal fauna: the AbyssBox project. *Deep. Res.*
1753 *Part II Top. Stud. Oceanogr.* 121, 137–145. doi:10.1016/j.dsr2.2015.05.002.

1754 Singh, S. C., Crawford, W. C., Carton, H., Seher, T., Combier, V., Cannat, M., et al. (2006). Discovery
1755 of a magma chamber and faults beneath a Mid-Atlantic Ridge hydrothermal field. *Nature* 442, 1029–
1756 32. doi:10.1038/nature05105.

1757 Sloyan, B. M., Wilkin, J., Hill, K. L., Chidichimo, M. P., Cronin, M. F., Johannessen, J. A., et al.
1758 (2019). Evolving the global ocean observing system for research and application services through
1759 international coordinatio. *Front. Mar. Sci.* 6. doi:10.3389/fmars.2019.00449.

1760 Smith, C. R., Tunnicliffe, V., Colaço, A., Drazen, J. C., Gollner, S., Levin, L. A., et al. (2020). Deep-
1761 Sea Misconceptions Cause Underestimation of Seabed-Mining Impacts. *Trends Ecol. Evol.* 35, 853–
1762 857. doi:10.1016/j.tree.2020.07.002.

1763 Smith, K. L., Sherman, A. D., McGill, P. R., Henthorn, R. G., Ferreira, J., Connolly, T. P., et al. (2021).
1764 Abyssal Benthic Rover, an autonomous vehicle for long-term monitoring of deep-ocean processes. *Sci.*
1765 *Robot.* 6, eabl4925. doi:10.1126/scirobotics.abl4925.

1766 Smith, L. M., Barth, J. A., Kelley, D. S., Plueddemann, A., Rodero, I., Ulses, G. A., et al. (2018). The
1767 Ocean Observatories Initiative. *Oceanography* 31, 16–35. doi:10.5670/oceanog.2018.105.

1768 Sohn, R. A. (2007). Stochastic analysis of exit fluid temperature records from the active TAG
1769 hydrothermal mound (Mid-Atlantic Ridge, 26°N): 1. Modes of variability and implications for
1770 subsurface flow. *J. Geophys. Res.* 112, B07101. doi:10.1029/2006JB004435.

1771 Spietz, R. L., Butterfield, D. A., Buck, N. J., Larson, B. I., Chadwick, W. W., Walker, S. L., et al.
1772 (2018). Deep-sea volcanic eruptions create unique chemical and biological linkages between the
1773 subsurface lithosphere and the oceanic hydrosphere. *Oceanography* 31, 128–135.
1774 doi:10.5670/oceanog.2018.120.

1775 St. Laurent, L., and Garrett, C. (2002). The Role of Internal Tides in Mixing the Deep Ocean. *J. Phys.*
1776 *Oceanogr.* 32, 2882–2899. doi:10.1175/1520-0485(2002)032<2882:TROITI>2.0.CO;2.

1777 Stefanni S., Mirimin L., Stanković D., Chatzivangelou D., Bongiorni L., Marini S., Modica M.V.,
1778 Manea E., Bonofiglio F., del Rio J., Cukrov N., Gavrilović A., De Leo F., Aguzzi J. 2022. Framing
1779 cutting-edge integrative taxonomy in deep-sea biodiversity monitoring via eDNA and optoacoustic
1780 augmented observatories. *Frontiers Marine Sciences*, 8: 1914.

1781 Stewart, L. C., Algar, C. K., Fortunato, C. S., Larson, B. I., Vallino, J. J., Huber, J. A., et al. (2019).
1782 Fluid geochemistry, local hydrology, and metabolic activity define methanogen community size and
1783 composition in deep-sea hydrothermal vents. *ISME J.* 13, 1711–1721. doi:10.1038/s41396-019-0382-
1784 3.

1785 Sweetman, A. K., Thurber, A. R., Smith, C. R., Levin, L. A., Mora, C., Wei, C.-L., et al. (2017). Major
1786 impacts of climate change on deep-sea benthic ecosystems. *Elem Sci Anth* 5, 4.
1787 doi:10.1525/elementa.203.

1788 Taylor, J., Krumpen, T., Soltwedel, T., Gutt, J., and Bergmann, M. (2017). Dynamic benthic
1789 megafaunal communities: Assessing temporal variations in structure, composition and diversity at the
1790 Arctic deep-sea observatory HAUSGARTEN between 2004 and 2015. *Deep. Res. Part I Oceanogr.*
1791 *Res. Pap.* 122, 81–94. doi:10.1016/j.dsr.2017.02.008.

1792 Taylor, J., Staufenbiel, B., Soltwedel, T., and Bergmann, M. (2018). Temporal trends in the biomass
1793 of three epibenthic invertebrates from the deep-sea observatory HAUSGARTEN (Fram Strait, Arctic
1794 Ocean). *Mar. Ecol. Prog. Ser.* 602, 15–29. doi:10.3354/meps12654.

1795 Theissen-Krah, S., Rüpke, L. H., and Hasenclever, J. (2016). Modes of crustal accretion and their
1796 implications for hydrothermal circulation. *Geophys. Res. Lett.* 43, 1124–1131.
1797 doi:<https://doi.org/10.1002/2015GL067335>.

1798 Thiel, H., Kirstein, K. O., Luth, C., Luth, U., Luther, G. W., Meyer-Reil, L. A., et al. (1994). Scientific
1799 requirements for an abyssal benthic laboratory. *J. Mar. Syst.* 4, 421–439.

1800 Thomson, R. E., Mlhály, S. F., Rabinovich, A. B., McDuff, R. E., Veirs, S. R., and Stahr, F. R. (2003).
1801 Constrained circulation at Endeavour ridge facilitates colonization by vent larvae. *Nature* 424, 545–
1802 549. doi:[10.1038/nature01824](https://doi.org/10.1038/nature01824).

1803 Thomson, R. E., Roth, S. E., and Dymond, J. (1990). Near-Inertial Motions Over a Mid-Ocean Ridge:
1804 Effects of Topography and Hydrothermal Plumes. *J. Geophys. Res.* 95, 7261–7278.

1805 Tivey, M. K., Bradley, A. M., Joyce, T. M., and Kadko, D. (2002). Insights into tide-related variability
1806 at seafloor hydrothermal vents from time-series temperature measurements. *Earth Planet. Sci. Lett.*
1807 202, 693–707.

1808 Tolstoy, M., Cowen, J. P., Baker, E. T., Fornari, D. J., Rubin, K. H., Shank, T. M., et al. (2006). A sea-
1809 floor spreading event captured by seismometers. *Science* (80-.). 314, 1920–1922.
1810 doi:[10.1126/science.1133950](https://doi.org/10.1126/science.1133950).

1811 Tomasi B., J. Preisig, G. B. Deane and M. Zorzi (2011). A Study on the Wide-Sense Stationarity of
1812 the Underwater Acoustic Channel for Non-coherent Communication Systems. 17th European Wireless
1813 2011 - Sustainable Wireless Technologies, pp. 1-6.

1814 Tomasi, B., Zappa, G., McCoy, K., Casari, P., and Zorzi, M. (2010). Experimental study of the space-
1815 time properties of acoustic channels for underwater communications. *Ocean. IEEE Sydney, Ocean.*
1816 2010. doi:[10.1109/OCEANSSYD.2010.5603667](https://doi.org/10.1109/OCEANSSYD.2010.5603667).

1817 Toomey, D. R., Jousselin, D., Dunn, R. A., Wilcock, W. S. D., and Detrick, R. S. (2009). Toomey et
1818 al. reply. *Nature* 458, E12–E13. doi:[10.1038/nature07888](https://doi.org/10.1038/nature07888).

1819 Tunnicliffe, V. (1991). The biology of hydrothermal vents - ecology and evolution. *Oceanogr. Mar.*
1820 *Biol.* 29, 319–407.

1821 Tunnicliffe, V., Juniper, S. K., and Sibuet, M. (2003). "Reducing environments of the deep-sea floor,"
1822 in *Ecosystems of the World: The Deep Sea*. Chapter 4 (Elsevier Press), 81–110.

1823 Van Ark, E., Detrick, R., Canales, J. P., Carbotte, S. M., Harding, A., Kent, G., et al. (2007). Seismic
1824 structure of the Endeavour Segment, Juan de Fuca Ridge: Correlations with seismicity and
1825 hydrothermal activity. *J. Geophys. Res.* 112. doi:10.1029/2005JB004210.

1826 van den Burg, S., Visscher, M., Sonneveld, A., Berges, B., Jansen, L., Sharp, F., et al. (2021). Uptake
1827 of new technology for ocean observation . *Eur. Marit. Fish. Fund.* doi:10.2926/37198 .

1828 Van Dover, C. L. (2014). Impacts of anthropogenic disturbances at deep-sea hydrothermal vent
1829 ecosystems: A review. *Mar. Environ. Res.* doi:10.1016/j.marenvres.2014.03.008.

1830 Van Dover, C. L. (2019). Inactive sulfide ecosystems in the deep sea: A review. *Front. Mar. Sci.* 6, 1–
1831 19. doi:10.3389/fmars.2019.00461.

1832 Van Dover, C. L., Colaço, A., Collins, P. C., Croot, P., Metaxas, A., Murton, B. J., et al. (2020).
1833 Research is needed to inform environmental management of hydrothermally inactive and extinct
1834 polymetallic sulfide (PMS) deposits. *Mar. Policy* 121, 104183. doi:10.1016/j.marpol.2020.104183.

1835 Vehling, F., Hasenklever, J., and Rüpke, L. (2021). Brine Formation and Mobilization in Submarine
1836 Hydrothermal Systems: Insights from a Novel Multiphase Hydrothermal Flow Model in the System
1837 $\text{H}_2\text{O}-\text{NaCl}$. *Transp. Porous Media* 136, 65–102. doi:10.1007/s11242-020-01499-6.

1838 Vic, C., Ferron, B., Thierry, V., Mercier, H., and Lherminier, P. (2021). Tidal and Near-Inertial Internal
1839 Waves over the Reykjanes Ridge. *J. Phys. Oceanogr.* 51, 419–437. doi:10.1175/jpo-d-20-0097.1.

1840 Vic, C., Garabato, A. C. N., Green, J. A. M., Spingys, C., Forryan, A., Zhao, Z., et al. (2018a). The
1841 lifecycle of semidiurnal internal tides over the Northern Mid-Atlantic Ridge. *J. Phys. Oceanogr.* 48,
1842 61–80. doi:10.1175/JPO-D-17-0121.1.

1843 Vic, C., Gula, J., Roullet, G., and Pradillon, F. (2018b). Dispersion of deep-sea hydrothermal vent
1844 effluents and larvae by submesoscale and tidal currents. *Deep. Res. Part I Oceanogr. Res. Pap.* 133, 1–
1845 18. doi:10.1016/j.dsr.2018.01.001.

1846 Waeles, M., Cotte, L., Pernet-Coudrier, B., Chavagnac, V., Cathalot, C., Leleu, T., et al. (2017). On
1847 the early fate of hydrothermal iron at deep-sea vents: A reassessment after in situ filtration. *Geophys.*
1848 *Res. Lett.* 44, 4233–4240. doi:10.1002/2017GL073315.

1849 Webb, T. J., Vanden Berghe, E., and O'Dor, R. (2010). Biodiversity's big wet secret: the global
1850 distribution of marine biological records reveals chronic under-exploration of the deep pelagic ocean.
1851 *PLoS One* 5, e10223. doi:10.1371/journal.pone.0010223.

1852 Werner, F. E., Cowen, R. K., and Paris, C. B. (2007). Coupled biological and physical models: Present
1853 capabilities and necessary developments for future studies of population connectivity. *Oceanography*
1854 20, 54–69. doi:10.5670/oceanog.2007.29.

1855 West, M., Menke, W., Tolstoy, M., Webb, S., and Sohn, R. (2001). Magma storage beneath Axial
1856 volcano on the Juan de Fuca mid-ocean ridge. *Nature* 413, 833–836. doi:10.1038/35101581.

1857 Wilcock, W. S. D., Tolstoy, M., Waldhauser, F., Garcia, C., Tan Yen, J., Bohnenstiehl, D. R., et al.
1858 (2016). Seismic constraints on caldera dynamics from the 2015 Axial Seamount eruption. *Science* (80-
1859 .). 354, 1395–1399. doi:10.1126/science.aah5563.

1860 Xu, G., and Di Iorio, D. (2012). Deep sea hydrothermal plumes and their interaction with oscillatory
1861 flows. *Geochemistry, Geophys. Geosystems* 13, 1–18. doi:10.1029/2012GC004188.

1862 Xu, G., Larson, B. I., Bemis, K. G., & Lilley, M. D. (2017). A preliminary 1-D model investigation of
1863 tidal variations of temperature and chlorinity at the Grotto mound, Endeavour Segment, Juan de Fuca
1864 Ridge. *Geochemistry, Geophysics, Geosystems*, 18(1), 75-92.

1865 Young, C. M., He, R., Emlet, R. B., Li, Y., Qian, H., Arellano, S. M., et al. (2012). Dispersal of Deep-
1866 Sea Larvae from the Intra-American Seas: Simulations of Trajectories using Ocean Models. *Integr.*
1867 *Comp. Biol.* 52, 483–496. doi:10.1093/icb/ics090.

1868 Zeppilli, D., Bellec, L., Cambon-Bonavita, M.-A., Decraemer, W., Fontaneto, D., Fuchs, S., et al.
1869 (2019). Ecology and trophic role of *Oncholaimus dyvae* sp. nov. (Nematoda: Oncholaimidae) from the
1870 lucky strike hydrothermal vent field (Mid-Atlantic Ridge). *BMC Zool.* 4, 6. doi:10.1186/s40850-019-
1871 0044-y.

1872 Zeppilli, D., Vanreusel, A., Pradillon, F., Fuchs, S., Mandon, P., James, T., et al. (2015). Rapid
1873 colonisation by nematodes on organic and inorganic substrata deployed at the deep-sea Lucky Strike
1874 hydrothermal vent field (Mid-Atlantic Ridge). *Mar. Biodivers.* 45, 489–504. doi:10.1007/s12526-015-
1875 0348-2.

1876

1877

1878 **Boxes****BOX 1 – Observatories at Mid Ocean Ridges and Vents**

Currently three observatories operate at vents on the Mid-Atlantic and Juan de Fuca Ridges including EMSO-Azores, part of the European Multidisciplinary Seafloor and water column Observatory Research Infrastructure (EMSO-ERIC), the Endeavour node of the Ocean Networks Canada NEPTUNE observatory (ONC) and the Axial Seamount component of the Ocean Observatories Initiative Regional Cabled Array (OOI-RCA). They provide real-time to nearly real-time open access data, tools for data visualization and download and resources for training and outreach.

EMSO-Azores

EMSO-ERIC website: <http://emso.eu/>

EMSO-Azores: <https://www.emso-fr.org/EMSO-Azores>

Data download: <https://www.emso-fr.org/EMSO-Azores/Data-download>

Data visualization tool: <http://www.emso-fr.org/charts/azores/>

Infrastructure design: <https://www.emso-fr.org/EMSO-Azores/Infrastructure-2021-2022>

Maintenance cruises: <https://campagnes.flotteoceanographique.fr/series/130/>

ONC-Endeavour

Ocean Networks Canada website <https://www.oceannetworks.ca/>

Data download: <https://data.oceannetworks.ca/DataSearch>

Data visualization:

<https://data.oceannetworks.ca/home?TREETYPE=1&LOCATION=11&TIMECONFIG=0>

Infrastructure: <https://www.oceannetworks.ca/observatories/pacific/endeavour>

Regional Cabled Array – Axial Seamount

OOI website: <https://oceanobservatories.org/>

University of Washington Educational Site: <https://interactiveoceans.washington.edu/>

Data access and visualization: <https://dataexplorer.oceanobservatories.org/>

Axial seamount

Live video stream <https://oceanobservatories.org/streaming-underwater-video/>

1879

1880

BOX 2 – List of main recommendations from workshop 2

1. Climate change

- Deploy an European Generic Instrument Module -EGIM- (Lantéri et al., 2022), or equivalent, to monitor key regional water mass characteristics at each site
- Sample bottom and full water column seawater to conduct ground truthing chemical measurements and enable sensor calibration
- Install cabled, instrumented profiling moorings for full water column measurements

2. Subsurface processes

- Conduct 2D/3D seismic surveys to image subsurface features that include magma-mush zones, sills, and faults
- Install arrays of broadband and short-period seismometers, low frequency hydrophones, and bottom pressure tilt instruments to monitor magma movement, seafloor deformation
- Install temperature -chemical sensors in vents to inform fluid-rock reactions in the subsurface that are vent fluid sources
- Utilize IODP capabilities for installation of cabled and uncabled CORKed Observatories that allow downhole measurements, sampling (fluid-biological), and cross hole hydrogeological experiments

3. Interface and biological response

- Compile a list of recommended standardised protocols provided by experts to be applied during maintenance including sampling (i.e. microplastics, eDNA), video acquisition (fluid flux estimation)
- Conduct sea floor routine transects with ROVs and AUV's to map megafauna abundance, geological and chemical features and litter distribution using common protocol acquisition and logging terminology (see 4.3)
- Consistently record vertical video transects during ascent and descent of submersibles
- Quantify the magnitude and distribution of heat, chemical and biological fluxes

4. Water column: deep circulation, megaplume formation, fluid dispersal and connectivity

- Deploy an array of full water column profiling moorings equipped with a diverse suite of instruments at distances of 500 m to 1 km to mimic the scales resolved by numerical models.
- Conduct standardized routine vertical transect with CTD measurements and discrete fluid sampling

BOX 3 – Outreach activities and materiel related to observatories

EMSO-Azores

Educational resources for the public and researchers: www.deepseaspy.com (see educational resources tab)

Artistic creations: <https://www.teatrpiba.bzh/en/project/>

3D immersive visit: <https://www.youtube.com/watch?v=hNK1MERlzaY>

Endeavour component of ONC

Training and outreach resources: <https://www.oceannetworks.ca/learning>

Sight and sounds: <https://www.oceannetworks.ca/sights-sounds>

Regional Cabled Array – Axial Seamount

Educational website <https://interactiveoceans.washington.edu/>

UW Regional Cabled Array educational Data Portal

<https://app.interactiveoceans.washington.edu/>

Blog to chronicle eruption forecasts at Axial Seamount

https://www.pmel.noaa.gov/eoi/axial_blog.html

1883

1884

1885 **Tables**

1886 Table 1. Themes and processes to be considered at vents as defined during the first workshop and
 1887 that can be addressed through observatories and their associated maintenance cruises.

Discipline	Processes
Biology	Connectivity between vents, mounds, ridges, peripheral zones Role of ocean circulation on larval dispersal Recruitment dynamics Energy flow and fluxes
Chemistry	Chemical signatures: time-scale, stability, low- and high-temperature Phase separation Dynamic coupling of diffuse/focused venting Magmatic chamber replenishment Mixing Mineral precipitation, chemical speciation, chemical fluxes
Geophysics	Seafloor dynamics: compliance and ground deformation Plumbing system and fluid flow geometry over a range of substrata Subsurface characterization Crustal geothermal processes, permeability and stress states Forcing of sub-seafloor processes on seafloor systems (volcanic, tectonic, alteration and precipitation of minerals)
Oceanography	Plume characterization and dispersal Kinetic energy dissipation and turbulent mixing Carbon cycle Geochemical and thermal fluxes impacts on ocean Forcing of ocean dynamics on seafloor systems

1888

1889

1890

1891
1892

Table 2. List of variables currently measured at the three vent observatory platforms and the corresponding observables.

Domain	Observable	Variable	Instrument/Sensor	Observatory
Biology	Species abundance	Visible species	Video camera	OOI – ONC – EMSO
Biology	Species behaviour	Animal activity	Video camera	OOI – ONC – EMSO
Biology	Microbial colonization	Fluid Samples	CISICS	EMSO
Biology	Microbial community composition	Fluid Samples	PPS	OOI – ONC
Chemistry	Salinity	Conductivity	CTD	OOI – ONC – EMSO
Chemistry	Chlorinity	Resistivity	BARS/TRPH	OOI – ONC – EMSO
Chemistry	pH, eH (redox potential), H ₂ S	Redox potential (V)	THSPH/TRPH	OOI – ONC
Chemistry	Oxygen concentration	Optic (phosphorescence quenching)	Optode	OOI – ONC – EMSO
Chemistry	Turbidity	Optical backscatter	Turbidity meter / Nephelometer	OOI – ONC – EMSO
Chemistry	Vent fluid chemistry	Iron concentration	CHEMINI	ONC – EMSO
Chemistry	Vent fluid chemistry	Fluid Samples	RAS	OOI – ONC
Chemistry	Vent fluid chemistry	Fluid samples	DEAFS	EMSO
Chemistry	Diffuse vent chemistry	Fluid Samples	OSMOI	OOI
Flow	Velocity, Flux	Particle displacement	Video camera (imagery/pixels)	OOI – ONC – EMSO
Physics	Seismicity	Seafloor acceleration	Seismometer	OOI – ONC – EMSO
Physics	Seismicity	Seafloor tilt	Tilt meter	OOI – ONC
Physics	Currents	Water movement	Current meter	OOI – ONC – EMSO
Physics	Currents	Particle displacement	ADCP	OOI – ONC – EMSO
Physics	Currents	Particle displacement	ADCP profiler	OOI – ONC – EMSO
Physics	Flux	Forward scattering	Acoustic scintillation	OOI – ONC
Physics & biology	Ocean soundscape	Passive acoustics	Hydrophone	OOI – ONC – EMSO
Physics	Deformation	Pressure	Bottom Pressure Tilt meter	OOI
Physics	Pressure	Pressure	Pressure gauge	OOI – ONC – EMSO
Physics	Seawater temperature	Temperature	CTD	OOI – ONC EMSO

Physics	High and low temperature	Temperature	Autonomous temperature sensors	OOI – ONC – EMSO
Physics	Diffuse vent temperature	Temperature	RAS	OOI – ONC – EMSO
Physics	Diffuse vent temperature	Temperature	TMPSF	OOI
Physics	High temperature	Temperature	BARS/TRHPH	OOI – ONC – EMSO

1893

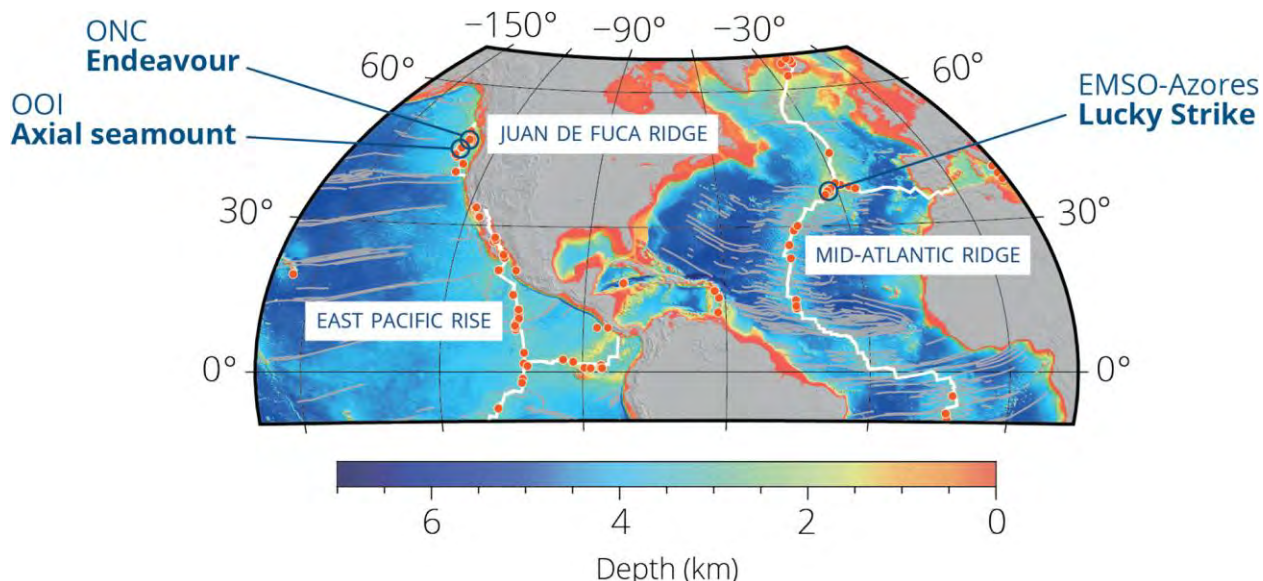
1894

1895 Table 3. Global Ocean Observing System (GOOS) Essential Ocean Variable (EOVs)
 1896 proposed by the Deep Ocean Observing Strategy (DOOS) and new observables specific to ridges
 1897 proposed by the InterRidge Integrated Multidisciplinary Observations at Vent Environments that can
 1898 be measured by seafloor vent observatories, their associated surface buoys and/or during annual
 1899 maintenance cruises (modified from Levin et al. 2019).

	Water column (Physics*)	Subsurface	Interface fluxes (Biogeochemistry*)	Interface Biological Responses (Biology and Ecosystems*)
GOOS EOVs	Sea state		Oxygen	Fish abundance and distribution
	Ocean surface stress		Nutrients	Hard coral cover and composition
	Sea surface height		Inorganic carbon	Ocean sound
	Sea surface temperature		Particulate matter	Microbe biomass and diversity
	Sea Surface currents		Transient tracer	Benthic invertebrate abundance and distribution
	Sea Surface salinity		Nitrous oxide	
	Subsurface salinity		Stable carbon isotopes	
			Dissolved organic Carbon	
DOOS EOVs	Ocean turbulence	Ocean bottom Pressure	Seafloor fluxes	Body size
			Seafloor labile organic matter	Seafloor sponge habitat cover
			Seafloor fluid and gas effluxes (focus on methane)	Connectivity of species
			Litter including microplastics	
IMOVES suggested observables	Ocean bottom temperature	Seafloor deformation	Heat and fluid fluxes and velocity	Engineer species cover
	Ocean bottom salinity	Seismicity	Chlorinity	Vent species behavior
	Ocean bottom oxygen concentration	Subsurface fluid flow	Fluid chemical composition	Pelagic species presence
	Bottom currents	Fluid chemical composition		

1901 **Figures**

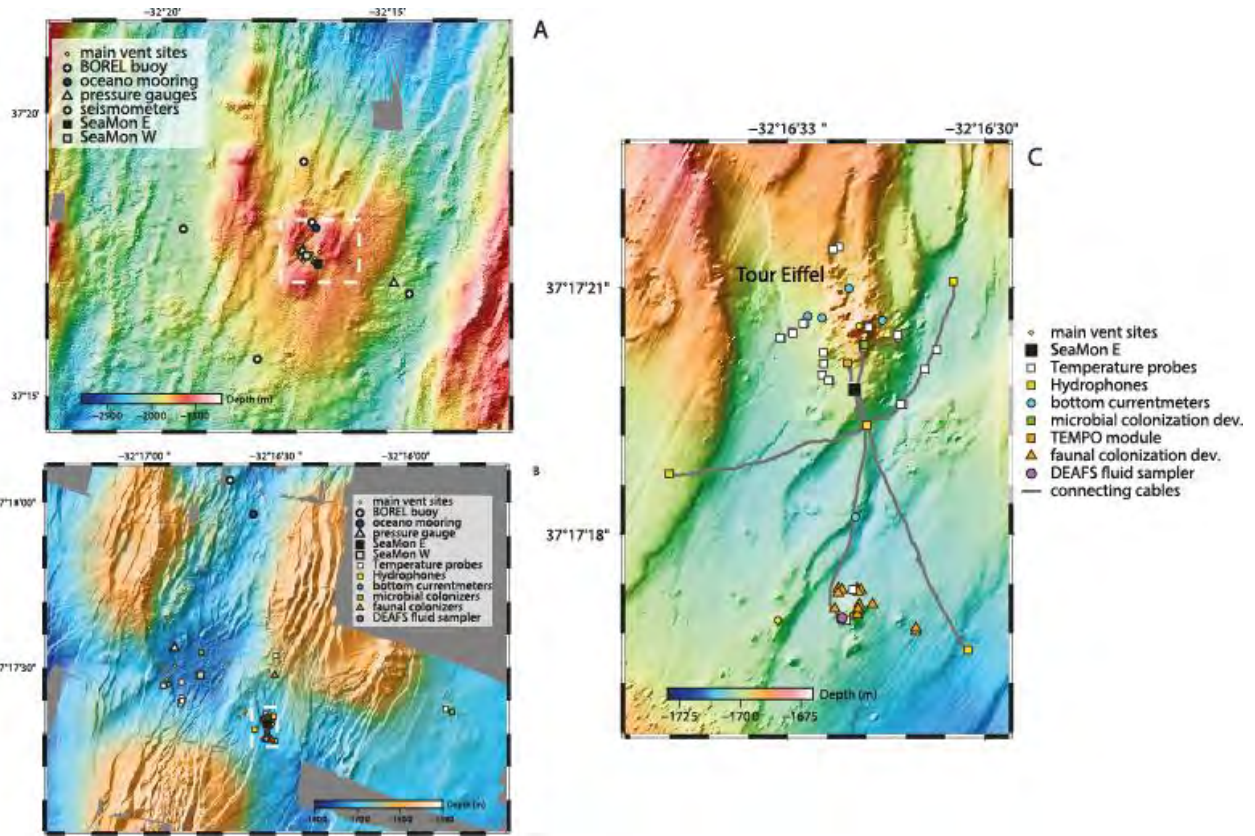
1902



1903

1904 Figure 1. Location of the three currently operating seafloor and water column mid-ocean ridges ocean
1905 observatories in the Pacific and Atlantic oceans. Orange dots represent active known felden.

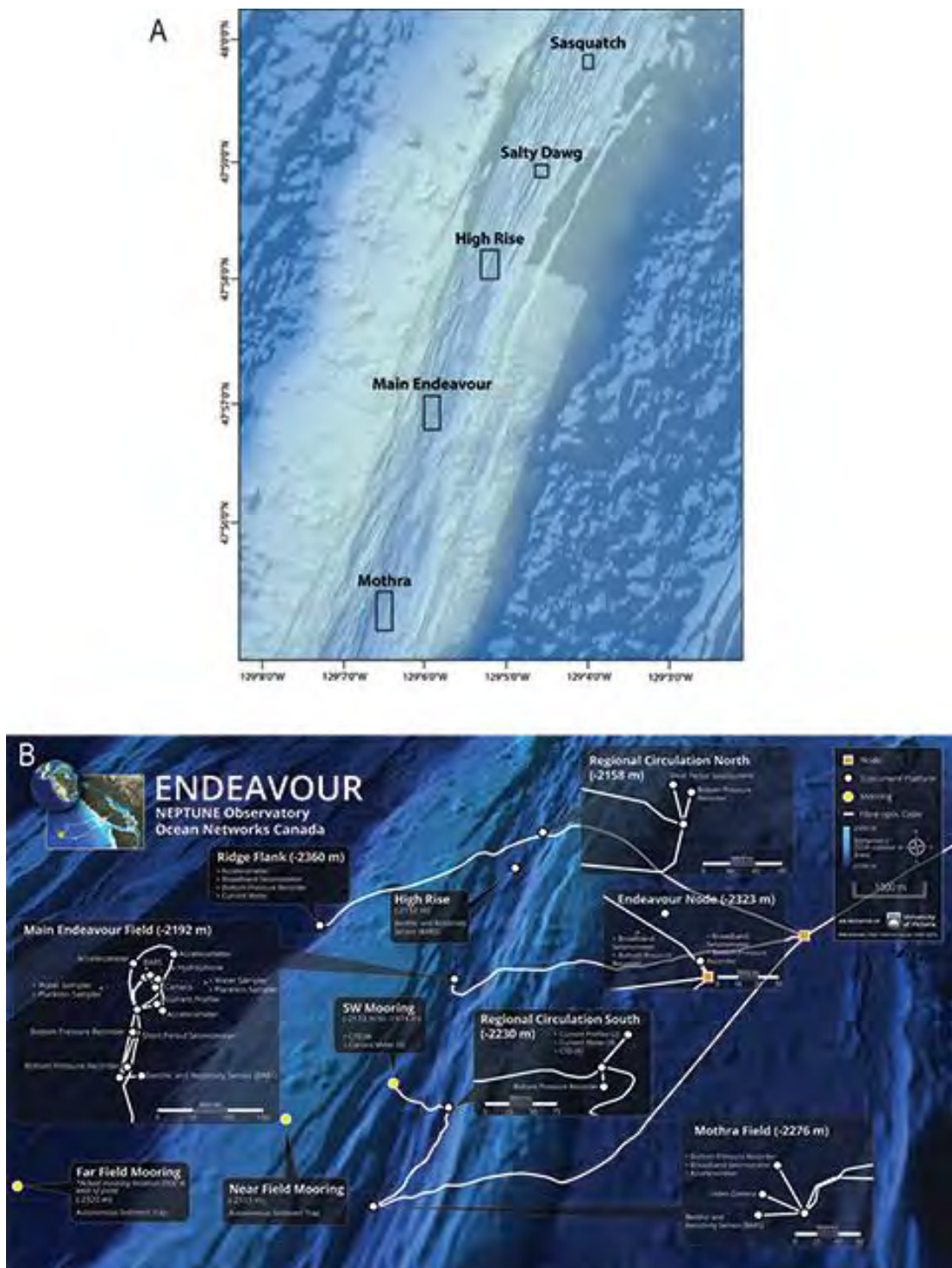
1906



1907

1908 Figure 2. The EMSO-Azores observatory displaying instruments location. A. Segment of the Mid-
 1909 Atlantic Ridge showing the location of the Lucky Strike vent field. B. The Lucky Strike vent field
 1910 showing the location of the EMSO-Azores observatory (area represented by the white dashed box in
 1911 A). C. Detail of the instrumentation at Tour Eiffel (area represented by the white dashed box in B).

1912



1913

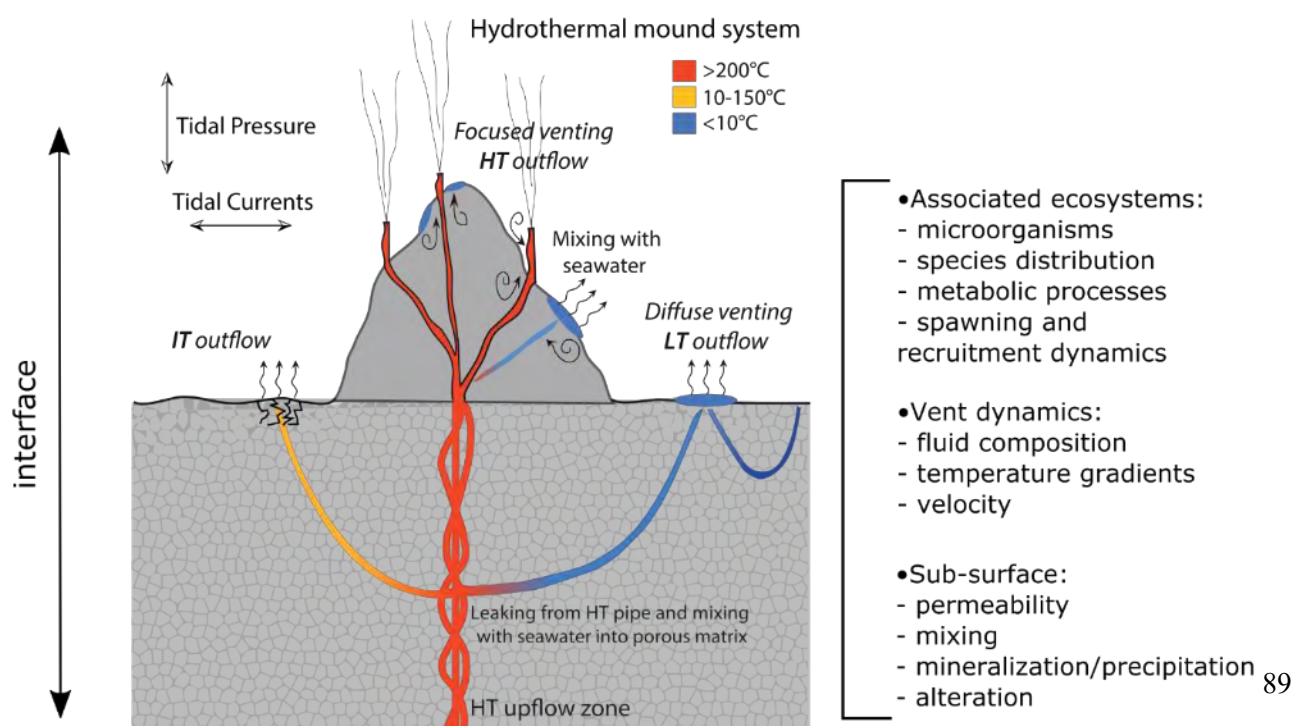
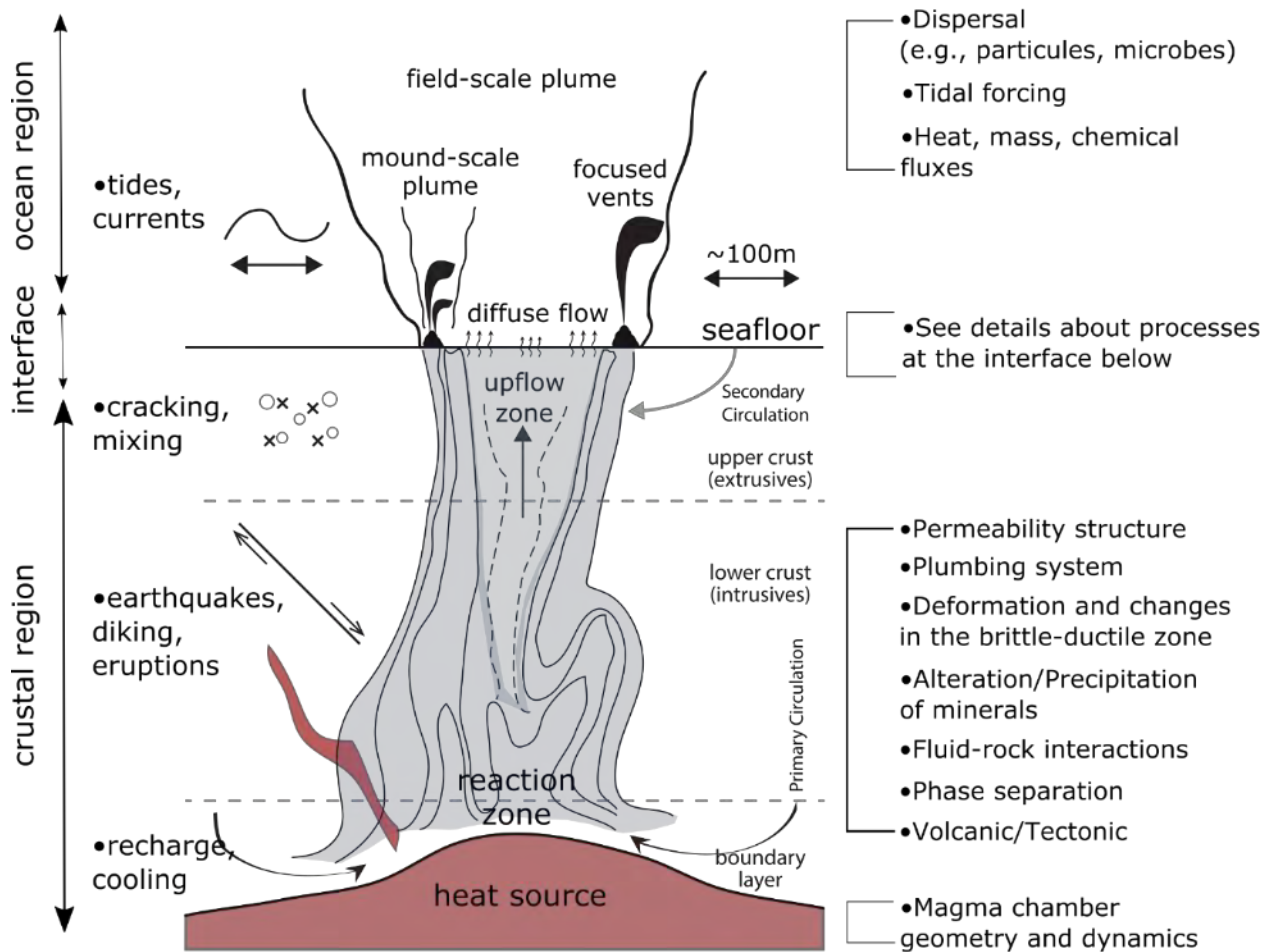
1914 Figure 3. The Ocean Networks Canada on the Endeavour segment of the Juan de Fuca Ridge. A.
 1915 Regional bathymetry showing the main hydrothermal vent fields. B. Details of the instruments location
 1916 at the Endeavour node.



1917

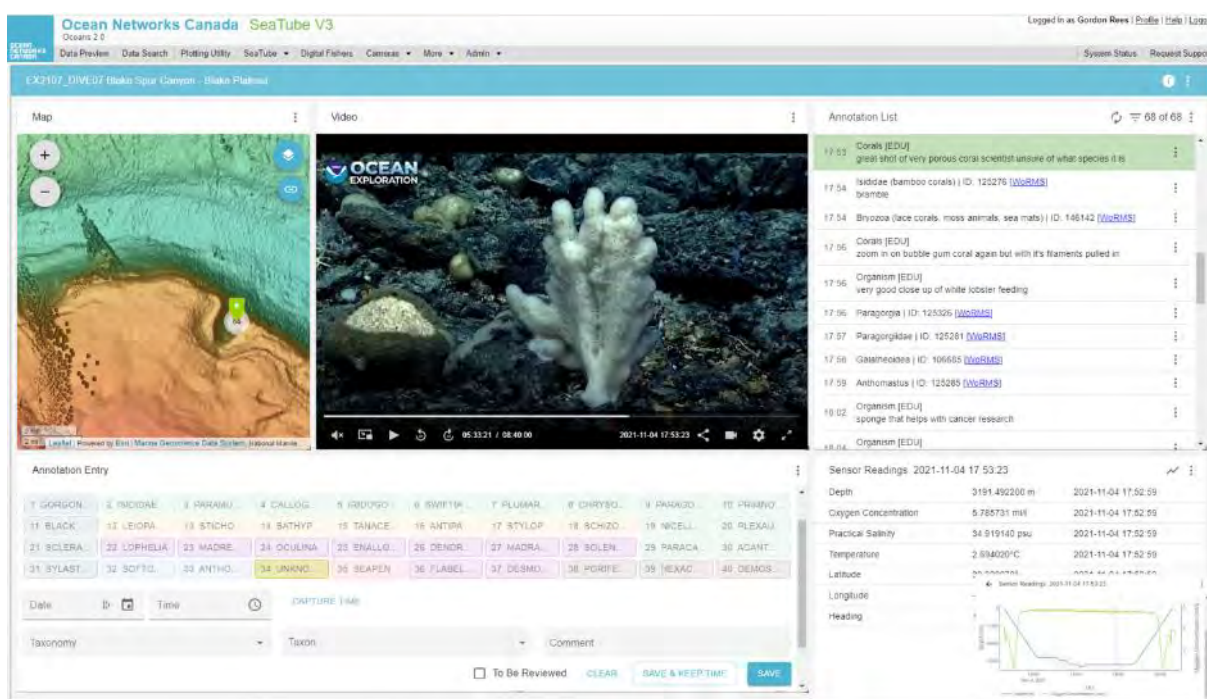
1918 Figure 4 The Ocean Observatory Initiative Axial Seamount array on the Juan de Fuca Ridge. A.
 1919 Regional bathymetry showing the main hydrothermal vent fields. B. Details of the instruments
 1920 locations within the axial caldera. * indicate instruments funded outside of OOI.

Forcing:



1922 Figure 5. (a) Conceptual model of a hydrothermal plumbing system at depth, with the upwelling of a
 1923 single plume above the magmatic heat source that is focused along high-permeability zones associated
 1924 with main faults and fractures networks. (b) Close-up of a hydrothermal mound edifice. High-
 1925 temperature (HT) outflow is directly fed by the high-temperature up-flow zone (here represented as an
 1926 anastomosing, interconnected series of conduits), intermediate-temperature (IT) outflow is fed from
 1927 leakage from the HT pipe and mixed with cold water into the porous matrix (i.e., hypothesis (1)) and
 1928 low-temperature (LT) outflow is fed from either hypothesis (1) or conductively heated bottom water
 1929 drawn into the seafloor as part of a secondary circulation system (i.e., hypothesis (2)). Modified from
 1930 Barreyre et al. [2014b].

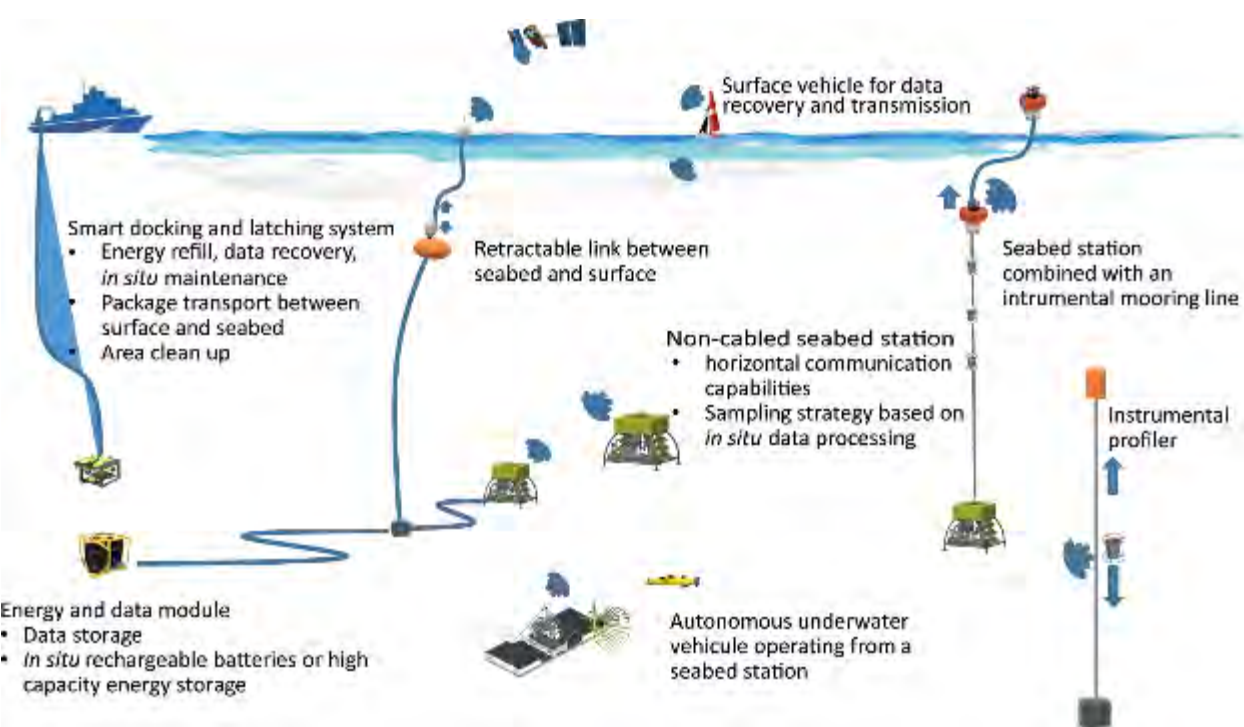
1931



1932

1933 Figure 6. Example of video annotation interface for SeaTube 3.0 showing location of ROV on seafloor
 1934 bathymetry, a deep-sea coral of interest, and the user-designed annotation options available for
 1935 identifying the coral. Sensor data from the ROV are also linked to the annotation. Screen capture
 1936 courtesy of NOAA Office of Ocean Exploration and Research.

1937



1938

1939 Figure 7. Illustration of future technological and operational breakthroughs to reduce deployment and
 1940 maintenance cost and reduce environmental footprint.

1941

1942

1943